DEFENSE DOCUMENTATION CENTER

FOR

SCIENTIFIC AND TECHNICAL INFORMATION

CAMERON STATION, ALEXANDRIA, VIRGINIA

Thermoelectric
Thermal-Barrier Microelements

Contract Nr. DA 36-039 SC-89212
DA Task Nr. 3A99-15-002-03

FINAL REPORT

1 April 1962 to 30 September 1962

Prepared for

U. S. ARMY ELECTRONICS RESEARCH
AND DEVELOPMENT LABORATORY
Fort Monmouth, New Jersey

MELPAR INC

3000 ARLINGTON BOULEVARD   FALLS CHURCH, VIRGINIA

ASTIA AVAILABILITY NOTICE

Qualified requesters may obtain copies of this report from the Armed Services Technical Information Agency (ASTIA), Arlington Hall Station, Arlington 12, Virginia.

ASTIA release to OTS is not authorized.

THERMOELECTRIC THERMAL-BARRIER MICROELEMENTS

Contract Nr. DA 36-039 SC-89212

U.S. Army Signal Corps Technical Requirement No. SCL-7635
dated 29 September 1961

DA Task Nr. 3A99-15-002-03

Final Report

1 April 1962 to 30 September 1962

The objective of this program was to develop, fabricate,
and evaluate thermoelectric thermal-barrier microelements.

Prepared by

F. K. Eggleston
P. A. Mullin
N. Fuschillo

D D C

JUL 18 1963

TISIA B

TABLE OF CONTENTS

LIST OF ILLUSTRATIONS

LIST OF ILLUSTRATIONS (Continued)

LIST OF ILLUSTRATIONS (Continued)

LIST OF ILLUSTRATIONS (Continued)

LIST OF TABLES

LIST OF TABLES (Continued)

GLOSSARY OF SYMBOLS

$\overline{A}$ = Area of either hot junction or cold junction, excluding the area associated with the thermoelectric legs (cm^2).

A' = Effective area of any necessary insulation such as the glass encapsulation (cm^2).

A_n = Area of the n-type thermoelectric leg (cm^2).

A_p = Area of the p-type thermoelectric leg (cm^2).

$A \pm A_n = A_p$ = Area of thermoelectric leg when the n-type leg is assumed to be the same as the p-type leg (cm^2).

B = Substitution made to simplify the algebra.

$$B = 2 \frac{(k_p - k_n) \Delta T}{\overline{S}^2 T_c^2} \quad (ohms)^{-1}.$$

C = Substitution made to simplify the algebra.

$$C = \frac{1 - B\rho_p}{\rho_n B + \left\{ \left(\frac{\rho_n}{\rho_p} \right) \left[1 + B(\rho_n - \rho_p) \right] \right\}^{1/2}} \quad (dimensionless).$$

C.O.P. = Coefficient of performance (dimensionless).

C.O.P.$_{(max)}$ = Maximum coefficient of performance (dimensionless).

C.O.P.$_{\dot{Q}(max)}$ = Coefficient of performance obtained when operating at maximum heat-pumping rate (dimensionless).

d = Width of a square thermoelectric leg (cm).

$\overline{\varepsilon}_1$ = Average emissivity of the hot junction surface area (dimensionless).

$\overline{\varepsilon}_2$ = Average emissivity of the cold junction surface area (dimensionless).

9

I = Current (amperes).

$I_{(\text{C.O.P.}_{(\text{max})})}$ = Current necessary to operate at maximum coefficient of performance (amperes).

$I_{(\text{max})}$ = Current necessary to produce maximum temperature difference (amperes).

$I_{(\dot{Q}_{(\text{max})})}$ = Current necessary to operate at maximum heat-pumping rate (amperes).

i = Ratio of operating current to current at maximum heat-pumping rate (dimensionless).

$\bar{k}$ = Average value of thermal conductivity of the n-type and p-type thermoelectric material over the appropriate temperature range $(\frac{\text{watts}}{\text{cm}^{\text{O}}\text{K}})$.

$k_{\text{insulation}}$ = Specific thermal conductivity of any nonthermoelectric material incorporated into the thermoelectric heat pump $(\frac{\text{watt}}{\text{cm}^{\text{O}}\text{K}})$.

k_n = Specific thermal conductivity of the n-type thermoelectric material averaged over temperature range used $(\frac{\text{watt}}{\text{cm}^{\text{O}}\text{K}})$.

k_p = Specific thermal conductivity of the p-type thermoelectric material averaged over temperature range used $(\frac{\text{watt}}{\text{cm}^{\text{O}}\text{K}})$.

K = Thermal conductance component of a couple due to the thermoelectric material $(\frac{\text{watts}}{{}^{\text{O}}\text{K}})$.

K_o = Geometrically optimized thermal conductance $(\frac{\text{watts}}{{}^{\text{O}}\text{K}})$.

$K_{\text{insulation}}$ = Thermal conductance component of the device caused by the nonthermoelectric materials $(\frac{\text{watts}}{{}^{\text{O}}\text{K}})$.

K_r = Thermal conductance component of the device caused by radiation through the nonthermoelectric part of the device $(\frac{watts}{^oK})$.

K' = Total thermal conductance of a thermoelectric device $(\frac{watts}{^oK})$.

$K' = K + K_{insulation} + K_r$.

$K_{(electron)}$ = Thermal conductance of thermoelectric material due to charge carriers $(\frac{watts}{^oK})$.

$K_{(lattice)}$ = Thermal conductance of the thermoelectric material due to phonon and photon energy transfers through the lattice $(\frac{watts}{^oK})$.

L = Length of the thermoelectric leg when the n-type leg is assumed to be the same length as that of the p-type leg (cm).

L_n = Length of the n-type thermoelectric leg (cm).

L_p = Length of the p-type thermoelectric leg (cm).

$m = \frac{Ir}{S}$ = Substitution made to simplify differentiation of equation defining coefficient of performance (^oK).

M = Dimensionless quantity used to describe the operating parameters of a thermoelectric couple operating at maximum coefficient of performance. $(M = \sqrt{1 + Z\bar{T}})$

N = Number of two-leg thermoelectric couples placed in series electrically.

n(subscript) = Denotes that a particular parameter is associated with the n-type thermoelectric material.

p(subscript) = Denotes that a particular parameter is associated with the p-type thermoelectric material.

P_o = Power input to the thermoelectric couple (watts).

$P_o \left(C.O.P._{(max)} \right)$ = Power input when operating at maximum coefficient of performance (watts).

$P_o \left(\dot{Q}_{(max)} \right)$ = Power input when operating at maximum heat-pumping rate (watts).

$\dot{Q}$ = Heat-pumping capacity of the system (watts).

$\dot{Q}_{(max)}$ = Maximum heat-pumping capacity (watts).

$\dot{Q} \left(C.O.P._{(max)} \right)$ = Heat-pumping capacity when the system is operating at maximum coefficient of performance (watts).

$\dot{Q}_t$ = Total heat load of the system including all heat losses (watts).

$\dot{Q}_r$ = Radiation heat loss (watts).

$\dot{Q}_{insulation}$ = Heat loss by conduction through any nonthermo-electric material (watts).

R = Electrical resistance of a single thermoelectric leg (ohms).

R_c = Contact resistance of a single solder connection (ohms).

R_c' = Contact resistance associated with both ends of a thermo-electric leg (ohms).

r = Electrical resistance component of a couple due to thermo-electric material (ohms).

r_c = Contact resistance associated with a two-leg thermoelectric couple (ohms).

r' = Total electrical resistance of a two-leg thermo-electric couple (ohms).

$r' = r + r_c$.

r_o = Geometrically optimized resistance (ohms).

$\overline{S} = (S_n - S_p)$ = Combined Seebeck coefficient of a thermo-electric couple made up of an n-type and a p-type leg averaged over temperature range used $(\frac{microvolts}{^{\circ}K})$.

S_n = Seebeck coefficient of the n-type thermoelectric leg averaged over temperature range used $(\frac{microvolts}{^{\circ}K})$.

S_p = Seebeck coefficient of the p-type thermoelectric leg averaged over temperature range used $(\frac{microvolts}{^{\circ}K})$.

T = Temperature ($^{\circ}K$).

T_c = Temperature of the cold junction ($^{\circ}K$).

T_h = Temperature of the hot junction ($^{\circ}K$).

T_L = Temperature of the thermal load ($^{\circ}C$).

T_{TG} = Temperature of thermal guard radiation shield ($^{\circ}C$).

$\overline{T}$ = 1/2 $(T_h + T_c)$ ($^{\circ}K$).

ΔT = Temperature difference between the hot and cold junctions ($^{\circ}K$).

$\Delta T = T_h - T_c$.

$\Delta T_{(max)}$ = Maximum temperature difference between the hot and cold junctions ($^{\circ}K$).

V_o = Seebeck voltage across the couple (volts).

$V \left(C.O.P._{(max)} \right)$ = Voltage when operating at maximum coefficient of performance (volts).

V = Voltage input to the thermoelectric couple (volts).

$V \left(\dot{Q}_{(max)} \right)$ = Voltage when operating at maximum heat-pumping rate (volts).

Z = Thermoelectric figure of merit $({}^{O}K)^{-1}$.

Z_O = Geometrically optimized figure of merit $({}^{O}K)^{-1}$.

Z' = Thermoelectric figure of merit which includes contact resistance $({}^{O}K)^{-1}$.

Z'' = Thermoelectric figure of merit which includes contact resistance and nonthermoelectric material thermal conductance $({}^{O}K)^{-1}$.

$\bar{\rho}$ = Average value of the electrical resistivity of the n-type and p-type thermoelectric material over the appropriate temperature range (ohm-cm).

ρ_n = Electrical resistivity of the n-type thermoelectric material averaged over temperature range used (ohm-cm).

ρ_p = Electrical resistivity of the p-type thermoelectric material averaged over temperature range used (ohm-cm).

ρ_c = Contact resistivity associated with both the n-type and p-type thermoelectric material (ohm-cm^2).

γ = Ratio of thermoelectric leg area to its length (cm).

γ = A/L.

1. PURPOSE

1.1 Objective

The objective of this contract was to develop, fabricate, and evaluate thermoelectric cooling devices which would be suitable for direct incorporation into Army micromodules as special microelements having the purpose of protecting heat-sensitive circuit elements. These devices, called Thermoelectric Thermal Barrier Microelements (TEB's), would be located between microelements bearing heat-sensitive and heat-generating circuit' elements. The performance requirements for these devices are given by Signal Corps Technical Requirement No. SCL-7635 and are summarized in table X.

1.2 Work Division

The work was divided into the following tasks and phases:

TASK A

Phase 1. THEORETICAL ANALYSIS

Part A. Design (including thermoelectric material considerations).

(1) Optimization of design.

Part B. Materials (other than thermo-electric).

Phase 2. MATERIALS ACQUISITION

Part A. Thermoelectric materials optimized for operation at 72.5°C and 100°C.

Part B. Micromodule substrates.

Part C. Insulating and structural member (based on Task A, Phase 1B).

Part D. Silicone and epoxy resins (standard types used in micro-module program).

Part E. Materials and supplies required for processing and testing devices.

TASK B

Phase 1. EXPERIMENTAL

Part A. Construct several devices of each type (from designs of Task A, Phase 1A).

Phase 2. EVALUATIONS EQUIPMENT

Part A. Construct necessary evaluation equipment.

(1) Material meter.

(2) Device evaluator.

Phase 3. EVALUATION OF EXPERIMENTAL MODELS

Part A. Evaluate all test models in preliminary test setup to determine whether performance is as expected.

TASK C

Phase 1. PRODUCTION OF DEVICES REQUIRED FOR DELIVERY

Part A. Construct at least 35 of each type, allowing for failures and destructive testing.

(1) Make jigs and fixtures required for production.

(2) Prepare materials for assembly.

Phase 2. EVALUATION OF DEVELOPMENT MODELS

Part A. Evaluate all devices for delivery, using equipment constructed in Task B, Phase 2A(2).

Phase 3. FINAL REPORT

Part A. Prepare Final Report.

16

The program essentially conformed to the schedule shown
on the following page, except for the final production of
devices. This was delayed one month because of slow delivery
of the metallized substrates from the vendor. Further delay
was incurred because of an unusual materials problem in which
the material parameters changed nonuniformly along the length
of a Bi_2Te_3 alloy ingot. The nonuniformity of the material
over a relatively short distance was not evident from
materials evaluations and this fact prompted additional
materials evaluation in the process.

PROGRAM SCHEDULE

TASK A

PHASE 1. THEORETICAL ANALYSIS

PHASE 2. MATERIALS ACQUISITION

TASK B

PHASE 1. EXPERIMENTAL

PHASE 2. EVALUATIONS EQUIPMENT

PHASE 3. EVALUATION OF EXPERIMENTAL MODELS

TASK C

PHASE 1. PRODUCTION OF DEVICES

PHASE 2. TESTING AND EVALUATION

PHASE 3. FINAL REPORT

2 9 16 23 30 | 7 14 21 28 4 | 11 18 25 2 9 | 16 23 30 6 13 20 27 | 3 10 17 24 1 | 8 15 22 30

APRIL   MAY   JUNE   JULY   AUGUST   SEPTEMBER   OCTOBER

LETTER REPORTS DUE - 5TH

FINAL REPORT DUE

18

2. ABSTRACT

2.1 Objective

The objective of this contract was to design, fabricate, and evaluate micromodule thermoelectric cooling devices which would be suitable for direct incorporation into Army micromodules as special microelements having the purpose of protecting heat-sensitive circuit elements. These devices, called Thermoelectric Thermal Barrier Microelements (TEB's) would be located between microelement wafers supporting heat-sensitive and heat-generating circuit elements.

Selective temperature control, as a new circuit design parameter, holds the promise of increasing the reliability and performance of electronic packaging of the high density required to reduce the space and weight requirements associated with defense electronic systems.

2.2 Design

The design theory related to Thermoelectric Thermal Barrier (TEB) microelements is developed and all equations used in the design are derived and discussed. Design criteria are established and the anticipated performance of the designs adopted to meet type I, II, III, and IV conditions (SCL-7635) is calculated.

2.3 Fabrication

An account is given of the characteristics of the thermoelectric material used and the process steps involved in the construction of type I to IV TEB devices, including a description of the test and performance evaluation methods developed for the devices. The normal precautions to be taken in the handling and manufacture of the TEB devices are also given.

19

2.4   Results

The results of performance evaluations of the prototype devices are presented for $T_h = 125^{\circ}C$ and thermal loads of 50, 100, and 200 mw (see figure 39). These results were obtained by measuring T_c as a function of current. The test data under type I to IV conditions is presented on each of the four batches of 25 units designed to meet type I to IV conditions. One hundred operational units were supplied to USAELRDL which had been tested to meet the required specifications.

Data are presented from more complete tests on six single-junction and six double-junction devices. These include ΔT and T_c vs. I curves for various heat loads, maximum temperature difference under zero applied heat load, and temperature difference vs. heat load for various constant currents.

The results of the evaluations are discussed in relation to the design theory. An effective device figure of merit of $2.5 \times 10^{-3} \left(^{\circ}K\right)^{-1}$ without encapsulation is deduced from the experimental results at the specified type I to IV operating points. The difference between this and a measured materials figure of merit of $2.8 \times 10^{-3} \left(^{\circ}K\right)^{-1}$ is shown to be attributable to the independently calculated values of radiation exchange between T_h and T_c and of contact resistance. A device figure of merit of $Z'' = 2.1 \times 10^{-3} \left(^{\circ}K\right)^{-1}$ was calculated when the magnitude of thermal conduction through the glass encapsulation was taken into account. This theoretical value agreed well with that deduced from the experimental results.

2.5   Conclusions

Several conclusions were drawn from a consideration of the design, fabrication, and device evaluation part of this work.

The principal conclusion is that the devices designed and constructed easily meet the required specifications of USAELRDL Technical Requirement No. SCL-7635. The excess heat-pumping capacity built into these devices will enable them to meet higher thermal loads, under type I to IV temperature-difference conditions, than specified in SCL-7635.

2.6 Recommendations

Although the devices developed in the present contract easily meet the specified type I - IV operational requirements, several worthwhile improvements can be made. These are:

a. Improvements of the present device configurations.

b. Improvement in the configurational design which is possible with improved materials fabrication and p - n junction contacting technology.

c. Additional cooling concepts.

3.   PUBLICATIONS, LECTURES, REPORTS, AND CONFERENCES

3.1 Publications

None.

3.2 Lectures

None.

3.3 Reports

Five Monthly Letter Reports were prepared as a part of this program. These were as follows:

a. First Monthly Letter Report, by N. Fuschillo, dated 2 May 1962, for the period 1 April through 30 April 1962.

b. Second Monthly Letter Report, by N. Fuschillo, dated 1 June 1962, for the period 1 May through 31 May 1962.

c. Third Monthly Letter Report, by N. Fuschillo, dated 2 July 1962, for the period 1 June through 30 June 1962.

d. Fourth Monthly Letter Report, by N. Fuschillo, dated 2 August 1962, for the period 1 July through 31 July 1962.

e. Fifth Monthly Letter Report, by N. Fuschillo, dated 31 August 1962, for the period 1 August through 31 August 1962.

3.4 Conferences

Four conferences between Signal Corps and Melpar personnel were held to discuss the progress of work during the period 1 April to 30 September 1962. Two meetings were held at USAELRDL and two were held at Melpar at approximately equally spaced intervals.

The authors acknowledge the cooperation and valuable guidance contributed to this program by Dr. H. J. Dagenhart and Mr. H. C. Frankel of USAERDL.

4. FACTUAL DATA

4.1 Introduction

This part of the report contains a discussion of the design, fabrication, and evaluation of Thermoelectric Thermal Barrier (TEB) microelement heat pumps. Early in the discussion, all of the relevant equations used in thermoelectric refrigerators are derived and discussed (subparagraph 4.2). This general treatment of thermoelectric cooling device theory is then applied to design of TEB microelement heat pumps (subparagraph 4.3).

Subparagraph (4.4), Fabrication, contains a detailed description of all process steps as well as related information. The testing and evaluation of the thermoelectric material and the completed devices are considered part of the TEB process and are described in paragraph 4.

The results of the device evaluations for type I, II, III, and IV devices (see table X), together with a discussion of the results, are given in subparagraph 4.5.

4.2 Theory

A theoretical analysis of thermoelectric heat-pumping systems is presented below. The final result is presented in tables I-III, which contain the equations used in thermoelectric design. These tables have been useful in the design of thermoelectric systems. Refer to Glossary of Symbols for terminology and meaning of symbols used in the following derivations.

4.2.1 Derivation of Standard Equations

4.2.1.1 General Case Theory: The heat which a thermo-electric cooler can pump from the cold junction is given by[1]*.

$$\dot{Q} = \overline{S}T_c I - 1/2\, I^2 r - K\Delta T. \tag{1}$$

where $\dot{Q}$ = heat pumped from cold junction.

$\overline{S}T_c I$ = Peltier heat pumped from the cold junction.

$1/2\, I^2 r$ = Fraction of Joule heat conducted to the cold junction.

$K\Delta T$ = Heat delivered to the cold junction by thermal conduction.

$\overline{S} = S_n - S_p$ = The combined Seebeck coefficients of the n-type and p-type legs averaged over the temperature range used.

$r = \dfrac{\rho_n L_n}{A_n} + \dfrac{\rho_p L_p}{A_p}$ = Electrical resistance of the thermoelectric couple.

ρ_n = Resistivity of the n-type leg averaged over the temperature range used.

ρ_p = Resistivity of the p-type leg averaged over the temperature range used.

L = The length of a thermoelectric element.

A = The cross-sectional area of a thermoelectric element.

$K. = \dfrac{k_n A_n}{L_n} + \dfrac{k_p A_p}{L_p}$ = Thermal conductance of the thermo-electric couple.

k_n = Thermal conductivity of the n-type leg averaged over the temperature range used.

k_p = Thermal conductivity of the p-type leg averaged over the temperature range used.

---

*The numbers in the square brackets indicate the reference from which the equations were taken. The references are listed at the end of this report.

$\Delta T = T_h - T_c$ = Temperature difference across the thermoelectric couple.

T_h = Temperature of the hot junction.

T_c = Temperature of the cold junction.

I = The current flowing through the thermoelectric couple.

The voltage across the thermoelectric couple is given by[2].

$$V = \bar{S}\Delta T + Ir. \tag{2}$$

V = Voltage applied to couple.

$\bar{S}\Delta T$ = Seebeck voltage due to temperature difference being maintained across the thermocouple.

Ir = Voltage drop due to a current flow through the thermoelectric couple.

The power necessary for the thermoelectric couple is given by[3].

$$P_o = VI = \bar{S}\Delta TI + I^2 r. \tag{3}$$

The normal criterion used to characterize a thermoelectric cooler is the Coefficient of Performance (C.O.P.). The C.O.P. of the cooler is given by[4] and [11].

$$C.O.P. = \frac{\dot{Q}}{P_o}$$

$$C.O.P. = \frac{\bar{S}T_c I - 1/2\, I^2 r - K\Delta T}{\bar{S}\Delta T\, I + I^2 r} \tag{4}$$

25

The normal criterion used to characterize a thermoelectric material is the thermoelectric figure of merit (Z). The Z of a thermoelectric couple is given by[5].

$$Z = \frac{\overline{S}^2}{rK} = \frac{(S_n - S_p)^2}{\left[\rho_n \frac{L_n}{A_n} + \rho_p \frac{L_p}{A_p}\right]\left[k_n \frac{A_n}{L_n} + k_p \frac{A_p}{L_p}\right]} \tag{5}$$

It will be shown later that the efficiency of a thermo-electric system will be maximized when Z is maximized geometrically. To maximize Z geometrically, the product, rK, could be minimized with respect to the ratio of the cross-sectional areas of the n-type and the p-type legs.

$$\frac{\partial}{\partial(A_n/A_p)}(rK) = 0.$$

Solving this equation and equating $L = L_n = L_p$ results in

$$\left[\frac{A_n}{A_p}\right]^2 = \frac{\rho_n}{k_n} \cdot \frac{k_p}{\rho_p} \tag{6}$$

or[6]

$$Kr_{(minimum)} = \left[\sqrt{k_n\rho_n} + \sqrt{k_p\rho_p}\right]^2.$$

The geometrically optimized figure of merit (Z_o) is given by[7]

$$Z_o = \frac{(S_n - S_p)^2}{\left[\sqrt{k_n\rho_n} + \sqrt{k_p\rho_p}\right]^2}. \tag{7}$$

Another common criterion used to characterize the thermo-electric cooler is the maximum temperature difference that can be maintained across it. By rearranging equation (1), we have[8]

$$\Delta T = \frac{\overline{S}\, T_c I - 1/2\, I^2 r - \dot{Q}}{K} \, .$$

(8)

It follows from equation (8) that, all other conditions remaining constant, ΔT will be increased as

$$\dot{Q} \longrightarrow 0$$

and will be maximum when $\dot{Q} = 0$.

This, then, allows equation (8) to become

$$\Delta T \left(\dot{Q} = 0 \right) = \frac{\overline{S}\, T_c I - 1/2\, I^2 r}{K} \, .$$

(9)

To maximize ΔT, we must let[9]

$$\frac{\partial (\Delta T)}{\partial I} = 0$$

$$0 = \overline{S}\, T_c - Ir$$

$$I_{max} = \frac{\overline{S}\, T_c}{r}$$

where I_{max} is the current which will produce the maximum temperature difference.

Substituting this value of I_{max} back into equation (9) results in[10]

$$\Delta T_{(max)} = \frac{\overline{S}^2 T_c^{\,2}}{2rK} = \frac{Z T_c^{\,2}}{2} \, .$$

(10)

From equation (10), it can be seen that from the measurements of two temperatures under the condition that they represent the maximum temperature difference maintainable by a thermoelectric couple, the effective figure of merit of the material in the couple can be determined directly.

So far, the discussion has been restricted to design criterions for ideal couples, i.e., ones which do not have contact resistances or thermal losses associated with them. The problem of contact resistance has hindered the development of very small thermoelectric couples. Figure 1 shows the effect of contact resistances with respect to element length for arbitrary values of electrical resistivity and contact resistivity of 10^{-3} ohm-cm and 10^{-5} ohm-cm^2, respectively. Although these values are arbitrary, they represent the mean value of $\bar{\rho}$ and ρ_c attainable under the present state of the art in thermoelectric fabrication. It is clear, then, that for any comprehensive analysis of microthermoelectric systems, modification must be made in the basic theory to account for the losses attributable to contact resistance.

The total resistance of a two-leg thermoelectric couple, r', can be defined by

$$r' = r + r_c$$

where r_c is the contact resistance.

$$r' = \frac{\rho_n L_n}{A_n} + \frac{\rho_p L_p}{A_p} + \frac{2\rho_c}{A_n} + \frac{2\rho_c}{A_p} \tag{11}$$

$$r' = r + \frac{2\rho_c}{A_n} + \frac{2\rho_c}{A_p}$$

$$L = \frac{2P_c}{\rho}\left[\frac{1}{r'r - 1}\right]$$

SEE REFERENCE [36]

LENGTH OF ELEMENT (CM)

10^{+0}

10^{-1}

10^{-2}

RATIO OF $r'r$

1.0   1.2   1.4   1.6   1.8   2.0   2.2   2.4
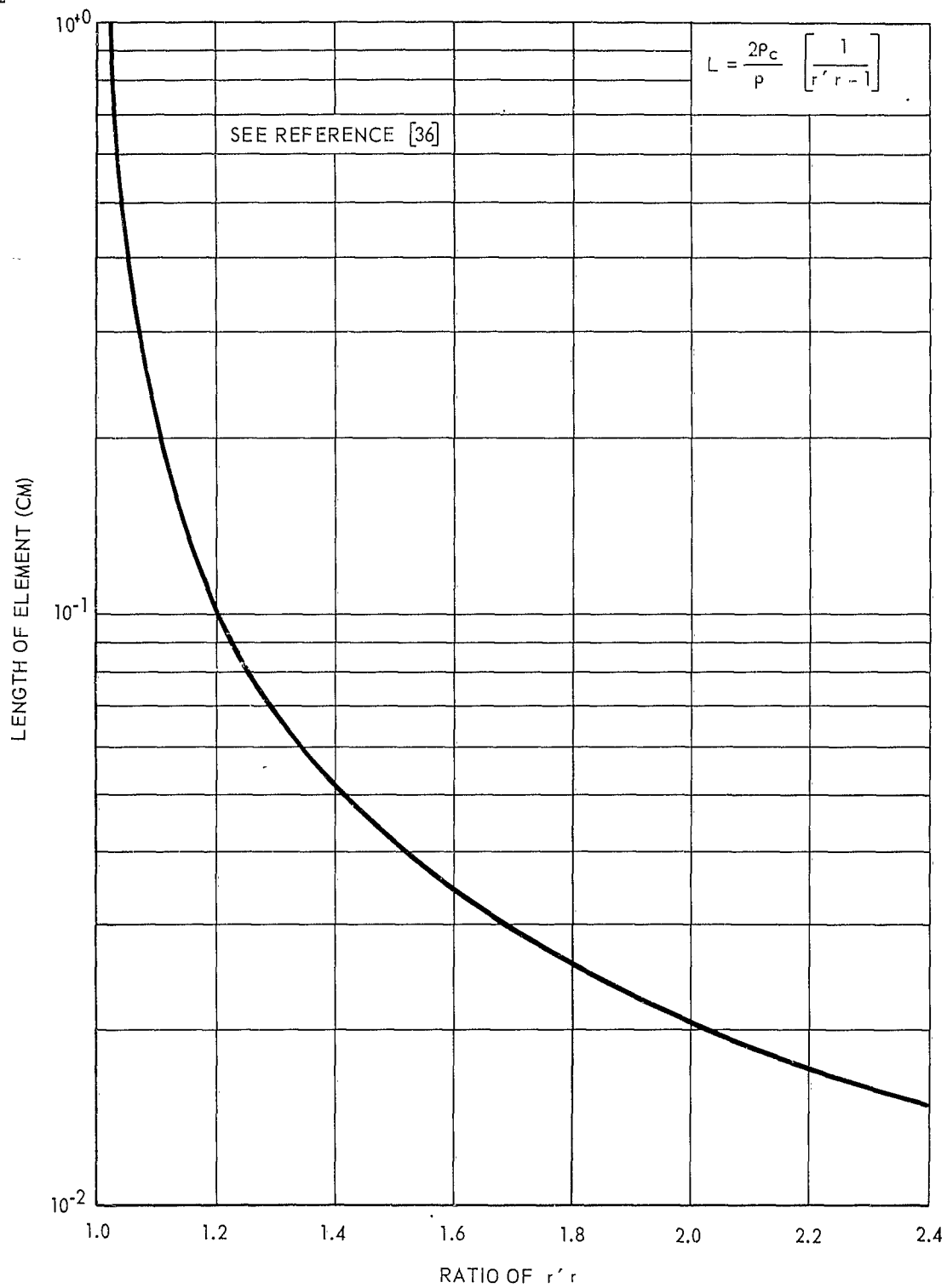
Figure 1.   Length of Elements Necessary To Obtain Specific Ratio of r'/r

29

where ρ_c = value of contact resistivity and for most cases, where $A_n = A_p = A$

$$r' = r + \frac{4\rho_c}{A} . \tag{12}$$

A new figure of merit can be defined to take into account the contact resistance

$$Z' = \frac{(S_n - S_p)^2}{r'K} .$$

If $\rho_n = \rho_p = \bar{\rho}$ and $L_n = L_p = L$, then Z' can be written as

$$Z' = \frac{Z}{1 + \dfrac{r_c}{r}} = \frac{Z}{1 + \dfrac{2\rho_c}{\bar{\rho} L}} \tag{13}$$

The total thermal conductance of a thermoelectric couple, K', can be defined by

$$K' = K + K_{(insulation)} + K_r \tag{14}$$

$$\text{where } K = K_{(lattice)} + K_{(electron)} \tag{15}$$

A new figure of merit is defined to take into account both contact resistance and thermal conductivity.

$$Z'' = \frac{(S_n - S_p)^2}{r'K'} \tag{16}$$

$$Z'' = \frac{Z}{\left(1 + \dfrac{r_c}{r}\right)\left(1 + \dfrac{K_r + K_{(insulation)}}{K}\right)} \tag{17}$$

It should be noted here that in all the equations given throughout the remainder of the design theory, r' can be used instead of r, K' can be used instead of K, and Z' and Z" are interchangeable with Z or Z_o.

4.2.1.2   Case of Maximum Coefficient of Performance: Equation (4) gave the definition of the coefficient of performance of a thermoelectric cooler as [11]

$$C.O.P. = \frac{\overline{S}T_c I - 1/2\ I^2 r - K\Delta T}{\overline{S}\Delta T\ I + I^2 r} \qquad (4)$$

$$\text{Let } m = \frac{Ir}{\overline{S}} \qquad (18)$$

and substitute into equation (4). The C.O.P. can then be written as [12]

$$C.O.P. = \frac{mT_c - 1/2\ m^2 - \dfrac{Kr\Delta T}{\overline{S}^2}}{m\Delta T + m^2} \qquad (19)$$

Equation (19) shows that the C.O.P. can be optimized by adjusting m, which is a function of I from equation (18), and by adjusting the product, Kr. Because C.O.P. is positive, it is maximized by minimizing the product, Kr. Assume that the length of the p-type leg is the same as that of the n-type leg ($L_n = L_p = L$). Then, to minimize the product, Kr, let

$$\frac{\partial}{\partial (A_n/A_p)}\ (Kr) = 0$$

The area ratio under this condition is given by equation (6).

31

This results in

$$r_o = \frac{L}{A_p} \left[\frac{\rho_n}{\left(\frac{\rho_n k_p}{\rho_p k_n}\right)^{1/2}} + \rho_p \right]$$

(20)

and

$$K_o = \frac{A_p}{L} \left[k_n \left(\frac{\rho_n k_p}{\rho_p k_n}\right)^{1/2} + k_p \right]$$

(21)

where r_o and K_o are the values of resistance and thermal conductance geometrically optimized for maximum C.O.P. Putting these values of r_o and K_o into equation (5) results in the geometrically optimized thermoelectric figure of merit as given by equation (7) on page 26 of this report.

Putting these values of r_o and K_o into equation (4) results in

$$C.O.P. = \frac{\overline{S} T_c I - 1/2\ I^2 r_o - K_o \Delta T}{\overline{S} \Delta T\ I + I^2 r_o}$$

(22)

To optimize C.O.P. with respect to the current, let

$$\frac{\partial (C.O.P.)}{\partial I} = 0.$$

32

Solving this gives[14]

$$I = \frac{\bar{S} \Delta T}{r_o (M - 1)} \qquad (23)$$

where
$$M = \sqrt{1 + Z\bar{T}} \qquad (24)$$

and
$$\bar{T} = 1/2 \, (T_h + T_c). \qquad (25)$$

Putting this value of I back into equation (22) gives[15]

$$C.O.P._{(max)} = \frac{T_c}{\Delta T} \cdot \left[\frac{M - \dfrac{T_h}{T_c}}{M + 1} \right]. \qquad (26)$$

Equation (26) shows that the $C.O.P._{(max)}$ is made up of two components: $\dfrac{T_c}{\Delta T}$, which is the C.O.P. of a Carnot refrigerator, and $\left(\dfrac{M - T_h/T_c}{M + 1} \right)$, which can be thought of as representing the degree to which the thermoelectric couple approaches an ideal Carnot refrigerator.

To obtain the amount of heat pumped under the condition of maximum Coefficient of Performance, the value of I from equation (23) is substituted back into equation (1). This results in

$$\dot{Q}\left(C.O.P._{(max)} \right) = \frac{\bar{S}^2 \Delta T}{r_o} \left[\frac{T_c}{M-1} - \frac{\Delta T}{2(M - 1)^2} - \frac{1}{Z_o} \right]. \qquad (27)$$

This same value of current substituted into equations (2) and (3) gives for the voltage[16] and power input[17] for $C.O.P._{(max)}$

$$^V\left(C.O.P._{(max)}\right) = \frac{\overline{S}\,\Delta TM}{M-1}. \tag{28}$$

$$^P\left(C.O.P._{(max)}\right) = \left(\frac{S\Delta T}{M-1}\right)^2 . \frac{M}{r_o} \tag{29}$$

4.2.1.3 Case of Maximum Heat-Pumping Rate: Equation (1) gives the equation for the amount of heat pumped by a thermo-electric couple as[1]

$$\dot{Q} = \overline{S}T_c I - 1/2\ I^2 r - K\Delta T. \tag{1}$$

To maximize $\dot{Q}$ with respect to current, let

$$\frac{\partial \dot{Q}}{\partial I} = 0.$$

This results in a value of current such that[18]

$$^I\left(\dot{Q}_{(max)}\right) = \frac{\overline{S}T_c}{r}. \tag{30}$$

Substituting this value of current back into equation (1) results in[19]

$$\dot{Q}_{(max)} = \frac{\overline{S}^2 T_c{}^2}{2r} - K\Delta T. \tag{31}$$

The geometrical optimization will be given now. As before, let $L_n = L_p = L$. The usual objective in designing for maximum heat-pumping rate is to obtain a given capacity with a minimum size or minimum weight, or to minimize the amount of thermo-electric material required. These objectives require that the total cross-sectional area, $A_T = A_n + A_p$, be as small as possible.

Therefore, the term which should be maximized is $\dfrac{\dot{Q}}{A_T}$. This is done by letting

$$\frac{\partial}{\partial (A_p)} \left(\frac{\dot{Q}}{A_T} \right) = 0.$$

The result is given by [20]

$$\frac{A_n}{A_p} = \frac{\rho_n B + \left\{ \left(\dfrac{\rho_n}{\rho_p} \right) \left[1 + B \left(\rho_n - \rho_p \right) \right] \right\}^{1/2}}{(1 - B\rho_p)} \qquad (32)$$

where [21]

$$B = \frac{2(k_p - k_n)\Delta T}{\overline{S}^2 T_c^2} .$$

This gives

$$r_o = \frac{L}{A_p} \left[\frac{\rho_n (1 - B\rho_p)}{\rho_n B + \left\{ \left(\dfrac{\rho_n}{\rho_p} \right) \left[1 + B \left(\rho_n - \rho_p \right) \right] \right\}^{1/2}} + \rho_p \right] \qquad (33)$$

and

$$K_o = \frac{A_p}{L} \left[k_n \frac{\rho_n B + \left\{ \left(\dfrac{\rho_n}{\rho_p} \right) \left[1 + B(\rho_n - \rho_p) \right] \right\}^{1/2}}{(1 - B\rho_p)} + k_p \right] \qquad (34)$$

where r_o and K_o are now the values of the resistance and thermal conductance of the thermoelectric couple geometrically optimized for maximum heat pumping.

The figure of merit for this case is given by

$$Z_o = \frac{(S_n - S_p)^2}{\rho_n k_n + \rho_p k_p + \rho_n k_p C + \dfrac{\rho_p k_n}{C}} \qquad (35)$$

where

$$C = \frac{1 - B\rho_p}{\rho_n B + \left\{\left(\dfrac{\rho_n}{\rho_p}\right)\left[1 + B\ (\rho_n - \rho_p)\right]\right\}^{1/2}}$$

The values substituted back into equation (31) give[22]

$$\dot{Q}_{(max)} = \frac{1}{L}\left\{\frac{\bar{S}^2 T_c^{\ 2}}{2\left(\dfrac{\rho_n}{A_n} + \dfrac{\rho_p}{A_p}\right)} - \Delta T\ (A_n k_n + A_p k_p)\right\}\ . \qquad (36)$$

The voltage for $\dot{Q}_{(max)}$ is given by[23]

$$V\left(\dot{Q}_{(max)}\right) = \bar{S}\ T_h \qquad (37)$$

and the input power is given by[24]

$$P_o\left(\dot{Q}_{(max)}\right) = \frac{\bar{S}^2 T_c T_h}{r_o}\ . \qquad (38)$$

From equations (4) and (30), the C.O.P. under the condition of maximum heat pumping rate is given by

$$C.O.P.\left(\dot{Q}_{(max)}\right) = \frac{1 - \dfrac{2\Delta T}{Z T_c^{\ 2}}}{2\ (1 + \dfrac{\Delta T}{T_c})}\ . \qquad (39)$$

4.2.1.4 <u>The Thermoelectric Refrigerator Equations in Terms</u>
<u>of $\Delta T_{(max)}$</u>: In paragraph 4.2.1.1, equation (10) defined a
quantity [10]

$$\Delta T_{(max)} = 1/2 \ zT_c^2.$$ (10)

Equation (10) states that the maximum temperature that can be
developed across a thermoelectric couple is dependent only on
the thermoelectric figure of merit and the temperature of the
cold junction of the thermocouple. It is interesting to note
that all of the equations derived previously for $\dot{Q}_{(max)}$,
$\dot{Q}\left(C.O.P._{(max)}\right)$, C.O.P._{(max)}, and C.O.P. $\left(\dot{Q}_{(max)}\right)$ can be written
to a first approximation in terms of $\Delta T_{(max)}$.

The term for $\dot{Q}_{(max)}$ as given in equation (31) becomes,
after using the substitution from equation (10), [25]

$$\dot{Q}_{(max)} = K\Delta T_{(max)} \left[1 - \frac{\Delta T}{\Delta T_{(max)}} \right].$$ (40)

Equation (39) becomes [26]

$$C.O.P.\left(\dot{Q}_{(max)}\right) = 1/2 \left(1 - \frac{\Delta T}{\Delta T_{(max)}} \right) \left(1 - \frac{\Delta T}{T_h} \right).$$ (41)

Equation (27) becomes [27]

$$\dot{Q}\left(C.O.P._{(max)}\right) \doteq K\Delta T \left(1 - \frac{\Delta T}{\Delta T_{(max)}} \right)$$ (42)

while equation (26) becomes [28]

$$C.O.P._{(max)} \doteq \frac{1 - \dfrac{\Delta T}{\Delta T_{(max)}}}{2\left(\dfrac{\Delta T}{\Delta T_{(max)}} + \dfrac{\Delta T}{T_c}\right)} \quad . \tag{43}$$

Using this notation, two more equations evolve, namely: [29,30]

$$\dot{Q}\left(C.O.P._{(max)}\right) \doteq \frac{\Delta T}{\Delta T_{(max)}} \dot{Q}_{(max)} \tag{44}$$

and

$$C.O.P.\left(\dot{Q}_{(max)}\right) \doteq \frac{\Delta T}{\Delta T_{(max)}} C.O.P._{(max)} \quad . \tag{45}$$

Comparing equations (44) and (45) leads to the following conclusion:

$$C.O.P.\left(\dot{Q}_{(max)}\right) \times \dot{Q}_{(max)} \doteq C.O.P._{(max)} \times \dot{Q}\left(C.O.P._{(max)}\right) \quad . \tag{46}$$

This is significant because it appears that the choice of operating at either maximum C.O.P. or maximum $\dot{Q}$ has no effect on the product of C.O.P. x $\dot{Q}$.

The general case equations can also be given in terms of $\Delta T_{(max)}$, and $I\left(\dot{Q}_{(max)}\right)$ where $I\left(\dot{Q}_{(max)}\right)$ = the current which gives maximum heat pumping [18]

$$I\left(\dot{Q}_{(max)}\right) = \frac{\overline{S}T_c}{r} \quad . \tag{30}$$

38

Equation (1) becomes [31]

$$\dot{Q} = K \Delta T_{(max)} \left(2i - i^2 - \frac{\Delta T}{\Delta T_{(max)}} \right) \qquad (47)$$

and equation (4) becomes [32]

$$C.O.P. = \frac{2i - i^2 - \frac{\Delta T}{\Delta T_{(max)}}}{2(i^2 + \frac{\Delta T}{T_c} i)} \qquad (48)$$

where [33]

$$i = \frac{I}{\left(\frac{I}{\dot{Q}_{(max)}} \right)} \qquad (49)$$

I = the current used for any operation.

4.2.1.5 The Concept of Effective Thermal Conductance:
Equations (1), (27), and (31) give the expressions for $\dot{Q}$,
$\dot{Q}_{C.O.P.}\big)_{(max)}$ and $\dot{Q}_{(max)}$ in terms of the basic parameters.
These equations can be rewritten in terms of an effective thermal
conductance by using the following substitution:

$$K = \frac{(S_n - S_p)^2}{Zr} . \qquad (50)$$

The advantage of using this form is that a good insight
as to what is happening physically can be seen from the equations,
and these equations lend themselves well to calculations.

Equation (1) becomes, upon using the substitution from equation (50),

$$\dot{Q} = -K\Delta T \left[1 + \frac{ZrI}{\overline{S}\Delta T}\left(\frac{Ir}{2\overline{S}} - T_c\right)\right]. \tag{51}$$

By the same substitution, equations (27) and (31) become

$$\dot{Q}\left(C.O.P._{(max)}\right) = \left\{-K\left[1 - \frac{Z}{(M-1)}\left(T_c - \frac{\Delta T}{2(M-1)}\right)\right]\right\}\Delta T \tag{52}$$

$$\dot{Q}_{(max)} = \left\{-K\left[1 - \frac{ZT_c^2}{2\Delta T}\right]\right\}\Delta T \tag{53}$$

As shown above, the resulting conductance terms in the curly brackets actually represent an effective negative thermal conductance as the thermoelectric couple pumps heat against a temperature gradient.

4.2.2 Design Equation Matrix

In the preceding subparagraphs, all of the equations necessary for thermoelectric refrigerator design were derived. The most useful of these equations are collected in tables I to III. The equations concerned were derived assuming one thermo-electric couple. The letter N was added to the equations in the tables to include those cases where more than one couple may be used. It is assumed that each of the N couples is connected electrically in series while being thermally in parallel.

Table I

EQUATIONS NECESSARY FOR THERMOELECTRIC REFRIGERATOR DESIGN

CALCULATIONS USING TABLES II AND III

$\overline{S} = S_n - S_p$ = Seebeck coefficient of couple   N = number of couples

$$r = \rho_n \frac{L_n}{A_n} + \rho_p \frac{L_p}{A_p} \qquad\qquad i = \frac{I}{I_{\left(Q_{(max)}\right)}}$$

$$r' = r + r_c$$

$$r' = r + \frac{4\rho_c}{A}$$

$$K = k_n \frac{A_n}{L_n} + k_p \frac{A_p}{L_p}$$

$$K' = K + K_{(insulation)} + K_r$$

$$Z = \frac{\overline{S}^2}{rK} = \frac{(S_n - S_p)^2}{k_n\rho_n + k_p\rho_p + k_n\rho_p \frac{A_n L_p}{L_n A_p} + k_p\rho_n \frac{L_n A_p}{A_n L_p}}$$

$$Z_o = \frac{(S_n - S_p)^2}{\left(\sqrt{k_n\rho_n} + \sqrt{k_p\rho_p}\right)^2} \cong \frac{\overline{S}^2}{\overline{\rho}\,\overline{k}}$$

$$Z' = \frac{\overline{S}^2}{r'K} \; ; \; Z' = \frac{Z}{1 + \frac{r_c}{r}} = \frac{Z}{1 + \frac{2\rho_c}{\rho L}}$$

$$Z'' = \frac{\overline{S}^2}{r'K'} = \frac{Z}{\left(1 + \frac{r_c}{r}\right)\left(1 + \frac{K_r + K_{(insulation)}}{K}\right)}$$

$M = \sqrt{1 + Z\overline{T}}$ where $Z = Z,\ Z_o,\ Z',$ or Z'' as defined above

$\overline{T} = 1/2 \left[T_h + T_c\right]$

$\Delta T_{(max)} = 1/2\ ZT_c^2$

Table II

GEOMETRICAL OPTIMIZATION OF THERMOELECTRIC COUPLE
PERFORMANCE WITH $L_n = L_p = L$

Condition / Parameter	Geometrically optimized for maximum heat pumping	Geometrically optimized for maximum coefficient of performance
Maximizing criterion	$$\frac{\partial}{\partial A_p}\left(\frac{\dot{Q}_c}{A_n + A_p}\right) = 0$$	$$\frac{\partial}{\partial(A_n/A_p)}(Kr) = 0$$
Resistance of couple, r (ohms)	$$r = \frac{L}{A_p}\left[\frac{\rho_n(1 - B\rho_p)}{\rho_n B + \left\{(\rho_n/\rho_p)\left[1 + B(\rho_n - \rho_p)\right]\right\}^{1/2} + \rho_p}\right]$$	$$r = \frac{L}{A_p}\left[\frac{\rho_n}{\left(\frac{\rho_n k_n}{\rho_p k_p}\right)^{1/2}} + \rho_p\right]$$
Thermal conductance of couple, K(Watts/°K)	$$K = \frac{A_p}{L}\left[\frac{k_n\left[\rho_n B + \left\{\left(\frac{\rho_n}{\rho_p}\right)\left[1 + B(\rho_n - \rho_p)\right]\right\}^{1/2}\right]}{(1 - B\rho_p)} + k_p\right]$$	$$K = \frac{A_p}{L}\left[k_n\left(\frac{\rho_n k_p}{\rho_p k_n}\right)^{1/2} + k_p\right]$$
Material figure of merit of couple, $z(°K)^{-1}$	$$z_o = \frac{\bar{S}^2}{\rho_n k_n + \rho_p k_p + \rho_n k_p C + \frac{\rho_p k_n}{C}}$$	$$z_o = \frac{\bar{S}^2}{\left(\sqrt{k_n \rho_n} + \sqrt{k_p \rho_p}\right)^2}$$

$$B = 2(k_p - k_n)\frac{\Delta T}{\bar{S}^2 T_c^2}$$

$$C = \frac{1 - B\rho_p}{\rho_n B + \left\{\left(\frac{\rho_n}{\rho_p}\right)\left[1 + B(\rho_n - \rho_p)\right]\right\}^{1/2}}$$

Table III

THERMOELECTRIC REFRIGERATOR DESIGN CALCULATIONS FOR SPECIFIC DESIGN CRITERION

Condition / Parameter	General Case	Maximum heat pumping $\frac{\partial \dot Q}{\partial I} = 0$	Maximum coefficient of performance $\frac{\partial (C.O.P.)}{\partial I} = 0$
Heat pumping rate ($\dot Q$)	$= N\left[\bar{S}T_c I - 1/2\, I^2 r - K\Delta T\right]$	$= N\left[\frac{\bar{S}^2 T_c^2}{2r} - K\Delta T\right]$	$= N\left[\frac{\bar{S}^2 \Delta T}{r}\right]\left[\frac{T_c}{(M-1)} - \frac{\Delta T}{2(M-1)^2} - \frac{1}{2}\right]$
	$= -NK\Delta T\left[1 + \frac{ZrI}{\bar{S}\Delta T}\left(\frac{Ir}{2\bar{S}} - T_c\right)\right]$	$= -NK\Delta T\left[1 - \frac{ZT_c^2}{2\Delta T}\right]$	$= -NK\Delta T\left[1 - \frac{Z}{(M-1)}\left(T_c - \frac{\Delta T}{2(M-1)}\right)\right]$
	$= NK\Delta T_{(max)}\left[2i - i^2 - \frac{\Delta T}{\Delta T_{(max)}}\right]$	$= NK\Delta T_{(max)}\left[1 - \frac{\Delta T}{\Delta T_{(max)}}\right]$	$\doteq NK\Delta T\left[1 - \frac{\Delta T}{\Delta T_{(max)}}\right]$
Coefficient of performance (C.O.P.)	$= \frac{\bar{S}T_c I - 1/2\, I^2 r - K\Delta T}{I\bar{S}\Delta T + I^2 r}$	$= \frac{\left[1 - \frac{2\Delta T}{ZT_c^2}\right]}{2\left[1 + \frac{\Delta T}{T_c}\right]}$	$= \left(\frac{T_c}{\Delta T}\right) \cdot \frac{M - T_h/T_c}{(M+1)}$
	$= \frac{2i - i^2 - \frac{\Delta T}{\Delta T_{(max)}}}{2\left(i^2 + \frac{\Delta T}{T_c} i\right)}$	$= 1/2\left[1 - \frac{\Delta T}{\Delta T_{(max)}}\right]\left[1 - \frac{\Delta T}{T_h}\right]$	$= \frac{1 - \frac{\Delta T}{\Delta T_{(max)}}}{2\left[\frac{\Delta T}{\Delta T_{(max)}} + \frac{\Delta T}{T_c}\right]}$
Current (I)	$= \frac{\bar{S}T_c}{r}\left[1 \pm \sqrt{1 - \frac{2r}{Z}\frac{\left(K\Delta T + \frac{\dot Q}{N}\right)}{(\bar{S}T_c)^2}}\right]$	$= \frac{\bar{S}T_c}{r}$	$= \frac{\bar{S}\Delta T}{r(M-1)}$
Seebeck Voltage across couple (V_o)	$= N\bar{S}\Delta T$	$= N\bar{S}\Delta T$	$= N\bar{S}\Delta T$
Voltage input to module (V)	$= N(\bar{S}\Delta T + Ir)$	$= N\bar{S}T_h$	$= \frac{N\bar{S}\Delta TM}{(M-1)}$
Power input (P_o)	$= N(I\bar{S}\Delta T + I^2 r)$	$= \frac{N\bar{S}^2 T_c T_h}{r}$	$= N\left[\frac{\bar{S}\Delta T}{(M-1)}\right]^2 \frac{M}{r}$
Maximum temperature difference ($\Delta T_{(max)}$)	$= 1/2\, ZT_c^2$	$= 1/2\, ZT_c^2$	$= 1/2\, ZT_c^2$

43

4.3 Design

4.3.1 Qualitative Design Analysis

Taking into account the special requirements of Thermo-
electric Thermal Barrier Microelements and the level of per-
formance desired, the optimum device design involves designing
for minimum current and the use of the maximum allowable element
height.

The requirements given in SCL-7635 are quite explicit in
defining the problem and the specifications which the TEB micro-
elements must meet. The requirements and specifications are
reviewed in the following subparagraphs.

4.3.1.1 <u>Thermoelectric Material</u>: The thermoelectric
material's figure of merit is required to be not less than
about $3 \times 10^{-3} \left({}^{\circ}K \right)^{-1}$. Bismuth telluride alloys are the only
materials currently available with this figure of merit.
Thermoelectric materials of this type are normally maximized
for operation at room temperature. The figure of merit for
Bi-Sb-Te-Se alloys decreases with temperature above $20^{\circ}C$. At
$125^{\circ}C$, the figure of merit for a p-type material can decrease
by as much as 30% from the value at $20^{\circ}C$, while n-type material
only suffers a decrease of the order of a few percent over the
same temperature range. Because the average operating tempera-
tures of the thermoelectric thermal barrier heat pumps are $100^{\circ}C$
and $72.5^{\circ}C$ in the two environments under consideration, it is
obviously desirable to optimize the figure of merit of the
thermoelectric material in this temperature range.

4.3.1.2 <u>Size</u>: Regarding the specification of size and
space available for TEB microelements (0.210" x 0.210" x 0.100"),
this is more than adequate. The maximum height specification

is influential in determining the maximum allowable cross-sectional area of the TEB microelement legs (because the operating current range is also specified). Using the design criterion of minimum current and recognizing the importance of minimum contact resistance fraction, it is desirable to have the maximum length for the thermoelectric elements. The maximum height of the TEB microelement assemblies should then be 0.1 of an inch.

4.3.1.3 Electric Power: A low driving current is specifically desired for the TEB microelements (less than three amperes). This can be achieved by choosing a proper geometry factor, A/L, where A = cross-sectional area of a thermoelectric junction leg and L = length of a thermoelectric junction leg. Because the area which gives the desired current range will be small and maximum length is defined by the height requirements, the feasibility of a current of less than three amperes is easily determined. It is possible for the required current to be less than one ampere.

4.3.1.4 Fabrication and Operational Stresses: The stresses encountered by TEB microelements during fabrication into micro-modules are not considered harmful to the thermoelectric portions of the TEB once it has been assembled into a unit. Small ·thermo-electric assemblies can successfully withstand the stresses associated with curing epoxy resins at 125°C. Ultrasonic cleaning techniques have been successfully used for cleaning thermoelectric devices after they had been assembled.

Regarding operational stresses, the effects of the operating temperature range, storage, and temperature cycling with accompanying thermal expansions and contractions should not cause any severe problems. Unpublished temperature-cycling experiments by one of the authors on other cooling devices have shown

excellent stability under both operating and storage conditions after several thousand hours.

4.3.1.5 <u>Design for Minimum Current</u>: In designing TEB heat pumps as specified in SCL-7635, there are three principal design modes:

a. Design for minimum current or maximum operational voltage.

b. Design for minimum element height (which affects TEB height).

c. Design for optimum compromise between minimum current and minimum element height.

The design for minimum current is best suited to the required specifications. Minimum current generally implies a high coefficient of performance and a high operational voltage (if the geometry factor is right). The maximum current specification of three amperes sets the geometry factor range because this defines the resistance. The height specification for the TEB sets the element length because it is desirable for the element resistance to be as great as possible. This is desirable for two reasons:

a. So that the contact resistance fraction can be as small as possible.

b. So that the current can be as low as possible. Knowing the approximate geometry factor and element length, the cross-sectional area is easily found.

The consideration of contact resistance is important because, if the contact resistance fraction of the total device resistance becomes appreciable, the effective Z of the device is reduced. Assuming a contact resistivity of approximately 1×10^{-5} ohm-centimeter^2 and using an area of 0.01 cm^2, this gives for one leg:

46

$$R_c = \frac{1 \times 10^{-5} \text{ ohm-cm}^2}{1 \times 10^{-2} \text{ cm}^2}$$

$$R_c' = 1 \times 10^{-3} \text{ ohm} \times 2 \text{ contacts} = 2 \times 10^{-3} \text{ ohm.}$$

The resistance of an element 0.2 cm long (0.08") is:

$$R = \frac{\rho L}{A} = \frac{1 \times 10^{-3} \text{ ohm-cm} \times 2 \times 10^{-1} \text{ cm}}{1 \times 10^{-2} \text{ cm}^2}$$

$$R = 2 \times 10^{-2} \text{ ohm}$$

and the total resistance is = 2.2×10^{-2} ohm for one leg.

This represents an appreciable resistance fraction, although the longest practical element height (greatest resistance) was used. The geometry factor is very near that which gives the optimum performance for the given element height. Figure 2 shows the effect of varying the cross-sectional area while the element height is maintained at its maximum practical value. As the area is decreased, and the current held constant, $\dot{Q}$ decreases because of increasing Joule heating in the element. When the area increases, $\dot{Q}$ decreases because of increasing thermal conductance. The effect of contact resistance on a Peltier heat pump can be seen by calculating a "device Z" or Z':

$$Z' = \frac{Z}{1 + \left(\dfrac{r_c}{r}\right)} .$$

Assuming $Z = 2.7 \times 10^{-3} \ (^{\circ}K)^{-1}$ and the above conditions,

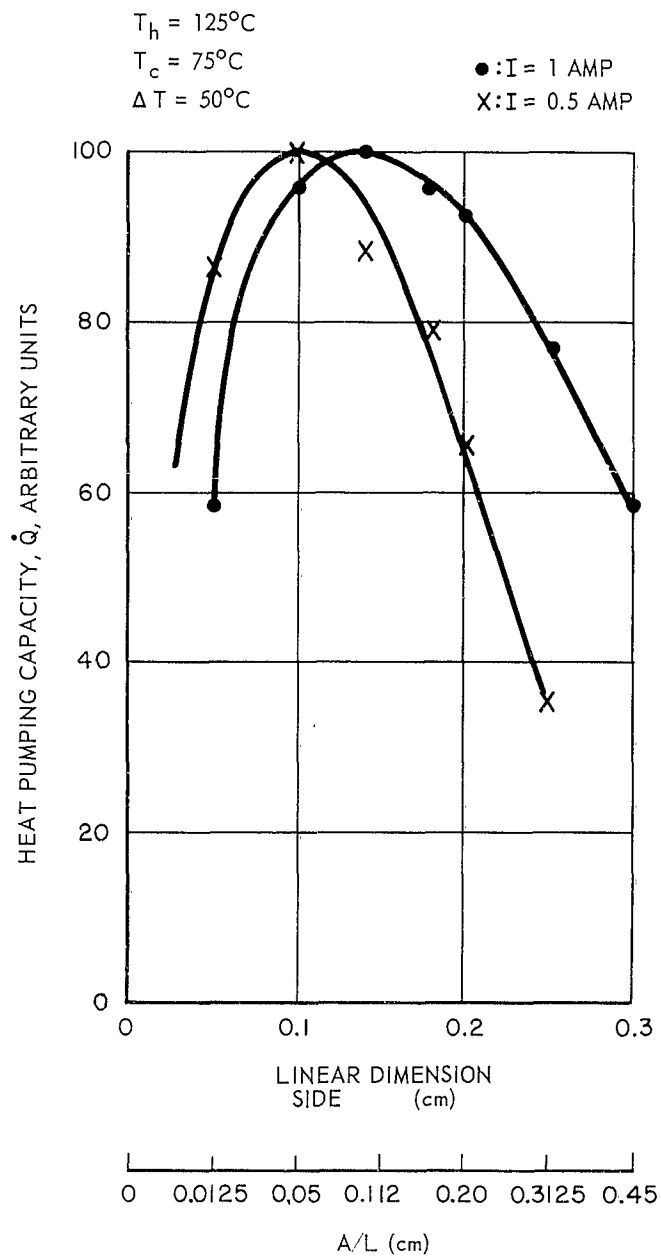$$Z' = 2.5 \times 10^{-3} (^{\circ}K)^{-1}.$$

Figure 2. Heat-Pumping Performance of Thermoelectric Cooling Device as
Function of Dimensions for Element Height of 0.2 cm (See page 56)

48

4.3.1.6 <u>Design For Minimum TEB Height</u>: From the consider-ations of contact resistance and heat pump performance vs. dimensional considerations shown in figure 2, this design mode can definitely be ruled out.

4.3.1.7 <u>Design For Optimum Compromise Between Minimum Current and Minimum Element Height</u>: This design mode suggests a compromise between minimum I and minimum height. This is ruled out on the same grounds as above because it requires further shortening of the heat pump elements which would result in even smaller effective device Z.

4.3.1.8 <u>Summary</u>: We are left with one design mode, the design for minimum current or highest operational voltage using the maximum practical element height. It is desirable to have as high a TEB voltage as possible to match more closely the power supplies commonly used in Signal Corps equipment. These considerations are discussed quantitatively in the following subparagraph.

4.3.2 <u>Design Calculations</u>

In the following design calculations we have considered the desirable thermocouple height to be limited to 0.2 cm by the maximum height of the TEB microelement specified in SCL-7635. The design problem then becomes one of reducing the area of cross section of the thermoelectric legs of the TEB to a minimum to minimize the current required to achieve type IV operating condition, which is the most demanding of the four conditions of device operation. This minimum cross-sectional area is calculated below and is impractically small from the standpoint of fabrication. Calculations are then performed for a cross-sectional area of .01 cm^2, which was considered the practical minimum because of the time scale of the contract.

All of the equations necessary to design any thermoelectric heat pump have been reviewed in subparagraph 4.2 and are summarized in tables I, II, and III. The utilization of these equations requires a precise knowledge of the n-type and the p-type material parameters. To facilitate the calculations in this subparagraph it will be assumed that the average values of the material parameters for the n-type material are the same as those for the p-type material. These average parameters are assumed to be as follows:

$$\overline{S} = \left|S_n\right| + \left|S_p\right| = 440 \frac{\text{microvolts}}{\text{deg Kelvin}}$$

$$\rho_n = \overline{\rho}_p = \overline{\rho} = 10^{-3} \text{ ohm-cm}$$

$$\rho_c = 10^{-5} \text{ ohm-cm}^2$$

$$k_n = k_p = \overline{K} = 1.76 \times 10^{-2} \frac{\text{watts}}{\text{cm-deg Kelvin}} .$$

With these average values of the material parameters, all of the device's operating parameters will be calculated.

From equation (7), the geometrical optimized figure of merit, Z_o, is given by

$$Z_o = \frac{(S_n - S_p)^2}{\left(\sqrt{\rho_n k_n} + \sqrt{\rho_p k_p}\right)^2} = \frac{\overline{S}^2}{\left(2\sqrt{\overline{\rho}\overline{K}}\right)^2}$$

$$= \frac{(440 \times 10^{-6})^2}{4(10^{-3})(1.76 \times 10^{-2})}$$

$$Z_o = 2.75 \times 10^{-3} \text{ (deg Kelvin)}^{-1}.$$

The specifications as to the dimensions of the TEB limited the height or length of the legs to 0.2 cm or less when taking into account the thickness of solder joints and ceramic and copper plates. The design calculations now proceed under the criterion of a thermoelectric leg length of 0.2 cm.

From equation (13), and assuming a length L = 0.2 cm,

$$Z' = \frac{Z_o}{1 + \frac{2\rho_c}{\bar{\rho}L}}$$

$$= \frac{2.75 \times 10^{-3}}{1 + \frac{2 \times 10^{-5}}{10^{-3} \times 2 \times 10^{-1}}}$$

$$Z' = 2.5 \times 10^{-3} \text{ (deg Kelvin)}^{-1}.$$

The operating temperatures were given for case III and case IV as

$$T_h = 398^\circ K = 125^\circ C$$

$$T_c = 348^\circ K = 75^\circ C$$

$$\Delta T = 50^\circ K.$$

From equation (25),

$$\bar{T} = \frac{1}{2} (T_h + T_c)$$

$$\bar{T} = 373^\circ K.$$

Using this value of $\bar{T}$ and the above value of Z' in equation 24.

$$M = \sqrt{1 + Z'\overline{T}}$$

$$= \left[1 + (2.5 \times 10^{-3})(3.73 \times 10^{2}) \right]^{1/2}$$

$$M = 1.39$$

4.3.2.1 <u>Calculations of Ideal Cross Section of Area and Associated Parameters of Thermoelectric Legs</u>: The first two sets of calculations were made to ascertain what areas would be associated with elements of length 0.2 cm operating either at maximum heat-pumping capacity or maximum coefficient of performance under the desired operating conditions of T_h, T_c, and $\dot{Q}$ for type IV conditions. These calculations would give the maximum voltages of operation possible under the operating conditions above with L = 0.2 cm.

For maximum heat-pumping capacity using a one-junction module, equation (53) was rearranged and solved for A where

$$A = \left(\frac{K}{k}\right)\left(\frac{L}{2}\right)$$

$$\dot{Q}_{(max)} = -\overline{k}\left(\frac{2A}{L}\right)\Delta T \left[1 - \frac{Z' T_c^{2}}{2\Delta T} \right]$$

$$50 \times 10^{-3} = -\left[\frac{(1.76 \times 10^{-2})\,2A(50)}{2 \times 10^{-1}} \right] \times$$

$$\left[1 - \frac{(2.5 \times 10^{-3})(3.48 \times 10^{2})^{2}}{2 \times 50} \right]$$

$$A = 2.8 \times 10^{-3} \, cm^{2} .$$

For a square element, the length of a side, d, is

$$d = 5.29 \times 10^{-2} \, cm.$$

For the two-junction module,

$$A = 1.4 \times 10^{-3} \, cm^{2}$$

and

$$d = 3.7 \times 10^{-2} \text{ cm.}$$

For Maximum Coefficient of Performance for a one-junction module, equation (52) was rearranged and solved for A

$$\dot{Q}_{\left(C.O.P._{max}\right)} = \frac{\bar{k} \; Z' \; 2A \; \Delta T}{L} \left[\frac{T_c}{(M-1)} - \frac{1/2 \Delta T}{(M-1)^2} - \frac{1}{Z'} \right]$$

$$50 \times 10^{-3} = \left[\frac{1.76 \times 10^{-2} \times 2.5 \times 10^{-3} \times 2A \times 50}{2 \times 10^{-1}} \right]$$

$$\times \left[\frac{348}{.39} - \frac{1/2(50)}{(.39)^2} - \frac{1}{2.5 \times 10^{-3}} \right]$$

$$A = 6.9 \times 10^{-3} \text{ cm}^2$$

$$d = 8.3 \times 10^{-2} \text{ cm.}$$

For the two-junction module,

$$A = 3.5 \times 10^{-3} \text{ cm}^2$$

$$d = 5.9 \times 10^{-2} \text{ cm.}$$

From these values of A, the resistance of the couples can be calculated, and from this, all of the other circuit parameters can be obtained. The results of these calculations are presented in tables IV and V. The calculations were also made

Table IV

CALCULATED VALUES OF AREA AND DEVICE PARAMETERS FOR OPERATION AT CONDITION OF MAXIMUM HEAT PUMPING CAPACITY $\left(\dot{Q}_{(max)}\right)$ WHEN THE LENGTH EQUALS .2 cm   ($T_h=125^{\circ}C$, $T_c=75^{\circ}C$)

	One junction (two legs)		Two junctions (four legs)	
	$\rho_c = 0$	$\rho_c=10^{-5}ohm-cm^2$	$\rho_c = 0$	$\rho_c=10^{-5}ohm-cm^2$
$\dot{Q}$ (watts)	5×10^{-2}	5×10^{-2}	5×10^{-2}	5×10^{-2}
A (cm^2)	2.4×10^{-3}	2.8×10^{-3}	1.2×10^{-3}	1.4×10^{-3}
d (cm)	.049	.053	.035	.037
r (ohm)	.16	.14	.66	.57
r' (ohm)	.16	.16	.66	.63
I (amp)	.93	.97	.47	.49
C.O.P.	.31	.29	.31	.29
V (volts)	.18	.17	.35	.35
P_o (watts)	1.6×10^{-1}	1.7×10^{-1}	1.6×10^{-1}	1.7×10^{-1}

Table V

CALCULATED VALUES OF AREA AND DEVICE PARAMETERS FOR OPERATION
AT CONDITION OF MAXIMUM COEFFICIENT OF PERFORMANCE
$(C.O.P._{(max)})$ WHEN THE LENGTH EQUALS .2 CM ($T_h=125^{\circ}C$, $T_c=75^{\circ}C$)

	One junction (two legs)		Two junctions (four legs)	
	$\rho_c = 0$	$\rho_c=10^{-5}$ohm-cm^2	$\rho_c=0$	$\rho_c=10^{-5}$ohm-cm^2
$\dot{Q}$ (watts)	5×10^{-2}	5×10^{-2}	5×10^{-2}	5×10^{-2}
A (cm^2)	6.4×10^{-3}	6.9×10^{-3}	3.2×10^{-3}	3.5×10^{-3}
d (cm)	.08	.083	.057	.059
r (ohm)	6.3×10^{-2}	5.8×10^{-2}	.25	.23
r' (ohm)	6.3×10^{-2}	6.3×10^{-2}	.25	.25
I (amp)	.84	.89	.42	.44
C.O.P.	.79	.72	.79	.72
V (volts)	.075	.079	.15	.16
P_o (watts)	6.3×10^{-2}	7.0×10^{-2}	6.3×10^{-2}	7.0×10^{-2}

for $\rho_c = 0$ to show what effect contact resistance has on the device parameters. This data is also included in the tables.

It is interesting to see how the heat-pumping capacity of the thermoelectric couple varies as the cross-sectional area of the legs is changed when their length is fixed at 0.2 cm. Equation (1) can be written in terms of the ratio of area to length by using the substitution

$$\gamma = \frac{\text{area}}{\text{length}} = \frac{A}{L} \text{ (cm)}$$

$$\dot{Q} = \overline{S} T_c I - 1/2 I^2 (2\overline{\rho}\frac{1}{\gamma}) - 2\overline{K} (\gamma) \Delta T. \tag{54}$$

Values of $\dot{Q}$ vs. γ were calculated for two values of current, I = .5 amperes and I = 1.0 amperes. The hot junction temperature and cold junction temperature were fixed at 125°C and 75°C, respectively. The values calculated were plotted in figure 2. It can be seen that the heat-pumping capacity falls off for γ's on either side of the γ which presents the maximum value of heat-pumping capacity.

The values of d which represented the optimum geometry for operating at maximum heat-pumping or maximum efficiency under the given operating conditions of T_h, T_c, and $\dot{Q}$ were so small that they could not be fabricated without considerable improvements in the present fabrication technology. Because this was not warranted by the application covered by the present contract, it was decided to make the legs with an area dimension as limited by our present fabrication technique. Thus, the value of d = 0.1 cm was used. Thus, the design criteria are determined

by dimensional limitations imposed by the contract specifications in regard to length of the elements and fabrication limitations in respect to the cross-sectional area. Therefore, the calculations for $\dot{Q}_{(max)}$, C.O.P.$_{(max)}$, and associated I, V, and P_O for a module made up of legs which were 0.2 cm x 0.1 cm x 0.1 cm in dimensions are now presented.

4.3.2.2 <u>Calculations for $\dot{Q}_{(max)}$ and C.O.P.$_{(max)}$ Using Practical Cross-sectional Area Dimensions and Associated Operating Parameters</u>: Before the system parameters were calculated, the resistance and thermal conductance of the one-junction and of the two-junction module were calculated.

For the one-junction module,

$$r = \frac{2\bar{\rho}L}{A} = \frac{2 \times 10^{-3} \times 0.2}{.01} = 4 \times 10^{-2} \text{ ohms}$$

$$r' = r + \frac{4\rho_c}{A} = 4 \times 10^{-2} + \frac{4 \times 10^{-5}}{10^{-2}} = 4.4 \times 10^{-2} \text{ ohms}$$

$$K = \bar{k}\frac{2A}{L} = 1.76 \times 10^{-2} \times \frac{2 \times 10^{-2}}{2 \times 10^{-1}} = 1.76 \times 10^{-3} \frac{\text{watts}}{\text{deg Kelvin}} \cdot$$

For the two-junction module,

$$r = \frac{4\bar{\rho}L}{A} = \frac{4 \times 10^{-3} \times 0.2}{.01} = 8 \times 10^{-2} \text{ ohms}$$

$$r' = r + \frac{8\rho_c}{A} = 8 \times 10^{-2} + \frac{8 \times 10^{-5}}{10^{-2}} = 8.8 \times 10^{-2} \text{ ohms}$$

$$K = \bar{k}\frac{4A}{L} = 1.76 \times 10^{-2} \times \frac{4 \times 10^{-2}}{2 \times 10^{-1}} = 3.52 \times 10^{-3} \frac{\text{watts}}{\text{deg Kelvin}} \cdot$$

57

As an illustration, the calculations are done here for a one-junction module considering contact resistance. Tables VI and VII give the values for one- and two-junction couples using a contact resistivity of 0 and 10^{-5} ohm $-$ cm^2.

Consider first operating under the condition of maximum heat pumping. Equation (53) gives

$$\dot{Q}_{(max)} = -K\Delta T \left[1 - \frac{Z' \, T_c^2}{2\Delta T} \right]$$

$$= -(1.76 \times 10^{-3}) \, (50) \left[1 - \frac{2.5 \times 10^{-3} \, (348)^2}{2 \times 50} \right]$$

$$\dot{Q}_{(max)} = .18 \text{ watt}$$

From equation (30)

$$I_{\left(\dot{Q}_{(max)}\right)} = \frac{\overline{S} \, T_c}{r'} = \frac{4.4 \times 10^{-4} \times 348}{4.4 \times 10^{-2}}$$

$$I_{\left(\dot{Q}_{(max)}\right)} = 3.5 \text{ amperes.}$$

From equation (39),

$$C.O.P._{(\dot{Q}_{(max)})} = \frac{1 - \dfrac{2\Delta T}{Z' \, T_c^2}}{2 \left[1 + \dfrac{\Delta T}{T_c} \right]}$$

$$= \frac{1 - \dfrac{2 \times 50}{2.5 \times 10^{-3} \, (348)^2}}{2 \left(1 + \dfrac{50}{348} \right)}$$

$$C.O.P._{(\dot{Q}_{(max)})} = .29$$

Since $C.O.P. = \dfrac{\dot{Q}}{P_o}$

Table VI

CALCULATED VALUES OF DEVICE PARAMETERS FOR OPERATION
AT CONDITION OF MAXIMUM HEAT PUMPING CAPACITY ($\dot{Q}_{(max)}$)
WHEN THE LENGTH EQUALS .2 cm AND THE CROSS SECTIONAL
AREA EQUALS .01 cm^2 (T_h=125°C, T_c=75°C)

	One junction (two legs)		Two junctions (four legs)	
	$\rho_c = 0$	$\rho_c=10^{-5}$ohm-cm^2	$\rho_c = 0$	$\rho_c=10^{-5}$ohm-cm^2
$\dot{Q}$ (watt)	.21	.18	.41	.36
I (amp)	3.8	3.5	3.8	3.5
C.O.P.	.31	.29	.31	.29
V (volt)	.18	.18	.35	.35
P_c (watt)	.67	.61	1.3	1.2

Table VII

CALCULATED VALUES OF DEVICE PARAMETERS FOR OPERATION
AT CONDITION OF MAXIMUM COEFFICIENT OF PERFORMANCE
$(C.O.P._{(max)})$ WHEN LENGTH EQUALS .2 cm AND CROSS-SECTIONAL
AREA EQUALS .01 cm^2 $(T_h = 125^{\circ}C,\ T_c = 75^{\circ}C)$

	One Junction (two legs)		Two junction (four legs)	
	$\rho_c = 0$	$\rho_c = 10^{-5}$ ohm-cm^2	$\rho_c = 0$	$\rho_c = 10^{-5}$ ohm-cm^2
$\dot{Q}$ (watt)	7.8×10^{-2}	7.2×10^{-2}	.16	.14
I (amp)	1.3	1.3	1.3	1.3
C.O.P.	.79	.72	.79	.72
V (volt)	.075	.079	.15	.16
P_c (watt)	9.9×10^{-2}	1.0×10^{-1}	2.0×10^{-1}	2.0×10^{-1}

$$P_{o(\dot{Q}_{(max)})} = \frac{\dot{Q}_{(max)}}{C.O.P._{(\dot{Q}_{(max)})}}$$

$$= \frac{.18}{.29}$$

$$P_{o(\dot{Q}_{(max)})} = .61 \text{ watt.}$$

Consider now maximum C.O.P. On rearranging equation (52),

$$\dot{Q}_{(C.O.P._{(max)})} = Z'K \Delta T \left[\frac{T_c}{M-1} - 1/2 \frac{\Delta T}{(M-1)^2} - \frac{1}{Z'} \right]$$

$$= \left[(2.5 \times 10^{-3}) \ (1.76 \times 10^{-3}) \ (50) \right]$$

$$x \left[\frac{348}{.39} - \frac{1}{2} \frac{50}{(.39)^2} - \frac{1}{2.5 \times 10^{-3}} \right]$$

$$\dot{Q}_{(C.O.P._{(max)})} = .072 \text{ watt.}$$

Using equation (23),

$$I_{(C.O.P._{(max)})} = \frac{\overline{S} \Delta T}{r'(M-1)}$$

$$= \frac{4.4 \times 10^{-4} \times 50}{4.4 \times 10^{-2} (.39)}$$

$$I_{(C.O.P._{(max)})} = 1.3 \text{ amperes.}$$

Using equation (26),

$$C.O.P._{(max)} = \frac{T_c}{\Delta T} \left[\frac{M - T_h/T_c}{M + 1} \right]$$

$$= \frac{348}{50} \left[\frac{1.39 - \frac{398}{348}}{2.39} \right]$$

$$C.O.P._{(max)} = .72$$

Again

$$P_o(C.O.P._{(max)}) = \frac{\dot{Q}_{\left(C.O.P._{(max)}\right)}}{C.O.P._{(max)}}$$

$$= \frac{.072}{.72}$$

$$P_o(C.O.P._{(max)}) = .10 \text{ watt.}$$

Tables VI and VII summarize these results.

4.3.2.3 Calculation of $\dot{Q}$, C.O.P., P_o and V as Function of Current for Practical Dimensions: The next calculations were made to find the variation of $\dot{Q}$, C.O.P., P_o, and V with current I under type IV operating conditions using the dimensions in the previous calculations. The equations of these parameters as a function of current are:

$$\dot{Q} = \overline{S}T_c I - 1/2 \ I^2 r' - K\Delta T \tag{1}$$

$$C.O.P. = \frac{\overline{S}T_c I - 1/2 \ I^2 r' - K\Delta T}{\overline{S}\Delta T I + I^2 r'} \tag{4}$$

$$P_o = \overline{S}\Delta TI + I^2 r' \tag{3}$$

$$V = \overline{S}\Delta T + Ir'. \tag{2}$$

These were calculated for values of current from 1 to 6 amperes. Tables VIII and IX summarize these results. Figures 3 and 4 show curves of the basic parameters as a function of current.

4.3.2.4 <u>Estimated Performance of Couples Under Types I to IV Operating Conditions</u>: We now calculate the device performances under types I to IV operating conditions as set forth in SCL-7635. These conditions are summarized in table X.

Using equation (1) for type I, we have:

$$\overset{\circ}{Q} = \overline{S}T_c I - 1/2\ I^2 r' - K\Delta T$$

$$5 \times 10^{-3} = (4.4 \times 10^{-4})(333)I - 1/2\ I^2(4.4 \times 10^{-2}) - 1.76 \times 10^{-3}(25)$$

$$I = .35\ ampere.$$

Using equation (2),

$$V = \overline{S}\Delta T + Ir'$$

$$= (4.4 \times 10^{-4})\ (25) + (.35)\ (4.4 \times 10^{-2})$$

$$V = 27.\ mv.$$

Because power is equal to the product of voltage and current,

$$P_o = IV$$

$$= (.35)\ (27)$$

$$= 9.4\ mw$$

Table VIII

CALCULATED VALUES OF CIRCUIT PARAMETERS

AS FUNCTION OF CURRENT FOR N JUNCTIONS

$(T_h = 125°C, \; T_c = 75°C, \; L = .2 \; cm, \; A = .01 \; cm^2)$

	I = 1 amp		I = 2 amp		I = 3 amp		I = 4 amp		I = 5 amp		I = 6 amp	
	$\rho_c=0$	$\rho_c=10^{-5}$	$\rho_c=0$	$\rho_c=10^{-5}$	$\rho_c=0$	$\rho_c=10^{-5}$	$\rho_c=0$	$\rho_c=10^{-5}$	$\rho_c=0$	$\rho_c=10^{-5}$	$\rho_c=0$	$\rho_c=10^{-5}$
$\dot{Q}$/N (Watts)	.045	.043	.14	.13	.19	.17	.20	.17	.18	.13	.11	.039
V/N (Volts)	.062	.066	.10	.11	.14	.15	.18	.20	.22	.24	.26	.29
P_o/N (Watts)	.062	.066	.20	.22	.43	.46	.73	.79	1.1	1.2	1.6	1.7
C.O.P.	.73	.65	.68	.59	.45	.37	.28	.22	.16	.11	.070	.023

$(\rho_c$ is given in ohm-cm^2.)

Table IX

CALCULATED VALUES OF CIRCUIT PARAMETERS

AS FUNCTION OF CURRENT FOR N=2 JUNCTIONS

$(T_h = 125^{\circ}C, \; T_c = 75^{\circ}C, \; L = .2 \text{ cm}, \; A = .01 \text{ cm}^2)$

	I = 1 amp		I = 2 amp		I = 3 amp		I = 4 amp		I = 5 amp		I = 6 amp	
	$\rho_c=0$	$\rho_c=10^{-5}$	$\rho_c=0$	$\rho_c=10^{-5}$	$\rho_c=0$	$\rho_c=10^{-5}$	$\rho_c=0$	$\rho_c=10^{-5}$	$\rho_c=0$	$\rho_c=10^{-5}$	$\rho_c=0$	$\rho_c=10^{-5}$
$\dot{Q}$ (watts)	.090	.086	.28	.26	.38	.35	.41	.35	.36	.26	.22	.070
V (volts)	.12	.13	.20	.22	.28	.31	.36	.40	.44	.48	.52	.57
P₀ (watts)	.12	.13	.41	.44	.85	.93	1.5	1.6	2.2	2.4	3.1	3.4
C.O.P.	.73	.65	.68	.59	.45	.38	.28	.22	.16	.11	.070	.023

ρ_c is given in ohm-cm^2.)

65

Figure 3.   Heat-Pumping Capacity, Coefficient of Performance, and Power
            Input for N Thermoelectric Couples as Function of Current
            Where N Is Number of Couples. $\left[T_h = 125\,°C,\ T_c = 75\,°C,\right.$
            $\left. L = .2\ cm,\ A = .01\ cm^2\right]$

66.
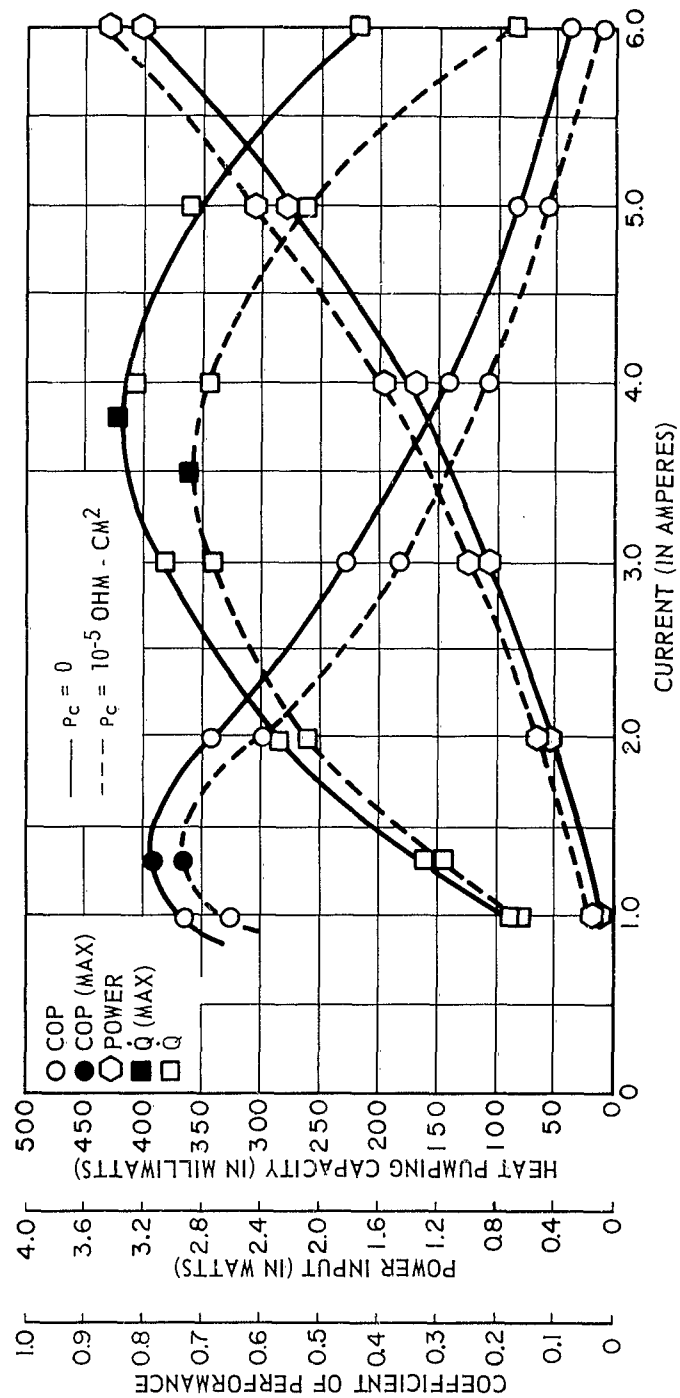
Figure 4. Heat-Pumping Capacity, Coefficient of Performance, and Power Input
For Two (N=2) Thermoelectric Couples as Function of Current
$\left[T_h = 125\,°C,\ T_c = 75\,°C,\ L = .2\ cm,\ A = .01\ cm^2 \right]$

67

Table X

PERFORMANCE REQUIREMENTS FOR THERMOELECTRIC THERMAL –
BARRIER MICROELEMENTS
(SCL- 7635)

Type Unit	T_h	T_c	$\overset{\circ}{Q}$	I
I	$85^{\circ}C$	$60^{\circ}C$ max	5 mw	< 3 amps
II	$85^{\circ}C$	$60^{\circ}C$ max	50 mw	< 3 amps
III	$125^{\circ}C$	$75^{\circ}C$ max	10 mw	< 3 amps
IV	$125^{\circ}C$	$75^{\circ}C$ max	50 mw	< 3 amps

$$\text{C.O.P.} = \frac{\overset{\circ}{Q}}{P_O}$$

$$= \frac{5 \text{ mw}}{9.4 \text{ mw}}$$

$$\text{C.O.P.} = .53$$

Table XI summarizes these results for type I conditions, together with those for types II, III, and IV. It should be noted that the TEB elements for achieving type I and II conditions consist of one couple, while those for achieving type III and IV contain two couples.

Comparison of the theoretical results of table XI for type IV TEB requirements and table IX and figure 3 clearly indicates that a device based on the dimensions used in the calculations would have $\overset{\circ}{Q}_{(max)}$ values in excess of those required to meet the performance requirements (table X) on $\overset{\circ}{Q}$ for currents under three amperes. This observation also applies to the less-demanding types I, II, and III TEB requirements. Thus the thermoelectric leg dimensions used in the calculations (0.2 cm x 0.1 cm x 0.1 cm) were employed in the construction of the devices.

4.3.3 Configurational Design

The mechanical configurations of the TEB devices are naturally based upon a standard micromodule substrate. The substrate is metallized in the center to the maximum allowable dimensions of 0.210" x 0.210". This is to help the heat transfer through the ceramic from the thermoelectric hot junction. The same area is allowed at the cold junction to permit adequate space for the mounting of the heat-sensitive components. A thin glass shell is placed around the periphery of the active area to reduce convection, to strengthen the assembly, and to keep out the plastic resins used in potting the micromodule stacks.

Table XI

CALCULATED VALUES OF MODULE PARAMETERS USING
REQUIREMENTS GIVEN IN TABLE X

Type	$\dot{Q}$	I	C.O.P.	P_o	V
I	5 mw	.35 amp	.53	9.4 mw	27. mv
II	50 mw	.72 amp	1.6	31. mw	43. mv
III	10 mw	.67 amp	.15	68. mw	101. mv
IV	50 mw	.84 amp	.51	99. mw	118. mv

Figures 5 and 6 show the basic TEB one-junction (type I and II conditions) and two-junction (type III and IV) designs resulting from the design analyses. Photographs of the devices are shown in figures 7 and 8. The dimensional and structural details for these devices are given in subparagraph 4.4.

The thermoelectric leg dimensions used in the construction of these devices were those used in the previous calculations in subparagraphs 4.3.2.2 through 4.3.2.4.
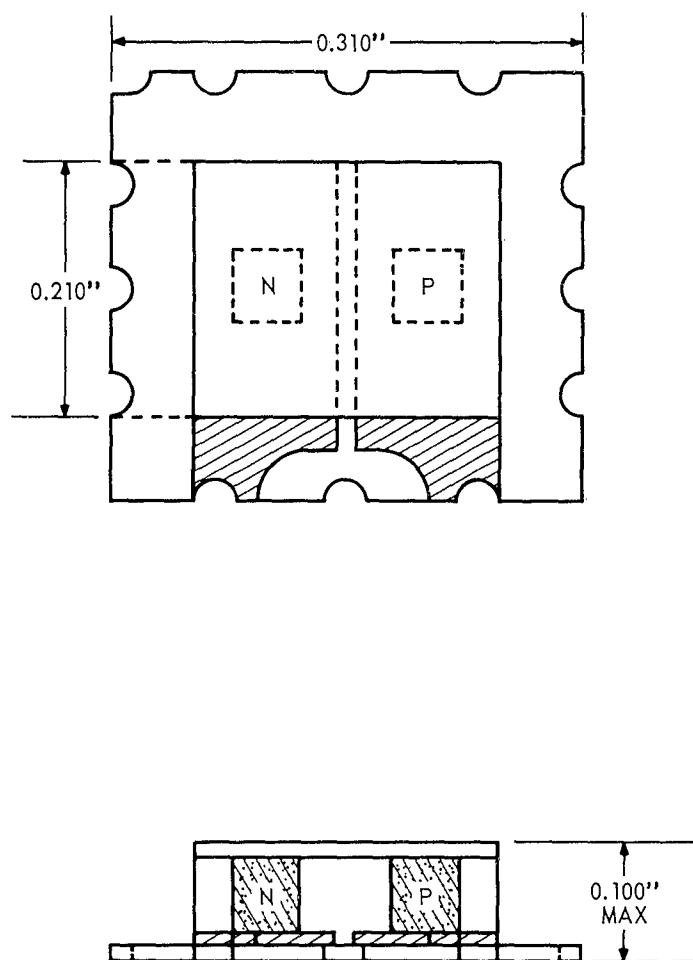
Figure 5.   One-Junction TEB, Type I or II
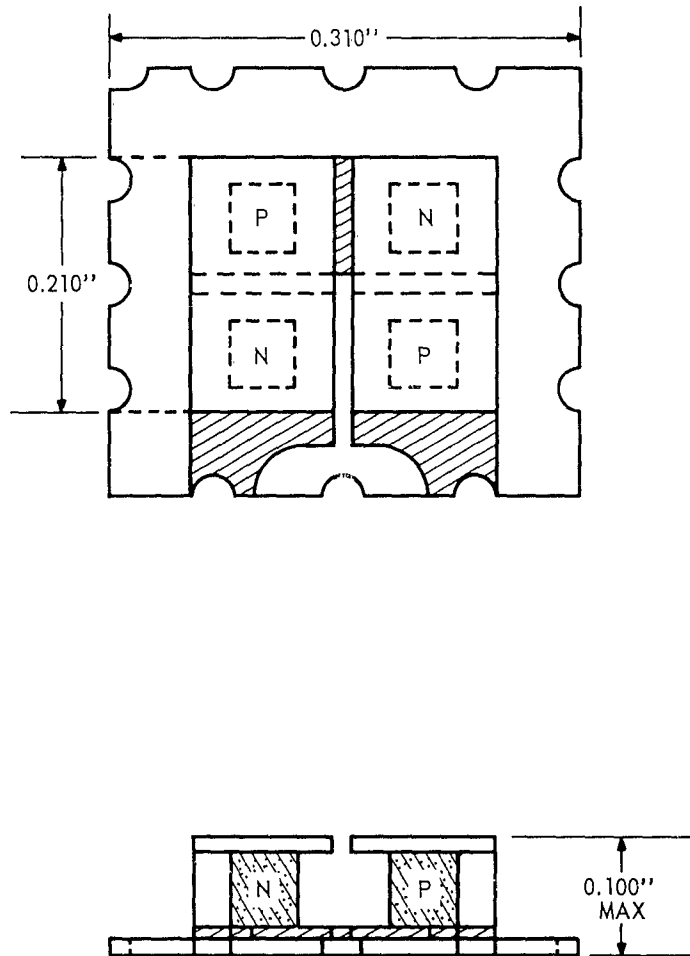
Figure 6. Two-Junction TEB, Type III or IV
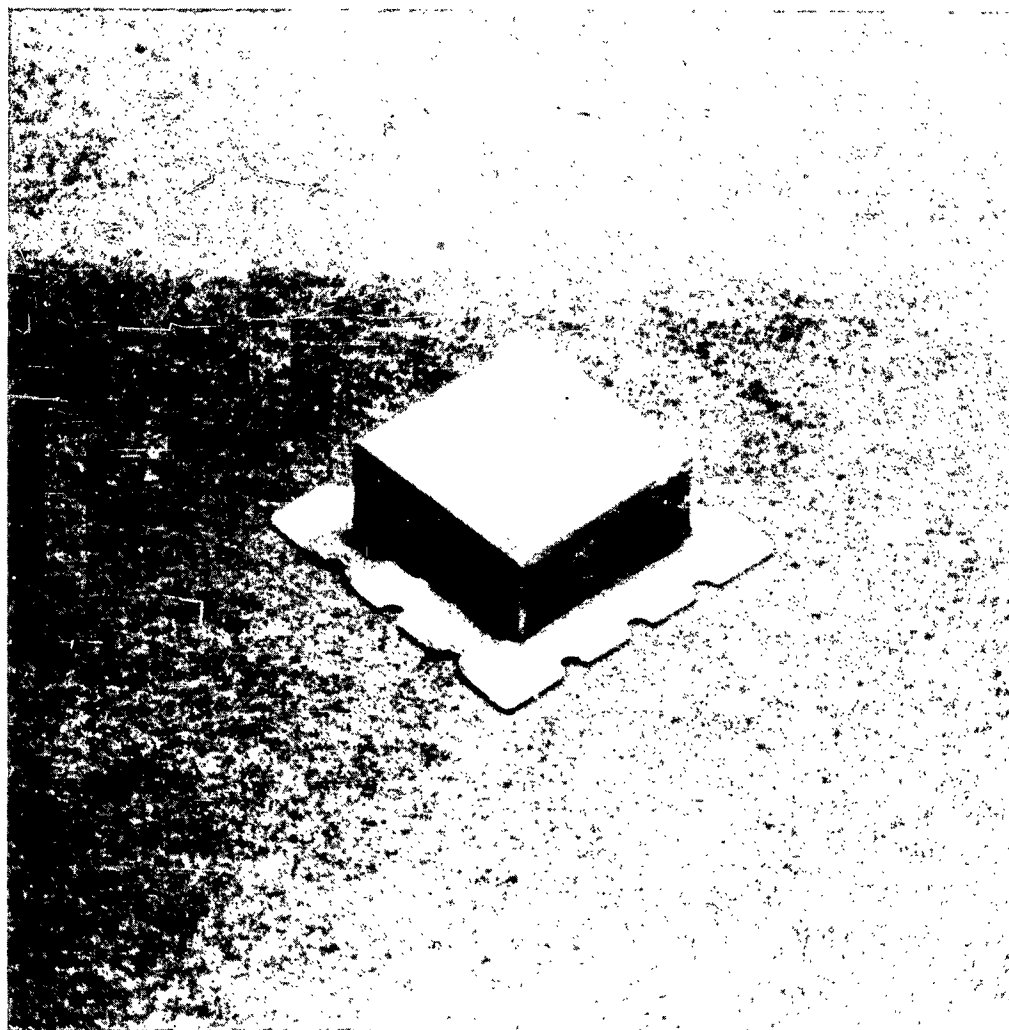
Figure 7.   Finished Single-Junction TEB, Type I or II
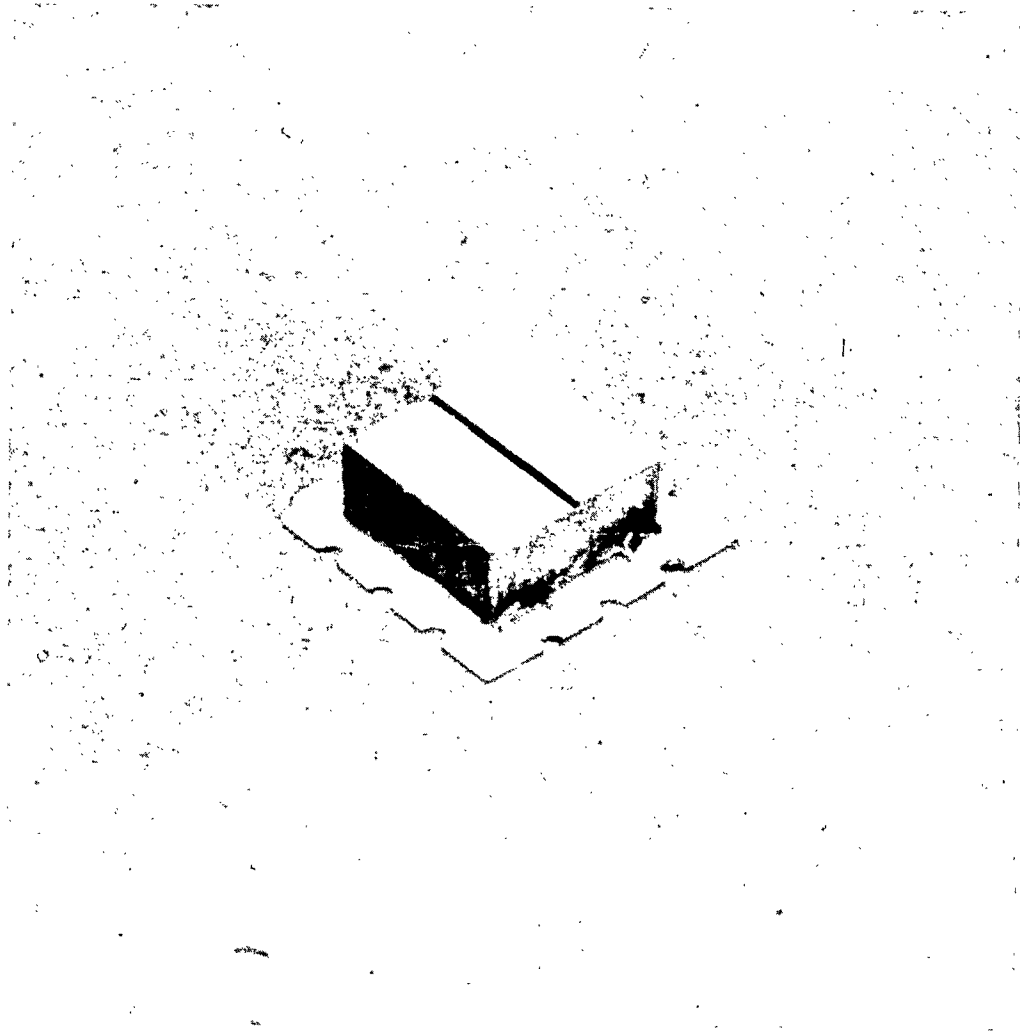
Figure 8.   Finished Two-Junction TEB, Type III or IV

4.4 Fabrication

4.4.1 Thermoelectric Material Source and Preparation

4.4.1.1 Source: The thermoelectric material used in the performance of this contract was obtained from Materials Electronics Products Company (Melcor), Trenton, New Jersey.

4.4.1.2 Preparation: The thermoelectric material used consisted of n- and p-type alloys in the quasiquaternary system $Bi_{2-x}Sb_xTe_{3-y}Se_y$ (where $0 \leq x \leq 2$ and $0 \leq y \leq 3$) based on Bi_2Te_3. This quasiquaternary system was first surveyed under the direction of the principal investigator of the present program at the Franklin Institute during 1957 and 1958.

It is a standard practice in the thermoelectrics industry for materials suppliers to withhold the exact composition, doping, and preparation steps from users as proprietary information. This has been true regarding the materials acquired for the performance of this program. The supplier would not release this information. Therefore, it is not possible to supply this information on materials used in this program. This material will be referred to as n- or p-type Bi_2Te_3 alloy.

4.4.2 Thermoelectric Material Parameters

The pertinent thermoelectric materials parameters, as measured by the Z-meter technique on typical materials used in the performance of this program, follow. This technique is discussed in subparagraph 4.4.3.3.

4.4.2.1 Bi_2Te_3 Alloy, n-Type:
   a. Seebeck coefficient, $S = -215$ $\mu v/^{O}K$.
   b. Electrical resistivity, $\rho = 9.75 \times 10^{-4}$ ohm-cm.
   c. Thermal conductivity, $k = 1.66 \times 10^{-2}$ $w/cm^{O}K$.
   d. Figure of merit, $Z = 2.85 \times 10^{-3} \left(^{O}K\right)^{-1}$.

4.4.2.2 $\underline{Bi_2Te_3\ Alloy,\ p\text{-}Type}$:

a. Seebeck coefficient, $S = 205\ \mu v/^{\circ}K$.

b. Electrical resistivity, $\rho = 7.50 \times 10^{-4}$ ohm-cm.

c. Thermal conductivity, $k = 2.01 \times 10^{-2}\ w/cm^{\circ}K$.

d. Figure of merit, $Z = 2.78 \times 10^{-3}\left(^{\circ}K\right)^{-1}$.

4.4.2.3 $\underline{Materials\ Figure\ of\ Merit\ Z}$: Using the values given above and the formula

$$Z = \frac{(S_n - S_p)^2}{\left(\sqrt{\rho_n k_n} + \sqrt{\rho_p k_p}\right)^2}$$

$$Z = \frac{\left[\left[(-215) - (205)\right]10^{-6}\right]^2}{\left(\sqrt{9.75 \times 10^{-4} \times 1.66 \times 10^{-2}} + \sqrt{7.50 \times 10^{-4} \times 2.01 \times 10^{-2}}\right)^2}$$

$$Z = 2.83 \times 10^{-3}\,(^{\circ}K)^{-1}.$$

4.4.3 $\underline{Device\ Process\ and\ Evaluation}$

A detailed description of the process for making Thermo-electric Thermal-Barrier Microelements having performance equal to or greater than that specified for types I, II, III, and IV TEB's in U.S. Army Signal Corps Technical Requirement SCL-7635, dated 29 September 1961, and summarized in table X, follows.

4.4.3.1 $\underline{Summary\ of\ Process\ Steps}$: The process steps are given in the process flow chart, figure 9. The Bi_2Te_3 alloy thermoelectric material is prepared or purchased before the following device-processing steps.

Step 1. Evaluation of thermoelectric material ingots.

Step 2. Slicing of thermoelectric material into pellets.

Step 3. Lapping of thermoelectric pellets to desired thickness.
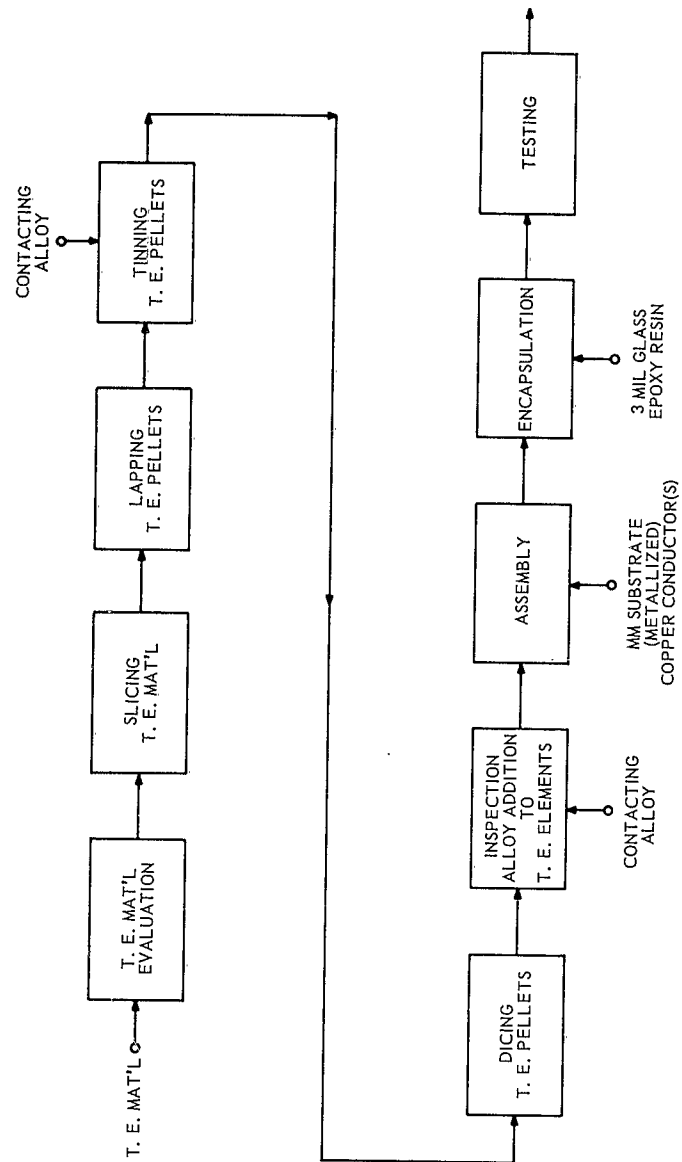
Figure 9. Flow Chart of TEB Process

Step 4. Tinning of thermoelectric pellets with contacting alloy.

Step 5. Dicing of thermoelectric pellets into elements.

Step 6. Inspection and addition of contacting alloy to thermoelectric elements.

Step 7. Assembly into TEB's.

Step 8. Encapsulation.

Step 9. Evaluation and testing.

4.4.3.2 Bill of Materials for TEB Devices: The bill of materials is summarized in table XII.

4.4.3.3 Process Description: The Thermoelectric Thermal-Barrier Microelements, types I, II, III, and IV, are prepared in nine basic processing steps and three subassembly processing steps. The thermoelectric elements are formed into the desired size and shape by mechanical means (see figure 10). Low contact resistance and high mechanical bond strength are obtained through the use of a special contacting alloy and flux. The device is assembled using a simple jig to hold the parts in position during the bonding operation. Finally, the device is partially encapsulated using a thin glass (microscope cover glass) shell to seal off the inner portion of the TEB from convection currents and restrict the entry of subsequent encapsulants into the inner portion. The glass shell also provides additional mechanical rigidity to the devices. See figures 7, 8, and 11.

Step 1. Evaluation of Thermoelectric Material Ingots

1.1 Equipment

1.1.1 Thermoelectric material Z-meter (see text)

1.1.2 Seebeck coefficient meter, Model 112B, Cambridge Systems, Inc., Newton, Mass.

Table XII

BILL OF MATERIALS FOR TEB DEVICES

| | Direct | | | Indirect | |
No.	Description	Quantity Required	No.	Description	Quantity Required
1	Thermoelectric element, n-type	1-2	3-1	Adhesive, Apiezon, Type W	--
2	Thermoelectric element, p-type	1-2	3-2	Abrasive paper, 600 grit SiC	6
3	Contacting alloy (See Section 4.4.3.3 for composition)	--	3-3	Trichloroethylene, tech.	1 liter
4	Micromodule substrate, metallized, type 1	1	3-4	Methanol, reagent	1 liter
or					
5	Micromodule substrate, metallized, type 2	1	4-5	Flux, stannous fluoborate solution	--
6	Copper conductor, type a	1	4-6	Water, deionized	1 liter
or					
7	Copper conductor, type b	2	5-7	Material mounting block	1
8	Substrate and copper conductor solder	1-2	7-8	Acetone, reagent	1 liter
9	Glass encapsulation pieces, 3 mils thick	4	7-9	Airbrasive abrasive	--
10	Paint, blue	--			
or					
11	Paint, green	--			
or					
12	Paint, yellow	--			

Table XII (Continued)

Direct			Indirect		
No.	Description	Quantity Required	No.	Description	Quantity Required
or					
13	Paint, red	--			
14	Epoxy resin, Armstrong A-1	--			

Note 1. The quantity required of direct materials is listed per device. Where "1 or 2" is listed under "quantity required," TEB types I and II require one and TEB types III and IV require two. Direct materials items listed "4 or 5" are two different type metallized substrates and only one type is used per device. Type 1 substrate is used for TEB types I and II, and type 2 substrate is used for TEB types III and IV. Similarly, for direct materials items 6 and 7, only one type is used per device with type a used for TEB I and II and type b used for TEB III and IV. Direct materials 10 through 13, inclusive, are paints used for color coding the device types: TEB I - blue, TEB II - green, TEB III - yellow, and TEB IV - red.

Note 2. The quantities required of indirect materials are listed per 100 devices.
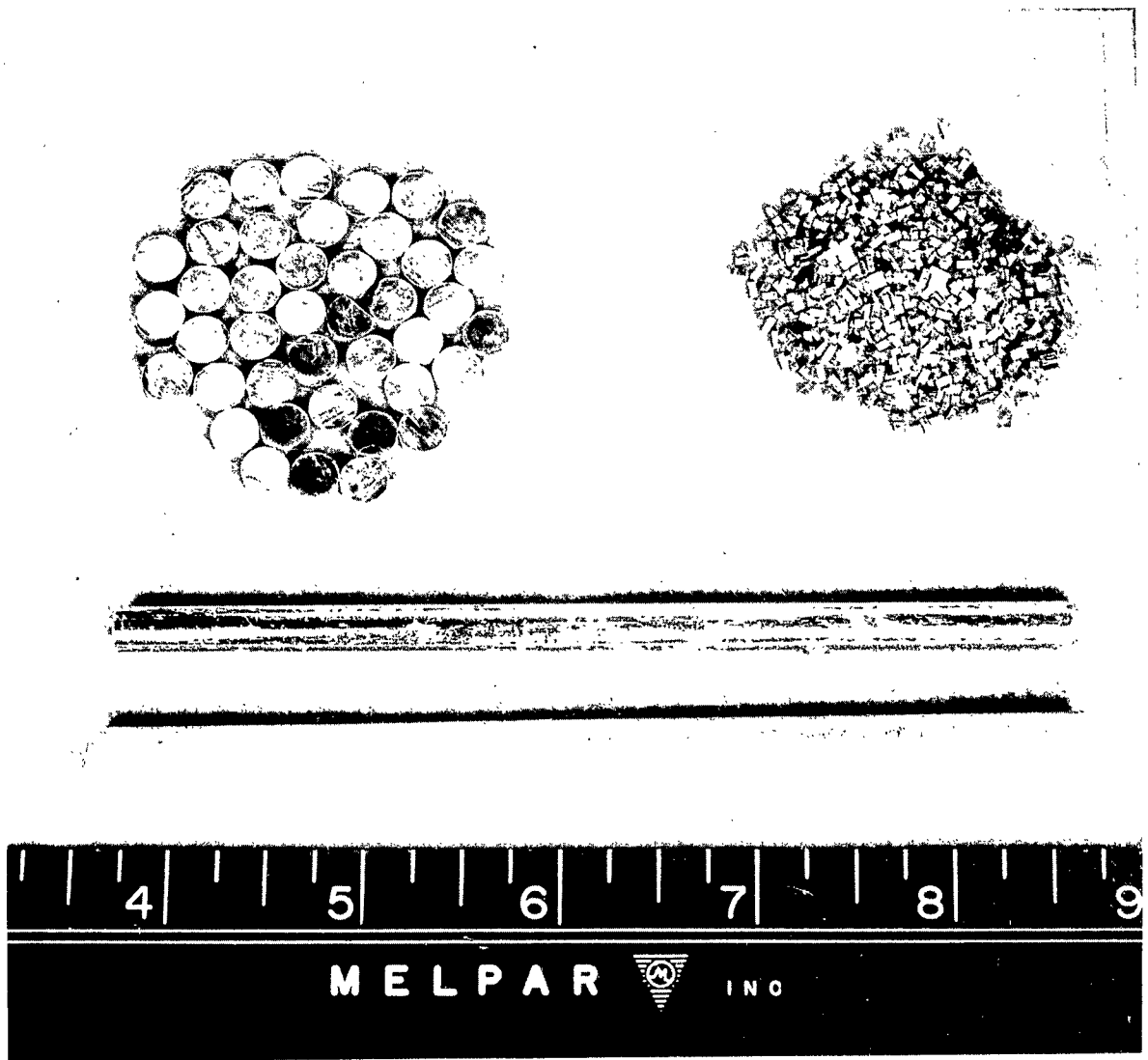
Figure 10.   Thermoelectric Material (Ingots, Pellets, and Elements)
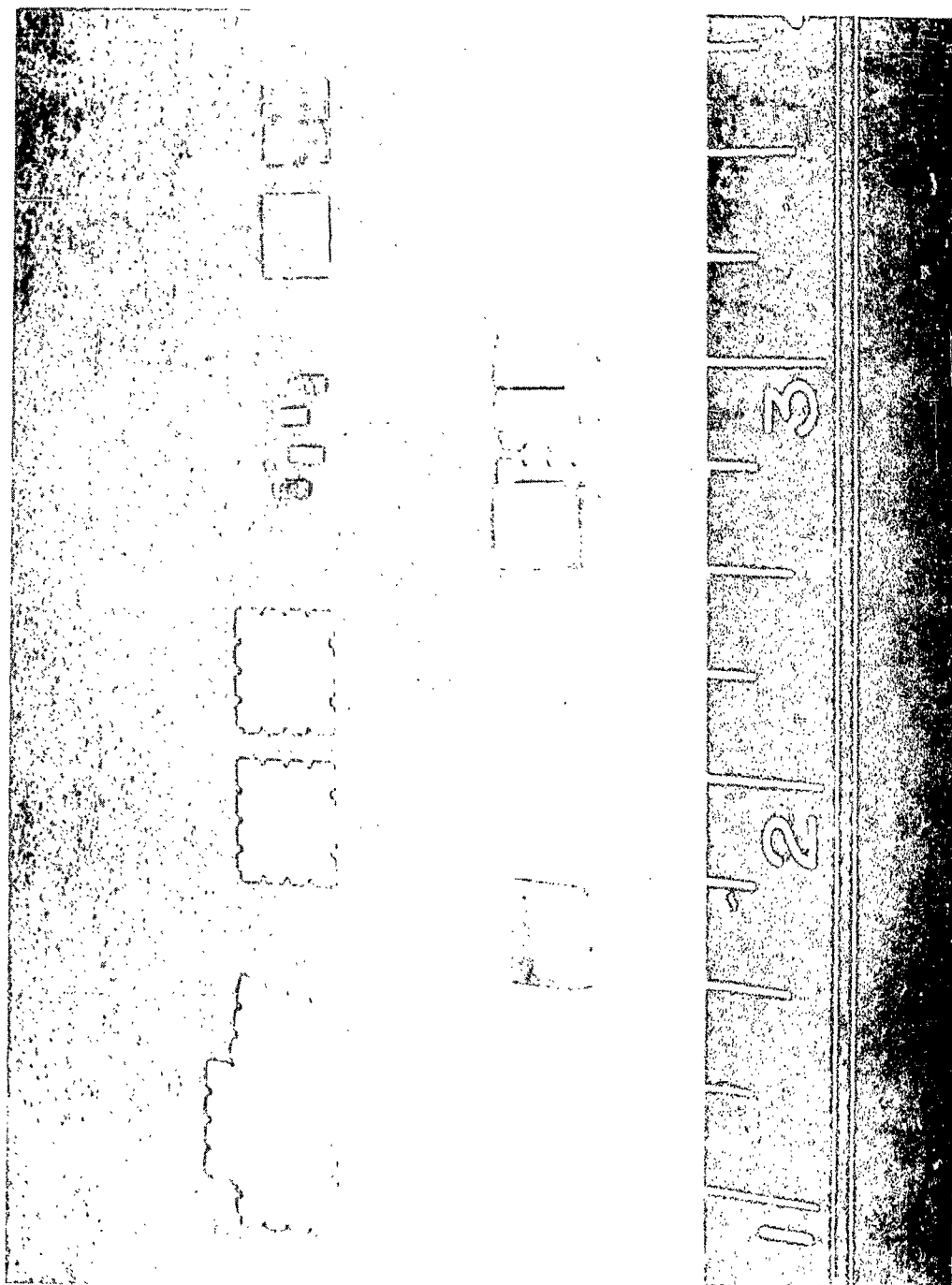
Figure 11. Direct Materials Involved in TEB Construction

1.1.3 Two-point resistivity meter, Model
113-2, Cambridge Systems, Inc.,
Newton, Mass.

1.1.4 Crystal slicing machine, Model WMA-2,
Micromech Mfg. Co., Union, N.J.

1.1.5 Thermoelectric material cutting
fixture (see figure 12).

1.1.6 Oryx miniature soldering iron, Model
6A, Oryx Elect. Labs., Ltd., Sussex,
England. (6 watts)

1.2 Materials

1.2.1 N-type Bi_2Te_3 alloy ingots, 7 mm
diameter.

1.2.2 P-type Bi_2Te_3 alloy ingots, 7 mm
diameter.

1.2.3 Contacting alloy (70Bi, 23Sn, 5Ag,
2Sb).

1.2.4 Stannous fluoborate flux solution
(45% to 48%).

1.3 Procedure

1.3.1 The Bi_2Te_3 ingots, both n- and p-type,
in the form of 7 mm diameter rods are placed in the thermo-
electric material cutting fixture as shown in figure 12. The
fixture holding the ingots is placed in the crystal slicing
machine and a section one inch long is cut from both the n-
and p-type material. It is cut from the approximate vicinity
from which the TEB elements will be prepared. The crystal
slicing machine is shown in figure 13.

1.3.2 The one-inch-long samples which
will be measured in the Z-meter to determine their parameter
values are tinned on each end using the contacting alloy and
stannous fluoborate flux. The contacting alloy consists of
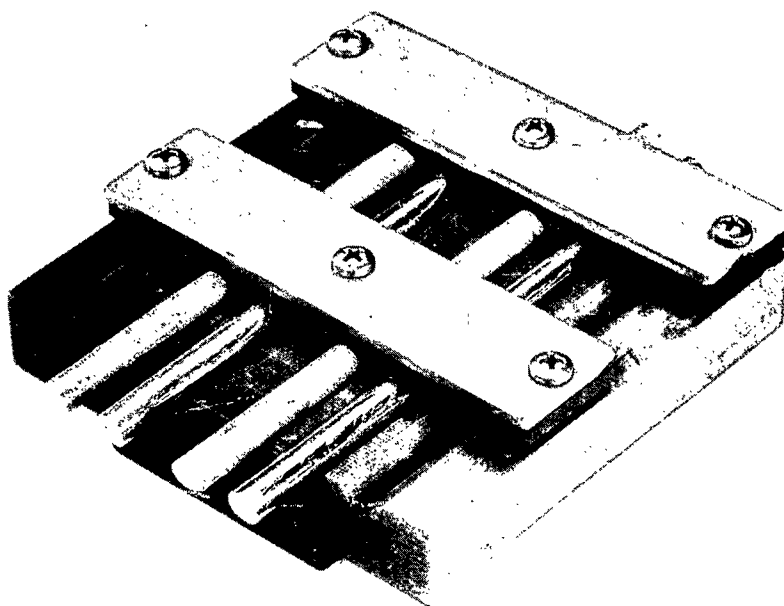
Figure 12.   Cutting Fixture
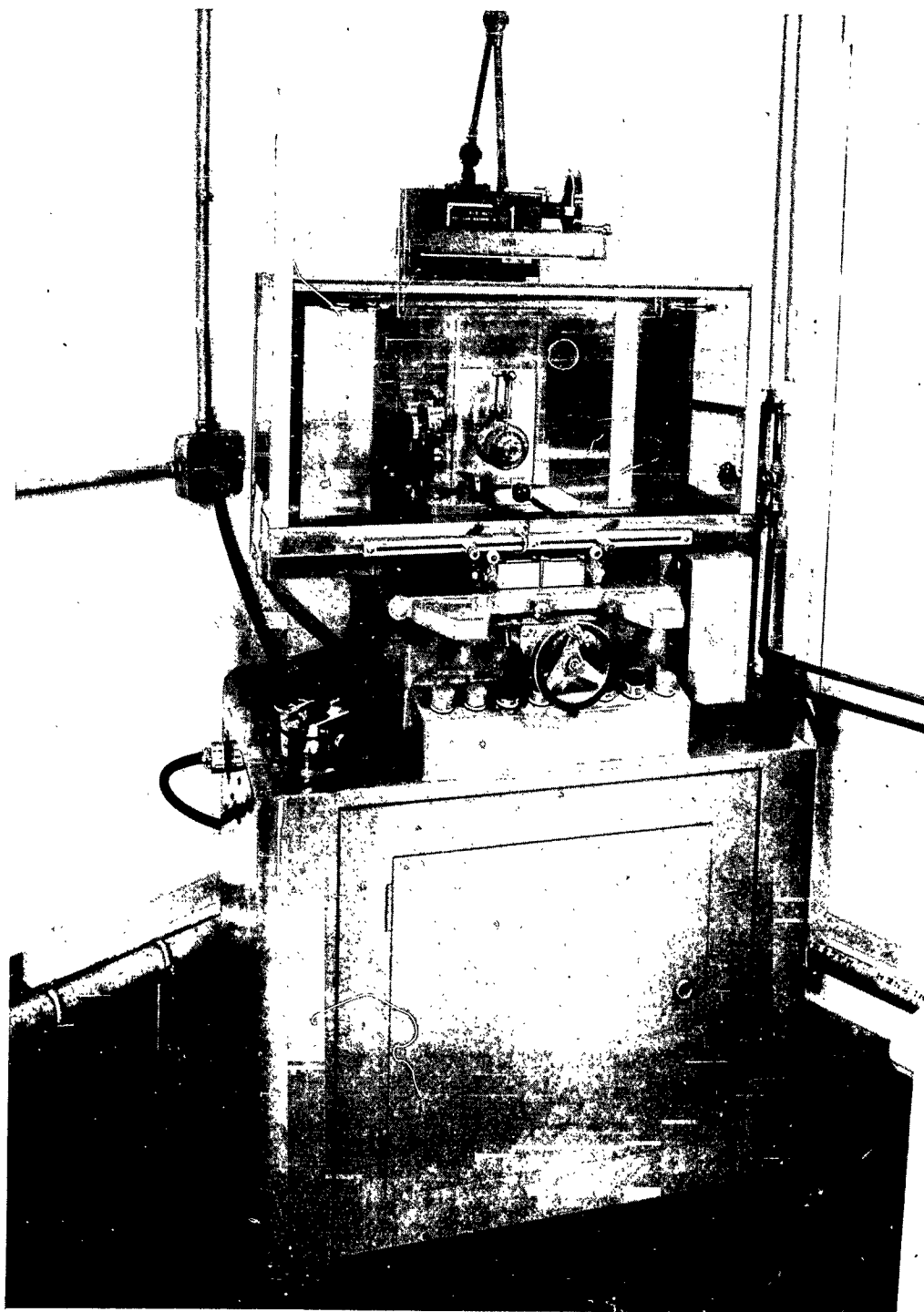
Figure 13. Semiconductor Crystal-Slicing Machine

a mixture of 70% Bi, 23% Sn, 5% Ag, and 2% Sb. They are tinned using an "Oryx" soldering iron.

      1.3.3 The samples are mounted one at a time in the Z-meter. The Z-meter is shown in figure 14. The evaluation is carried out, yielding values for S, ρ, k, and Z. Material whose Z is less than $2.7 \times 10^{-3} (^{\circ}K)^{-1}$ is rejected for use in the TEB application. No upper limit is set.

The Z-meter used was based upon the technique reported by Harman $\left[34\right]$. The unit provides a high vacuum with a radiation-shielded bell jar. Thermocouple and electrical feedthroughs are used to bring the measurement voltages out of the vacuum. The exact technique used is explained in detail in reference $\left[34\right]$.

      1.3.4 To determine the relative uniformity of the ingots to be used, additional measurements of Seebeck coefficient, S, and electrical resistivity, ρ, are made by probing the entire length of the ingot section to be used. The ends of the ingots are tinned in the same manner as described in procedure 1.3.2. A two-point probe is used to measure ρ with the current contacts made to the tinned ends of the ingot (figure 15). For the S measurement, a heated probe which has a constant temperature differential between the probe and the base block holding the ingots is probed along the length of the ingots in the region to be used (figure 16).

    Step 2. Slicing of thermoelectric material into pellets

      2.1 Equipment

          2.1.1 Crystal Slicing Machine

          2.1.2 Thermoelectric material cutting fixture

      2.2 Materials

          2.2.1 N-type Bi_2Te_3 alloy ingots, 7 mm diameter.
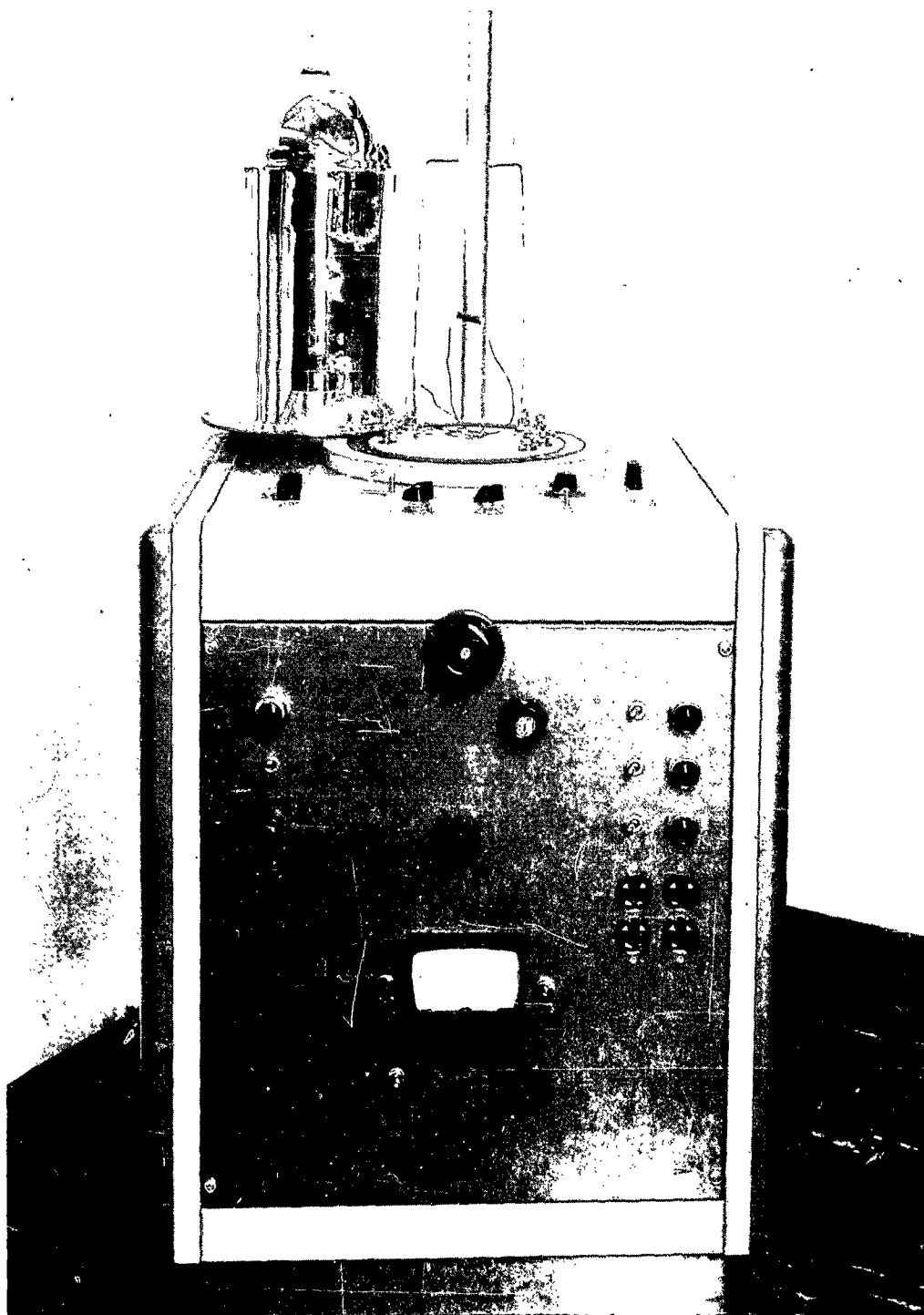
Figure 14. Thermoelectric Z Meter
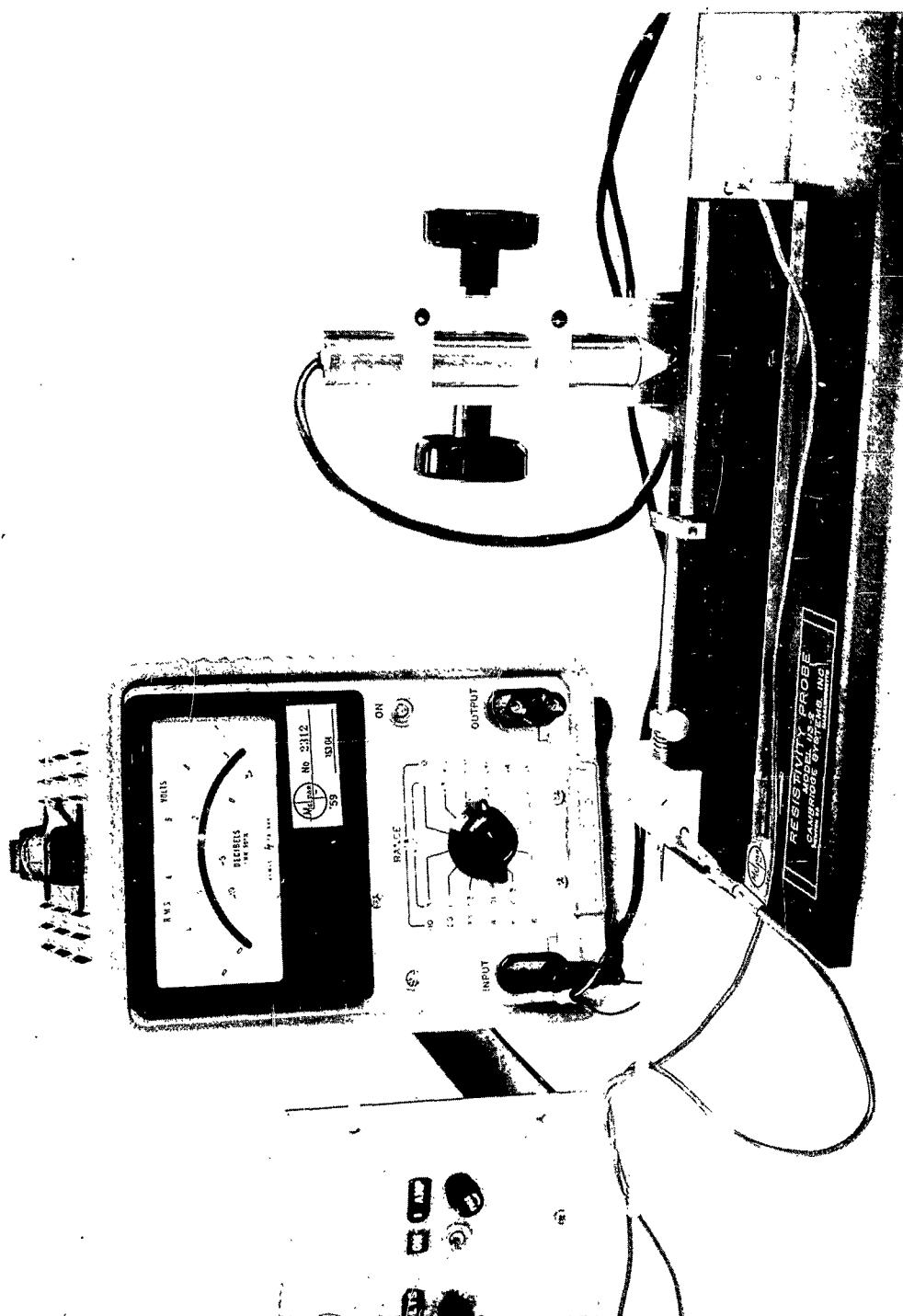
Figure 15.   Resistivity Meter For Thermoelectric Materials
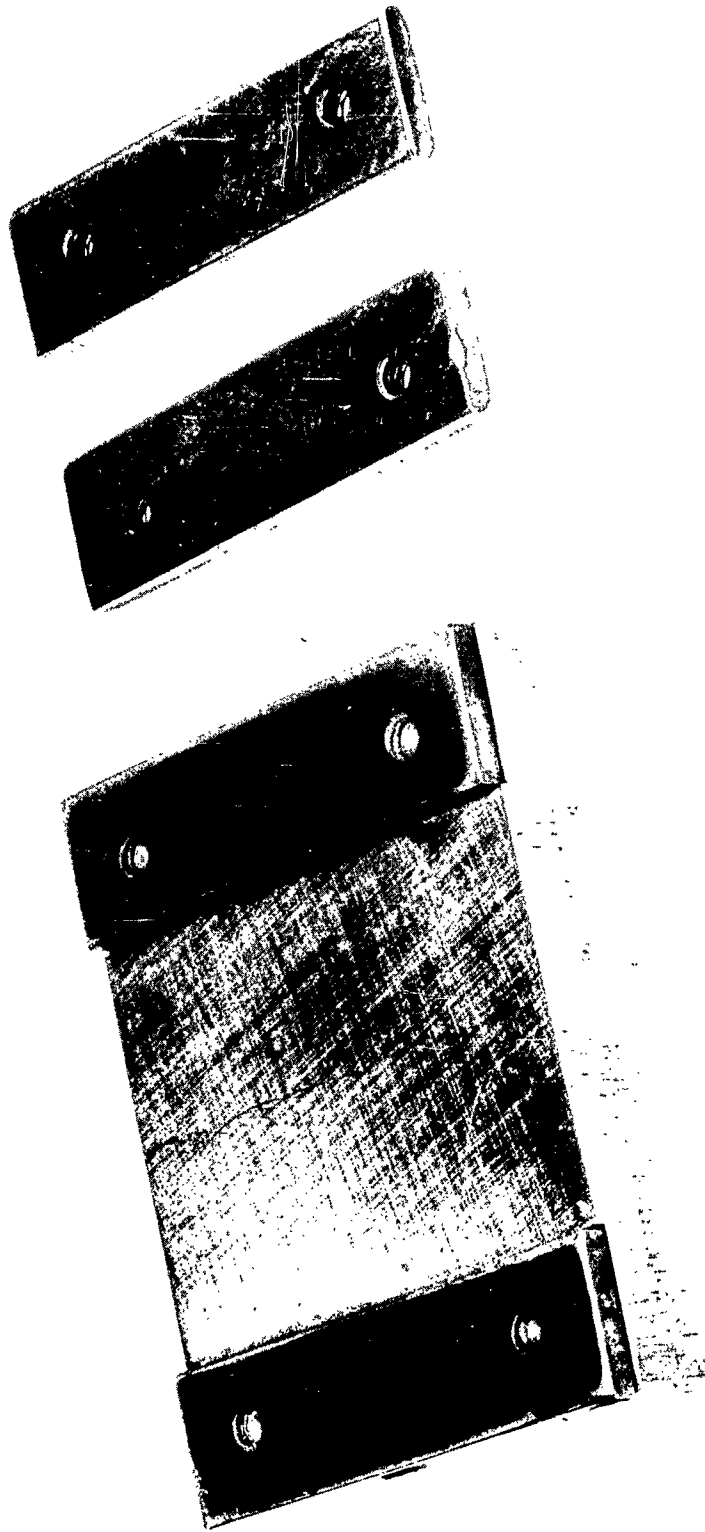
Figure 16.   Seebeck Coefficient Meter

2.2.2 P-type Bi_2Te_3 alloy ingots, 7 mm diameter.

2.3 Procedure

2.3.1 The n- and p-type Bi_2Te_3 alloy ingots are placed in the thermoelectric materials cutting fixture (figure 12). This fixture is placed in the crystal slicing machine and pellets are sliced off using a 3" x 0.010" diamond blade to a length of $0.090" \; ^{+0.002"}_{-0.000"}$. It is not necessary to keep the two types of material separate at this point so, for convenience, they are kept together.

Step 3. Lapping of the thermoelectric pellets to desired thickness

3.1 Equipment

3.1.1 Buehler grinding wheel, 8", Buehler, Ltd., Chicago, Ill.

3.1.2 Thermoelectric material lapping fixture (see figure 17).

3.1.3 Hot plate, Temco Model 1900, Thermolyne Corp., Dubuque, Iowa.

3.1.4 Surface temperature thermometer, Model 573 cm, Pacific Transducer Corporation, Los Angeles, Calif.

3.1.5 Micrometer caliper, 1" (calibrated to 0.0001").

3.1.6 Tweezers, coarse point.

3.2 Materials

3.2.1 N- and p-type Bi_2Te_3 alloy pellets, 7 mm dia. x 0.090".

3.2.2 Adhesive, Apiezon type W.

3.2.3 Abrasive paper, 8" dia. discs, 600 qrit SiC .

3.2.4 Trichloroethylene, technical grade.

3.2.5 Methanol, reagent grade.
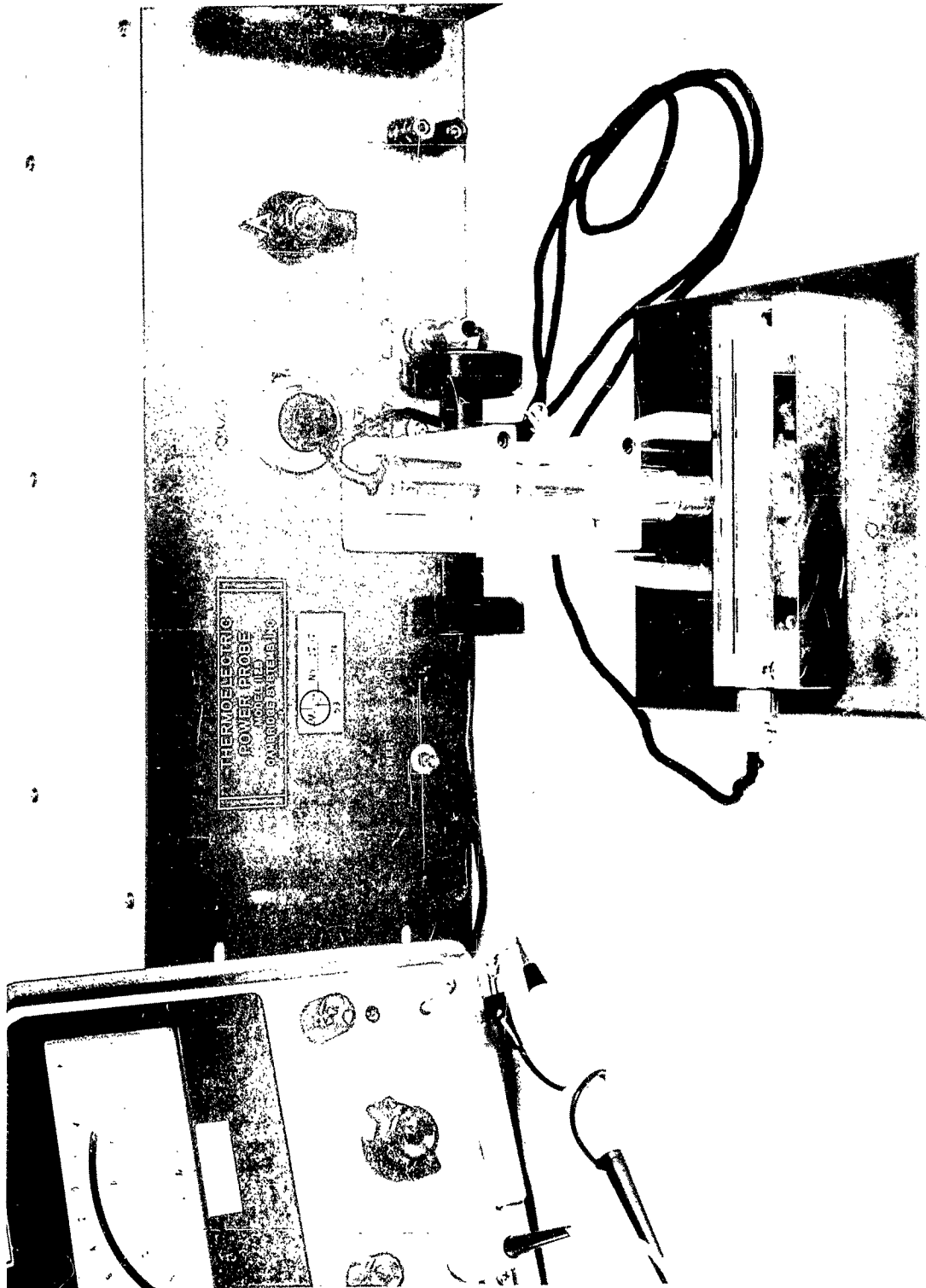
Figure 17.   Lapping Fixture

3.3 Procedure

3.3.1 The 7-mm-diameter x 0.090" thermo-electric pellets are mounted, using tweezers, on the thermoelectric material lapping fixture with a very thin film of Apiezon W. No attempt is made to differentiate between n- and p-type material at this stage. Figure 17 shows the lapping fixture. The Apiezon W is a thermoplastic material which melts between 80° and 90°C. The temperature is measured with a surface-temperature thermometer. This operation is performed on a hot plate which is set at approximately 90°C.

3.3.2 The lapping fixture is composed of two sections. One is the base upon which the elements are mounted close to the surface with a thin film of adhesive. The other is two sets of two hard steel gauge plates which control the thickness or length to which the pellets are lapped. The gauge plate set is mounted with one gauge plate at each end of the base piece. The first set of gauge plates is thicker than the desired pellet length. These are used to finish one side of the pellets and to leave enough material to finish the other side. With the first set of gauge plates installed, the pellets are lapped on the Buehler rotary grinding wheel on 600 grit SiC abrasive paper. Water is used as a coolant and to carry away the Bi_2Te_3 which is lapped away. The pellets are lapped until the gauge plates come down onto the lapping surface.

3.3.3 The lapping fixture and pellets are rinsed with water and dried. The fixture is placed back on the hot plate and the pellets removed. The Apiezon W is cleaned from the elements and the fixture with hot trichloroethylene.

The pellets are rinsed in methanol and dried. They are then
turned over with the recently lapped side down and mounted
to the lapping fixture base in the manner previously described
in procedure 3.3.1. The other set of gauge plates is installed.
These plates are the thickness to which the pellets must be
finished.

      3.3.4 The pellets are lapped on this side
until they are lapped flush with the finish gauge plates. A
micrometer is used to check each pellet to ensure that each
is coming down evenly. The fixture and pellets are again
rinsed with water and dried. The pellets are removed and
cleaned as described in procedure 3.3.3. After cleaning,
they are checked again with micrometers and any pellet outside
the limits 0.079" to 0.080" is rejected or reprocessed.

    Step 4. Tinning of thermoelectric pellets with
                contacting alloy.

      4.1 Equipment

          4.1.1 Oryx miniature soldering iron, with
                   stainless steel tip, 0.020" diameter.

          4.1.2 Hot plate.

          4.1.3 Surface-temperature thermometer.

          4.1.4 Tweezers, coarse.

      4.2 Materials

          4.2.1 N- and p-type lapped Bi_2Te_3 alloy
                   pellets, 7-mm-diameter x 0.080".

          4.2.2 Contacting alloy.

          4.2.3 Stannous fluoborate flux.

          4.2.4 De-ionized water.

          4.2.5 Methanol, reagent grade.

4.3 Procedure

This is a critical step because the quality of the electrical contact is determined by correctness of the following operations.

4.3.1 With the hot plate set at 190°C, as measured by the surface-temperature thermometer, a thermoelectric pellet is placed on the hot plate and stannous fluoborate flux is applied to the entire top surface. The pellet is allowed to come to temperature. As the fluxed pellet is coming to temperature, a small quantity of contacting alloy (enough to form a small bead at the end of the 0.020" diameter stainless steel soldering tip) is taken onto the small soldering iron. When the flux is beginning to boil off of the pellet, the pellet is held in position on the hot plate with tweezers and the soldering iron carrying the contacting alloy is brought in contact with the pellet surface. Immediately, the soldering iron is moved in a manner that spreads the contacting alloy over the entire pellet top surface. This is accomplished by moving the iron rapidly in a small circular motion until this motion has covered the whole pellet top surface. If some areas do not wet completely, more flux may be added and the process repeated. The result should be a thin even coating of solder over the whole top surface of the pellet.

4.3.2 The thermoelectric pellet is turned over and procedure 4.3.1 repeated on the other end surface. The pellets are tinned at this stage to ensure good wetting over the entire end-surfaces of resulting elements and because greater yields of diced elements can be obtained due to the extra strength provided by the solder.

4.3.3 The tinned pellets are cleaned in hot (80° to 90°C) de-ionized water for 15 minutes. After this treatment, they are rinsed in methanol and dried.

Step 5. Dicing of thermoelectric pellets into elements.

5.1 Equipment

5.1.1 Crystal slicing machine.

5.1.2 Dicing fixture (see figure 18).

5.1.3 Hot plate.

5.1.4 Surface temperature thermometer.

5.1.5 Stereoscopic microscope with calibrated measuring reticle.

5.1.6 Tweezers, coarse.

5.1.7 Tweezers, fine.

5.2 Materials

5.2.1 N- and p-type tinned pellets, 7 mm-diameter x 0.080".

5.2.2 Apiezon adhesive, type W.

5.2.3 Material mounting block, Chalk Tile, Jerrill Engrg Co., Fanwood, N.J.

5.2.4 Trichloroethylene, tech. grade.

5.2.5 Methanol, reagent grade.

5.3 Procedure

5.3.1 The tinned pellets are mounted to the material mounting block with Apiezon adhesive, type W. This is accomplished, as previously described, on a hot plate. The pellets are lined up in straight rows with coarse-pointed tweezers so that a maximum number of elements may be diced from them at one time. All the spaces between the pellets are filled in with the Apiezon adhesive up to the top surface and also filled up around the edges of the pellet rows. This
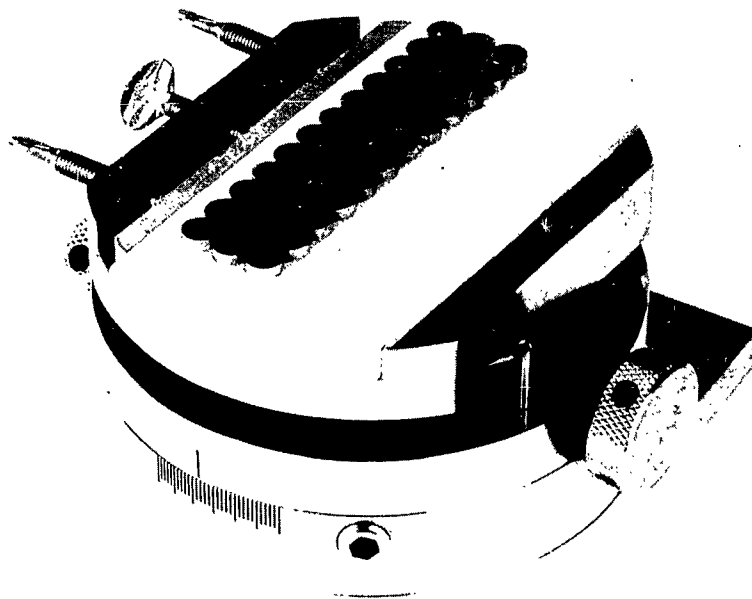
Figure 18.   Dicing Fixture

serves to give necessary support for the cut sections and keep them from breaking loose from the mounting block. The mounting block is mounted into the dicing fixture. The dicing fixture is shown in figure 18.

      5.3.2 The dicing fixture is mounted into the crystal slicing machine and 0.040" cuts are made in one direction along the rows of pellets. The first two cuts are checked with a calibrated microscope to ensure the desired dimensions in resulting elements. They must be within 0.040" $\pm$0.0005".

      5.3.3 After the first cut, the pellets are removed from the crystal slicing machine and the material mounting block is placed on the hot plate. The thermoplastic adhesive is melted and the cut rows are moved together such that the space between sliced pieces is eliminated and the pieces lie against each other. Additional adhesive is added around the outside of the resulting congregation of thermo-electric pieces. All sections of the thermoelectric material that are odd-shaped or broken and that will not result in good elements are removed at this time. The block is removed from the hot plate and placed in the dicing fixture. The fixture, holding the thermoelectric pellets, is placed in the crystal slicing machine and cuts are made perpendicular to the previous cuts. These cuts are also made to result in 0.040" wide pieces. The first two cuts are checked with the microscope as done in the previous dicing step. The same tolerances are maintained.

      5.3.4 The mounting block is heated on a hot plate. The resulting elements are removed with fine-pointed

tweezers. The elements are cleaned in hot trichloroethylene
for 15 minutes, rinsed in reagent methanol and dried.

Step 6. Inspection and addition of contacting alloy
to thermoelectric elements,

6.1 Equipment

6.1.1 Thermoelectric Probe (see text).

6.1.2 Stereoscopic microscope, 30X, Bausch and Lomb, Rochester, N.Y.

6.1.3 Hot plate.

6.1.4 Surface-temperature thermometer.

6.1.5 Tweezers, fine.

*6.1.6 Seebeck coefficient meter.

*6.1.7 Resistivity Meter, Modified (see figure 19).

*Required only when thermoelectric material properties are
changing rapidly along the length of an ingot.

6.2 Materials

6.2.1 Diced thermoelectric elements, 0.040" x 0.040" x 0.080".

6.2.2 Contacting alloy.

6.2.3 Stannous fluoborate flux,

6.2.4 Deionized water,

6.2.5 Methanol, reagent grade.

6.3 Procedure

6.3.1 The thermoelectric elements must
now be separated into n- and p-types. This is accomplished
with a "thermoelectric probe." This consists of a heated
probe and an unheated probe which are electrically connected
to a galvanometer. When an element is contacted by these probes,
a temperature difference is created and thermoelectric voltage
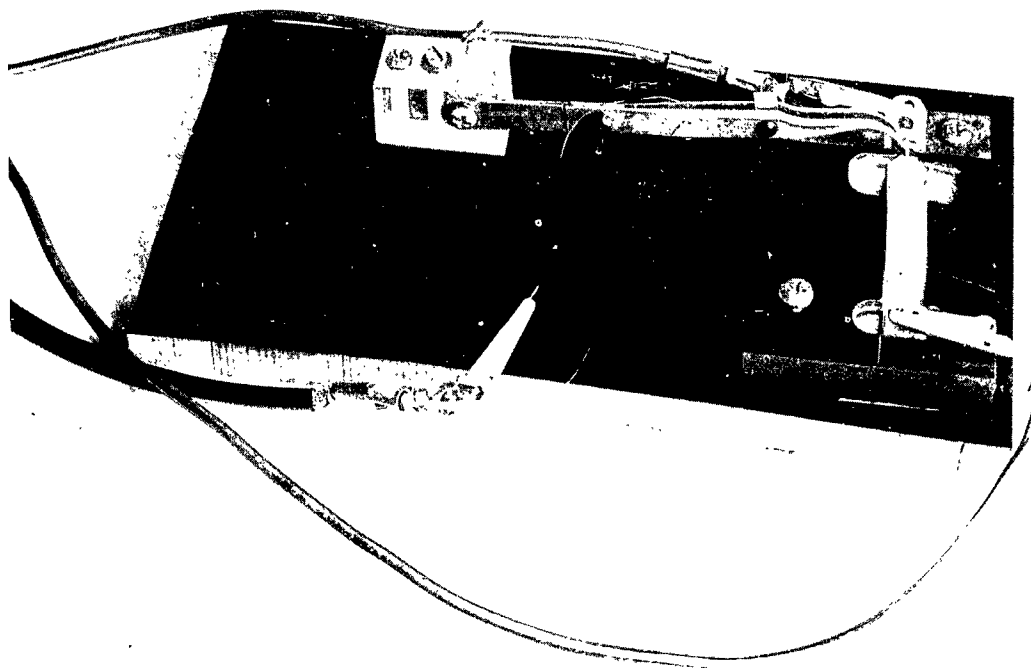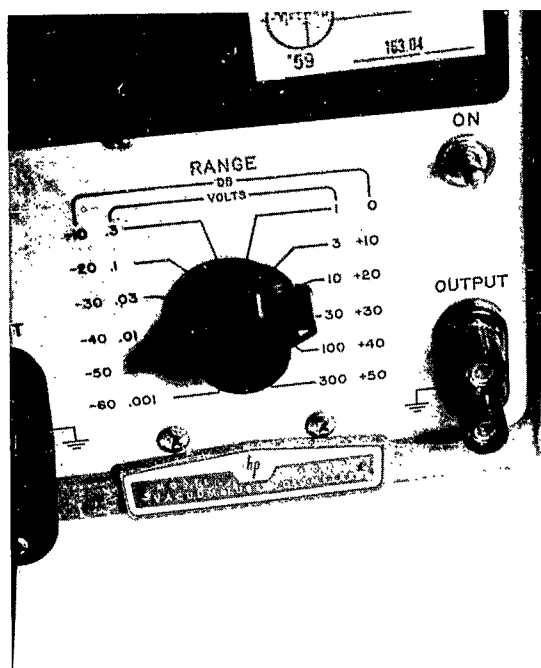
Figure 19. Resistivity Meter For Thermoelectric Elements

is generated. The direction of the deflection is an indication
of the polarity of the thermoelectric power (Seebeck coefficient)
of the element.

6.3.2 After the elements have been separated
into the two types, additional contacting alloy must be added
to the ends of the elements in order to obtain the desired
bonds in the finished devices. It is extremely difficult to
apply this alloy in the correct amounts during the original
tinning of the elements.

This addition of contacting alloy is accomplished by placing
a small volume of the alloy (approximately 1/4" cube) on a
microscope slide which is heated on a hot plate to 190°C. The
temperature is monitored by a surface-temperature thermometer.
On another microscope slide, placed beside the hot plate, a
small amount of stannous fluoborate flux is spread out in a
thin film. This is so that the elements may be coated with
a small amount of the flux at each end.

Using a stereoscopic microscope to observe the operation
and fine-pointed tweezers to handle the elements, the addition
of the contacting alloy is performed. The elements are grasped
in the middle with the tweezers and fluxed on both ends. While
observing through the microscope the element is brought into
contact with the melted hemisphere of contacting alloy and
held for one second. At the end of this time it is pulled
away rapidly from the surface of the contacting alloy. This
operation is repeated on the other end of the element. The
result should be a smooth spherical surface covering the entire
area of each end of the element, with the spherical radius
being approximately 0.030" to 0.035". As each element is looked

at under the microscope it is visually inspected and rejected
if found to be broken or misshaped.

6.3.3 The elements are placed in hot
de-ionized water (80° to 90°C) as they are processed. After
the batch has been completed, the elements (now being kept
separated into n- and p-type categories) are rinsed in reagent
methanol and dried.

6.3.4 After the application of additional
contacting alloy the Seebeck coefficient and resistivity of
the elements may be checked. This operation is to be included
when gross material variations are being experienced. Because
this occurs infrequently, it is not considered necessary as a
standard part of the process. In large-scale production it
may have advantage when material from several ingot sources
are grouped together in a batch of elements.

In this operation the s-meter is used in the same manner
as it was used in the ingot evaluations. The same measurement
method is used for the resistivity as was used for the ingot
evaluation except that a smaller set of probes is used on
the elements. The probe consists of a pair of tweezers with
electrically insulated points. The current is passed through
the tinned ends of the elements and the voltage drop taken
across a 1 mm spacing at the tweezer tips. See figure 19.

Step 7. Assembly into TEB's.

7.1 Equipment

7.1.1 Assembly jig (see figure 20).

7.1.2 Hot Plate.

7.1.3 Surface-temperature thermometer.

7.1.4 Stereoscopic microscope, 10X.

7.1.5 Jig cooling block (brass 4" x 4" x 1").
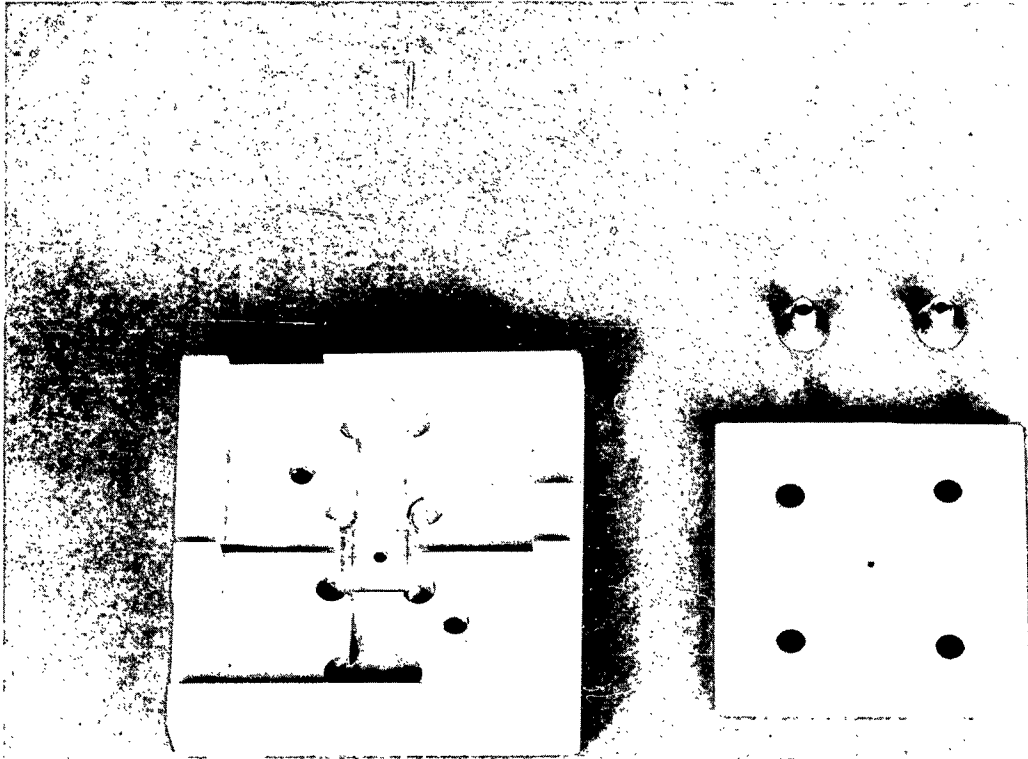
Figure 20.   TEB Assembly Jig Ready For Loading

7.1.6 Airbrasive unit, Model C, S.S. White Dental Mfg. Co., N.Y., N.Y.

7.1.7 Small screwdriver.

7.1.8 Tweezers, fine.

7.2 Materials

7.2.1 Thermoelectric elements, 0.040" x 0.040" x 0.080", with additions of contacting alloy at each end.

7.2.2 Stannous fluoborate flux.

7.2.3 Acetone, reagent grade.

7.2.4 De-ionized water.

7.2.5 Methanol, reagent grade.

7.2.6 Thermal grease, Dow Corning, Type XC-20106.

7.2.7 Copper conductors, Type a or type b.

7.2.8 Metallized micromodule substrates, 0.010" thick.

7.2.9 Airbrasive abrasive, Type No. 1.

7.3 Procedure

7.3.1 Figures 20, 21, 22, 23, 24, 25, and 26 apply to this procedure description. Figure 26 is a dimensional drawing of the assembly jig. The assembly jig (figures 20 and 25) is designed for use in constructing both one and two junction TEB's. It consists of:

1. One aluminum base part with a device cavity and several locating surfaces.

2. Two C-pieces which hold the elements in position when one junction TEB's are being made or two E-pieces when two junction TEB's are being made.

3. A glass strip which separates the elements held by the C or E-pieces.
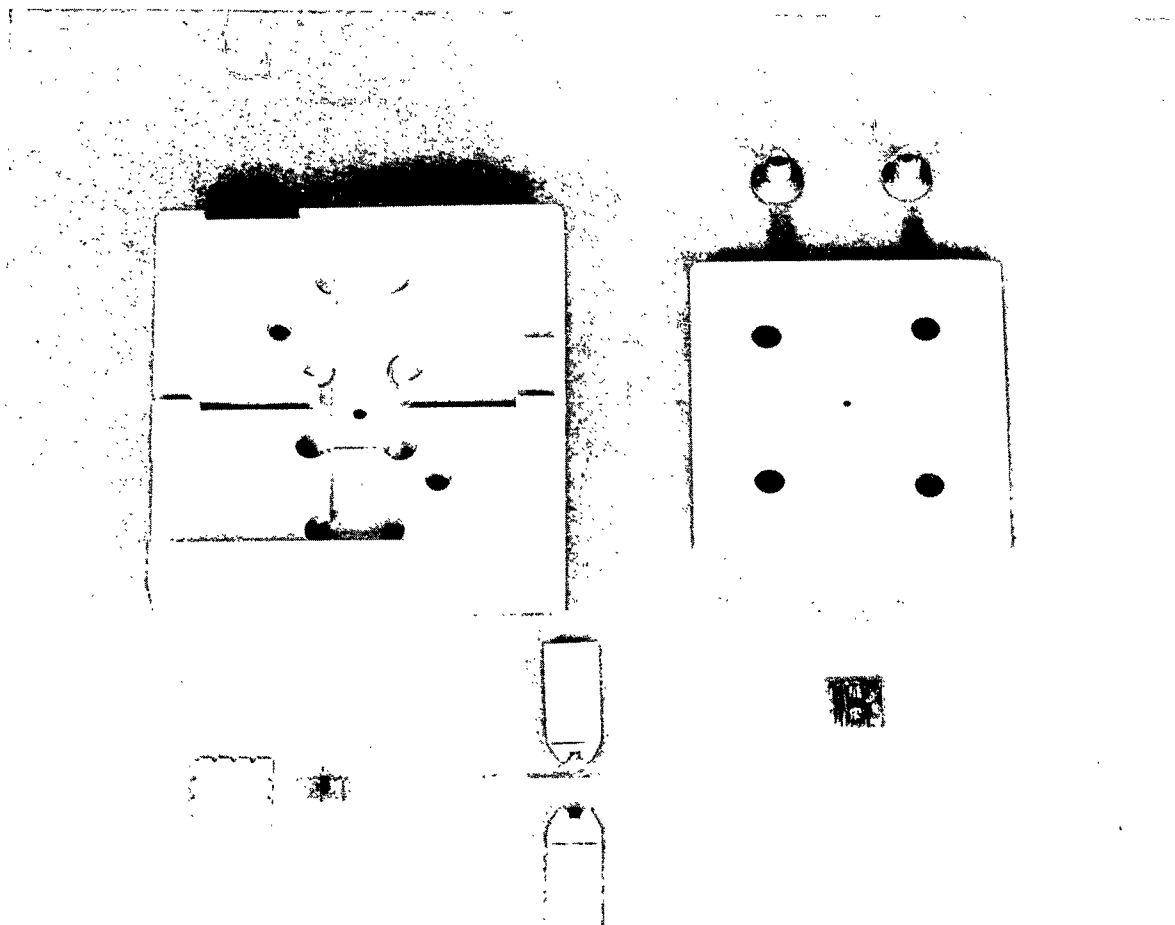
Figure 21.   TEB Assembly Jig Showing Parts For One-Junction Device
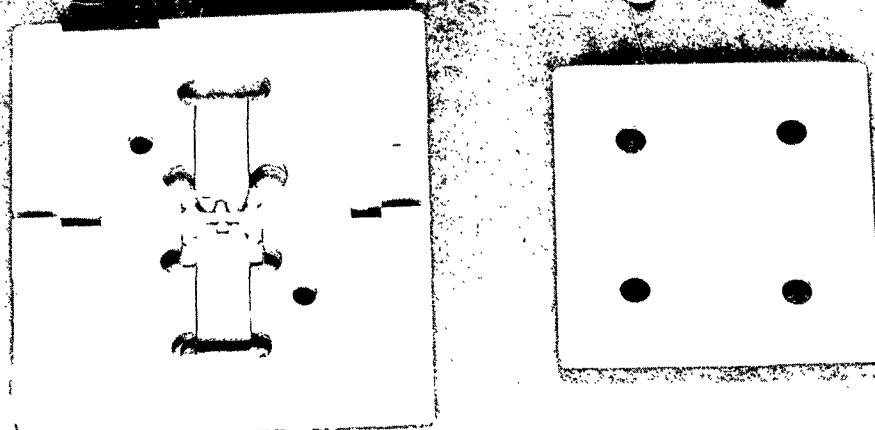
Figure 22.   TEB Assembly Jig Showing Parts For One-Junction Device Loaded
Into Position in Jig
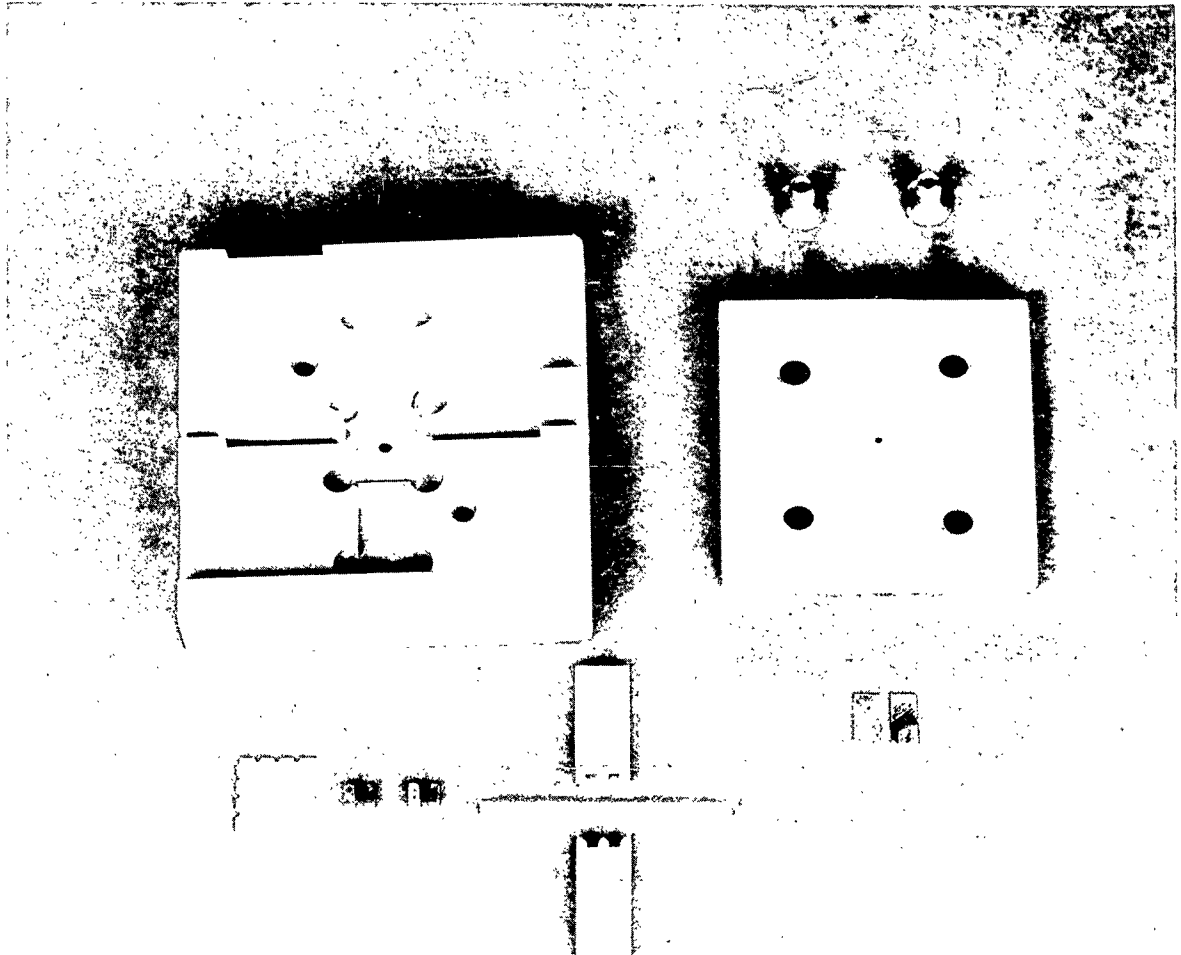
Figure 23.   TEB Assembly Jig Showing Parts For Two-Junction Device
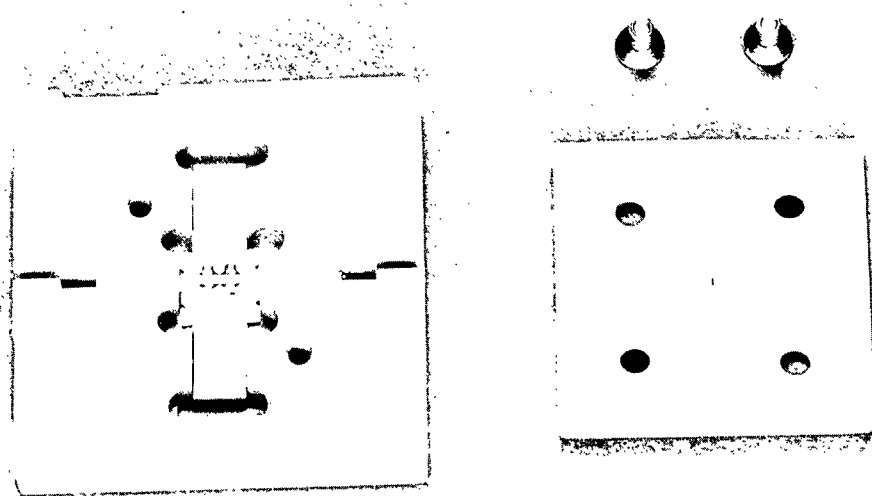
Figure 24.   TEB Assembly Jig Showing Parts For Two-Junction Device
Loaded Into Position in Jig
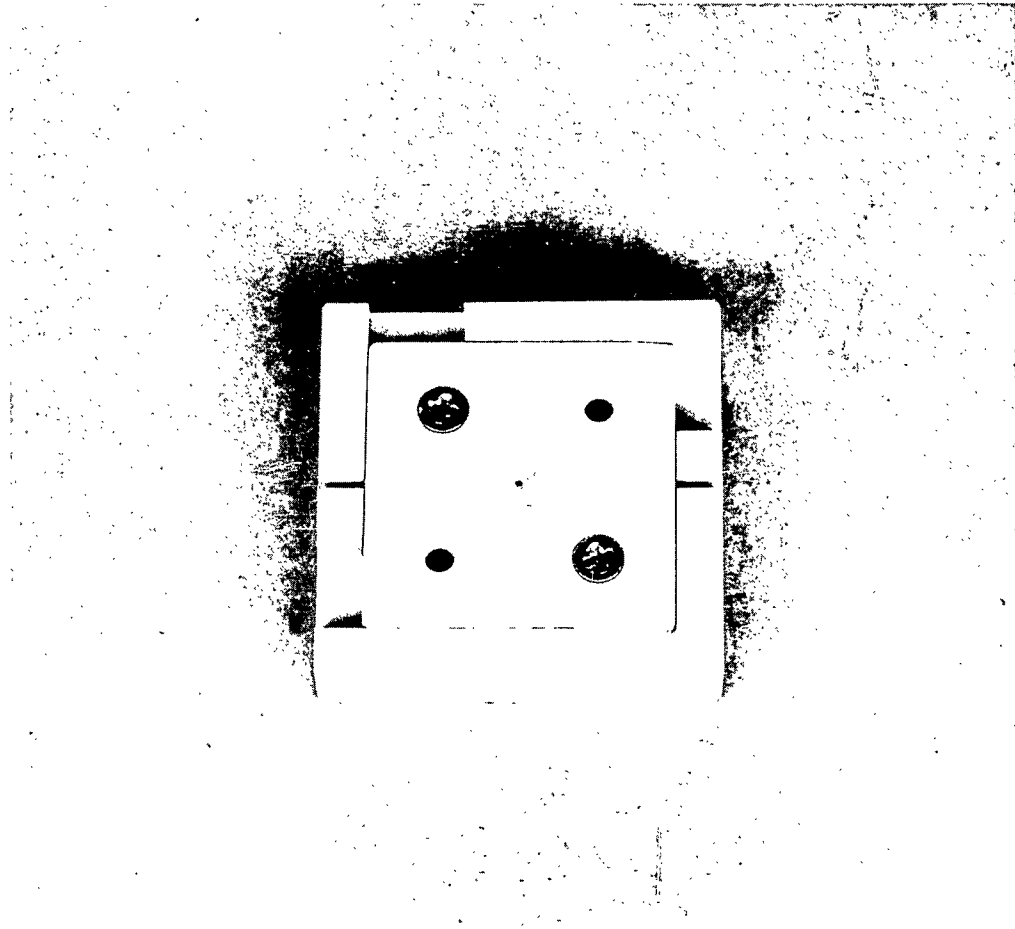
Figure 25.   TEB Assembly Jig Ready for Processing

R4690

1.625 SQ.

.8125

1.241

3/8 TYP

2 4-40 TAP HOLES
LOCATE FROM TOP PLATE
DET 2

.192 TYP

3/8

.210
.105

7/32

9/16

1.241

A   A

.1575

.315±.001 SQ. POCKET
.094 DEEP ON ₵

.042

1/8

.094 ±.001
.010

A-A

①

MATERIAL: ALUMINUM

1.240 SQ.   SLIP FIT

1/4
1/4

.005   .010   .216   .108

₵

TOP
TWO
L

.212
.106

1/8

PO

②

.1065

.1065   .213

.213

1/4

BO
C

1/4

DR. & CTR. SK 4

S

1

SLIP FIT IN DET I

1.240 SQ

.216
.108

1/4

1/4

TOP OF DET. 2
TWO JUNCTION
LOCATOR

.212
.106

1/8

POCKETS .004 ±.000
DEEP

.1065
.213

.1065

.213

BOTTOM OF DET. 2
ONE JUNCTION
LOCATOR

1/4

1/4

DR. & CTR. SK 4-40.

SCALE 1/1

.490
±.003

.040

23/64

.042

.042
+.001
-.000

.020

.208

.040

.045

.060

.020

.021

.042
+.001
-.000

TWO JUNCTION
LOCATOR
2 REQD

45° CHMF

ONE JUNCTION
LOCATOR
2 REQD

SCALE 2/1

2

Figure 26.   Detail Drawing of Assembly Fixture

110

4. A top plate which holds one type-a copper conductor part or two type-b conductor parts. Type-a is used for one-junction TEB's and type-b for two-junction TEB's. One side of the top plate is cut for type-a parts, the other side for type-b. The copper conductors are illustrated in figure 27.

5. Two 4/40 screws, used to tighten the top plate down onto the jig proper. These are necessary to obtain the desired overall TEB thickness.

See figures 21 and 23. The procedural difference between making one- and two-junction TEB's is simply the use of either C-pieces or E-pieces, loading of the proper number of elements, the proper copper conductors and the correct side of the top plate.

Because the assembly is similar except for the above-noted differences, a description of the assembly of only the two-junction TEB is given.

While observing through a stereoscopic microscope, the parts are loaded into the jig with fine-pointed tweezers. See figures 23 and 24. The parts are loaded in the following order as shown in the photographs:

1. The metallized micromodule substrate.

2. The glass separator strips.

3. The two E-pieces, relieved side down.

4. Two n-type and two p-type thermoelectric elements, highly fluxed with stannous fluoborate flux, are positioned so that they will be series-connected by virtue of their positions on the substrate and the two copper conductors.

The two type-b copper conductors are now placed in position with tinned side out on the appropriate cavities of the top plate.
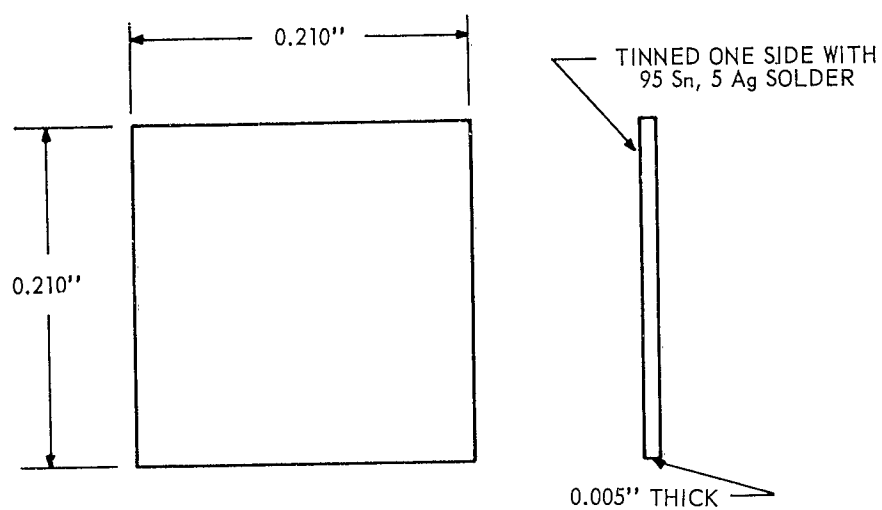
a. TYPE a
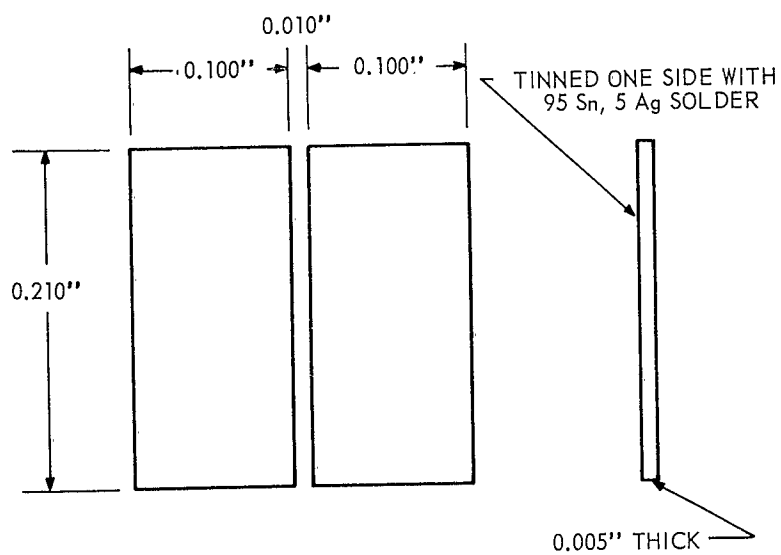
b. TYPE b

Figure 27. Copper Conductors

They are kept in position and held in the cavity by a thin film of silicon grease. This concludes the loading of the parts into the jig.

7.3.2 The base part of the jig and the top plate are now placed on the hot plate which is held at a temperature of $190^{\circ}C$ and monitored by a surface temperature thermometer. A small amount of stannous fluoborate flux is applied to the copper conductors' tinned surfaces. When the flux begins to evaporate, the top plate is placed in position on the jig base. The plate is oriented such that the copper conductors bear the proper relation to the elements for series connections. By this time the contact alloy on the ends of the elements has melted and the top may be pushed down (very carefully and gently) until it bottoms flat against the inner surface of the jig. The two 4/40 screws are placed in and tightened down gently assuring absolute bottoming and flatness of the top plate. This assures parallel device surfaces and eliminates any excess thickness not caused by improperly sized parts.

The surface-temperature thermometer is placed on top of the closed jig and the jig is allowed to remain on the hot plate until the top of the jig as measured by the surface thermometer is at $190^{\circ}C$. This requires approximately one minute. The jig is then removed and placed on a cooling block where the temperature of the jig is reduced to approximately $50^{\circ}C$ in one minute.

7.3.3 The jig is unloaded. Because of the presence of flux in the jig, the devices usually stick in the jig. Acetone is used to free these devices by applying a small quantity to the areas which are sticking.

7.3.4 The assembled TEB is then cleaned in hot (80° to 90°C) de-ionized water for 15 minutes, then rinsed with methanol and dried. An additional cleaning step is used. The device is lightly blasted all over with an Airbrasive Unit, using No. 1 abrasive. The Airbrasive Unit is shown in figure 28. This cleans the last vestige of foreign material from the ceramic, copper, and element areas of the TEB. A final rinse in methanol is used.

Step 8. Encapsulation

    8.1 Equipment

        8.1.1 Stereoscopic microscope, 20X.

        8.1.2 Tweezers, fine.

        8.1.3 Epoxy resin applicator (round toothpick).

        8.1.4 Oven, 100°C.

    8.2 Materials

        8.2.1 TEB assemblies.

        8.2.2 Three-mil glass encapsulation subassemblies.

        8.2.3 Epoxy resin, Armstrong Type A-1 and Activator A, Armstrong Products Co., Warsaw, Ind.

    8.3 Procedure

        8.3.1 Two glass encapsulation subassemblies, each consisting of two 3-mil-thick pieces of glass bonded to each other at right angles with epoxy resin (see figures 11 and 29), are used. The operation is performed under the microscope. The area on the substrate which will be directly under the glass encapsulant is coated with a narrow line of Armstrong A-1 epoxy resin (mixed 3 drops of catalyst per gram) all the way
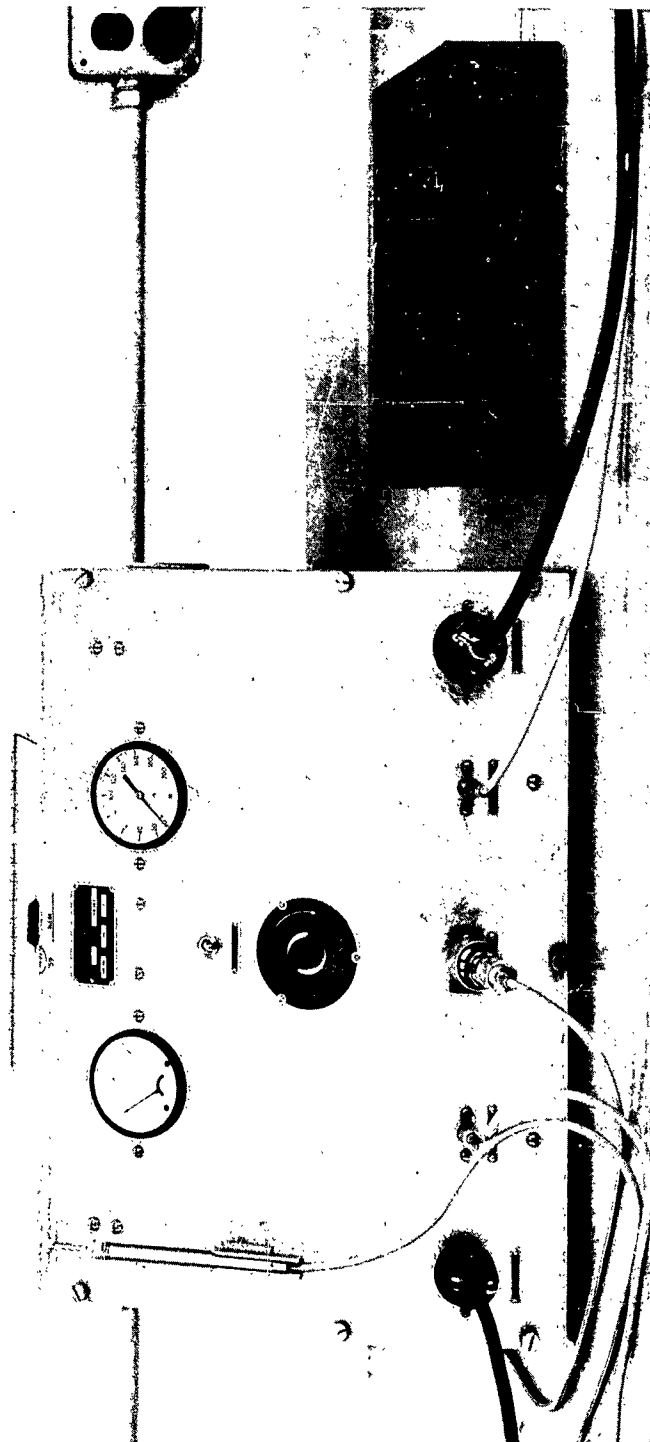
Figure 28. Airbrasive Unit
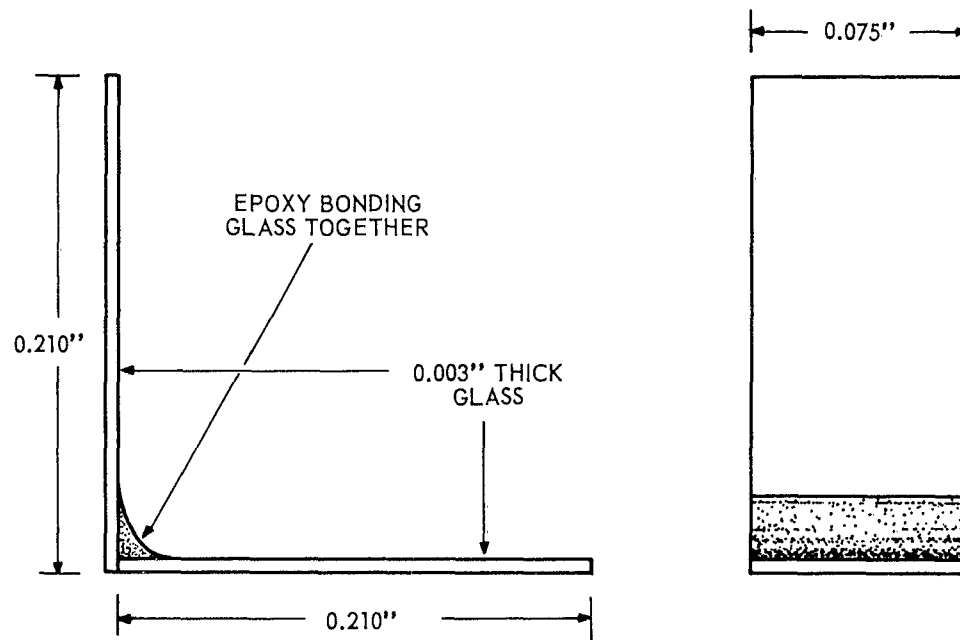
Figure 29.   Glass Encapsulation Subassembly

around, using a round toothpick as the applicator. The glass
subassemblies are placed in correct position on the device.

8.3.2 The units are placed in an oven
for one hour at $100^{\circ}C$. The TEB's are then removed from the
oven.

8.3.3 After cooling, more A-1 epoxy
is added, filling in any holes or gaps at the bottom and sealing
the glass to the copper conductors at the top.

8.3.4 The TEB's are placed back in
the oven and cured for one hour at $130^{\circ}C$. At the end of this
time, they are removed and allowed to cool.

Step 9. Evaluation and testing.

9.1 Equipment

9.1.1 Vacuum System (10^{-4} - 10^{-5} mm
Hg).

9.1.2 A-C and D-C power supplies.

9.1.3 A-C and D-C current and voltage
meters.

9.1.4 Potentiometer and sensitive
galvanometer, Model K-3, Leeds
and Northrup Co., Philadelphia,
Pa.

9.1.5 No. 40 gauge Chromel-Alumel
thermocouples.

9.2 Materials

9.2.1 TEB's, Types I, II, III, and IV.

9.2.2 Thermal grease, Dow Corning
type XC-20106.

9.3 Procedure

9.3.1 Figures 30, 31, and 32 are
applicable to this procedure. To determine the performance
of TEB's the devices are tested in a vacuum system (pressures
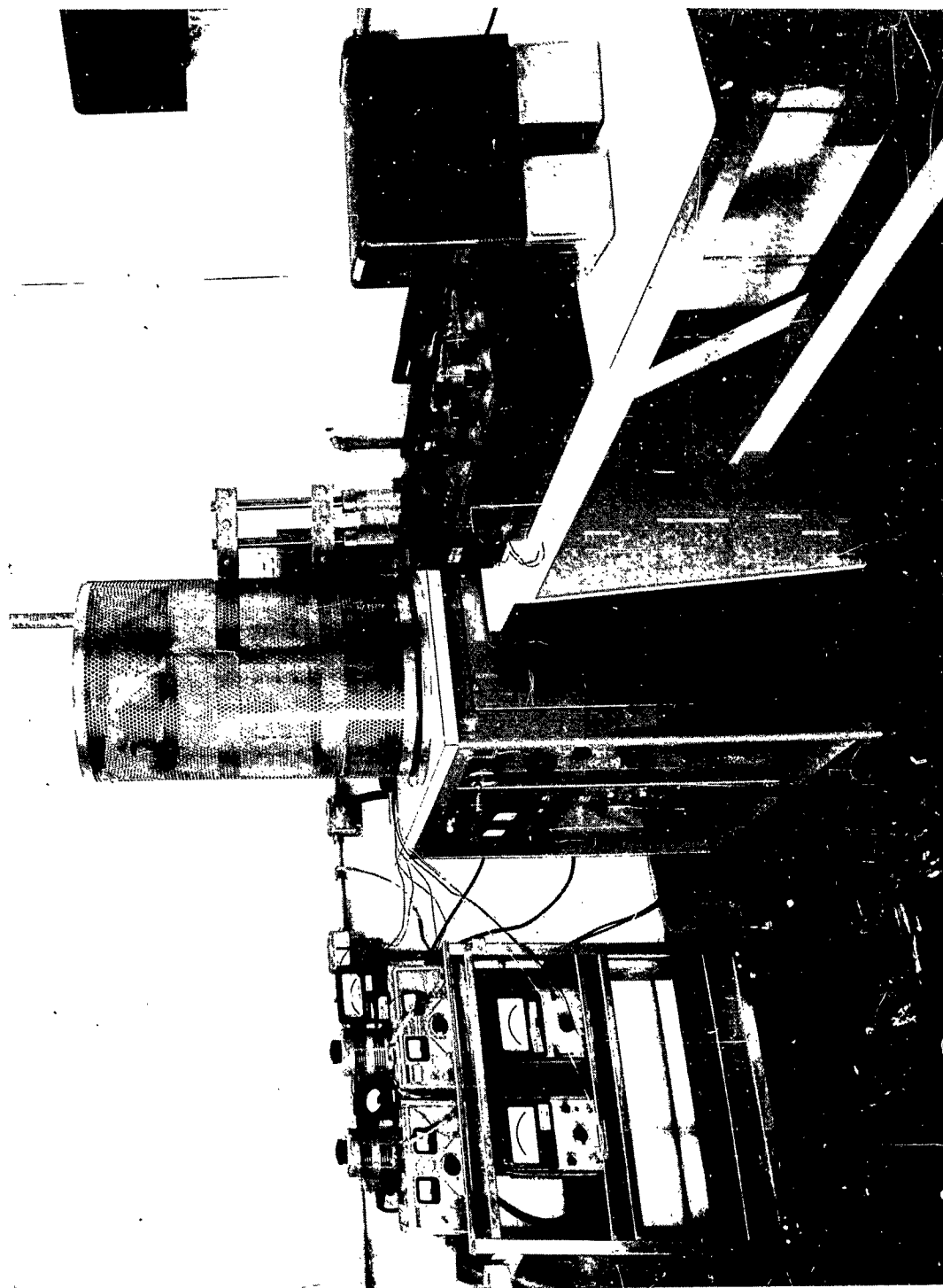
Figure 30.   TEB Evaluation System
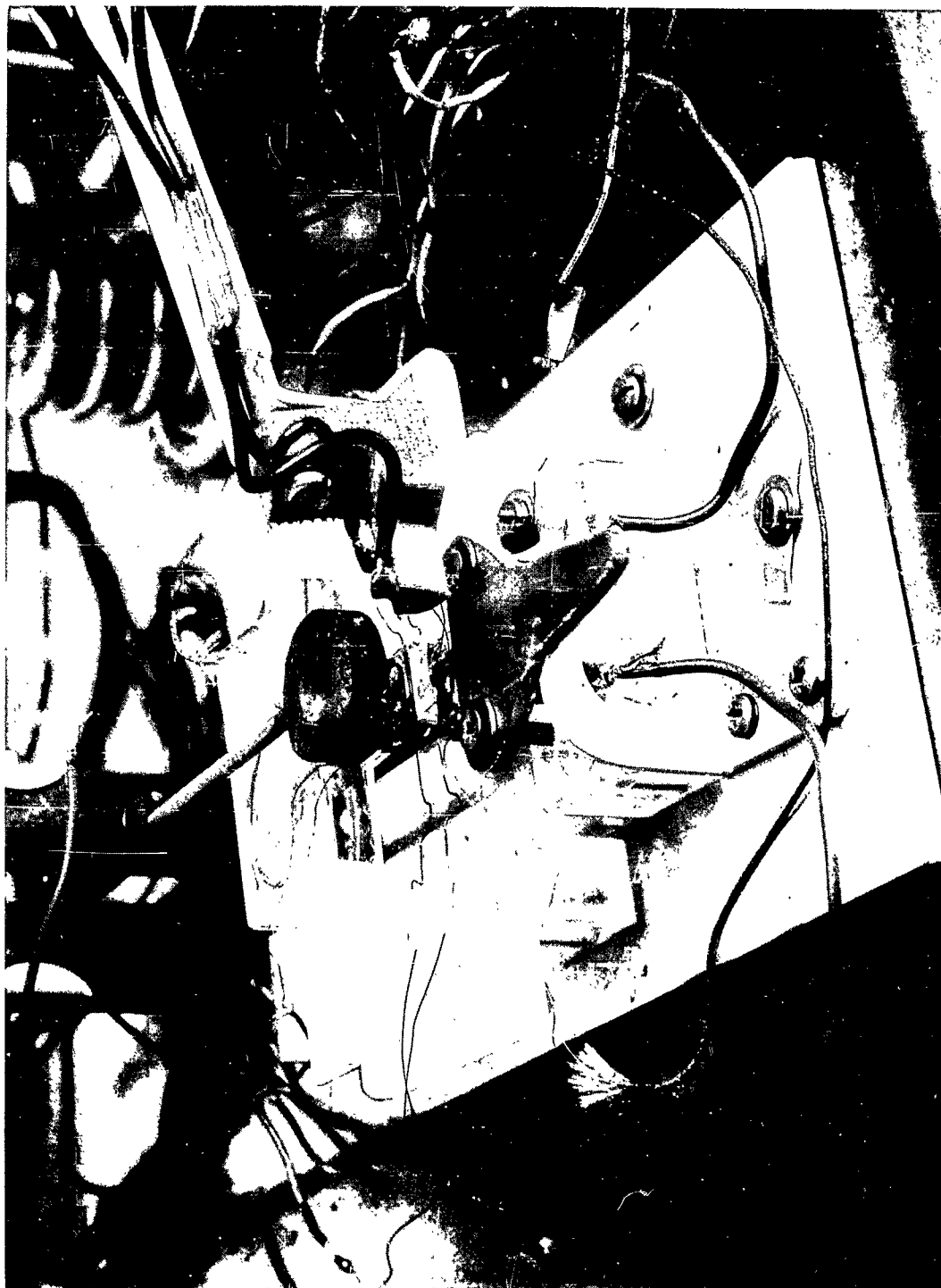
Figure 31.   TEB Performance Evaluator
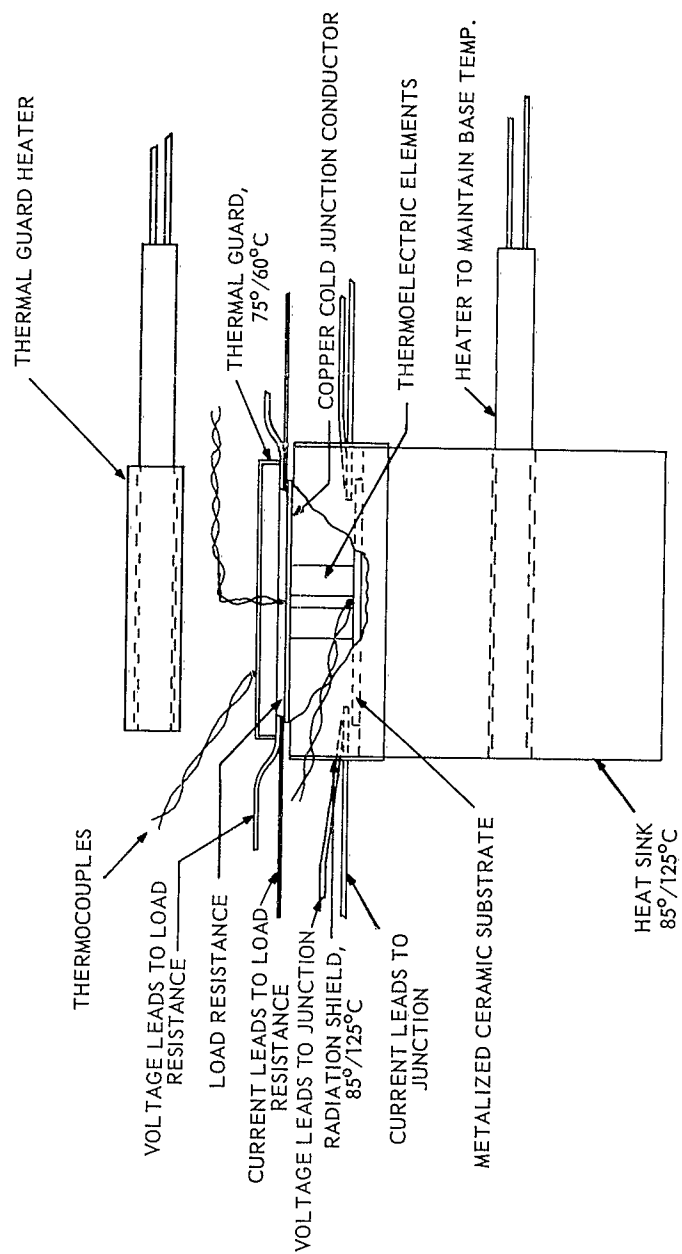
Figure 32.   TEB Evaluator — Thermal Guard Model

THERMAL GUARD HEATER

THERMAL GUARD, 75°/60°C

COPPER COLD JUNCTION CONDUCTOR

THERMOELECTRIC ELEMENTS

HEATER TO MAINTAIN BASE TEMP.

THERMOCOUPLES

VOLTAGE LEADS TO LOAD RESISTANCE

LOAD RESISTANCE

CURRENT LEADS TO LOAD RESISTANCE

VOLTAGE LEADS TO JUNCTION

RADIATION SHIELD, 85°/125°C

CURRENT LEADS TO JUNCTION

METALIZED CERAMIC SUBSTRATE

HEAT SINK 85°/125°C

120

of 10^{-3} to 10^{-5} mm of mercury were used with no detectable effect from varying the pressure between these limits). The actual operating conditions as defined in U.S. Army Signal Corps Technical Requirement SCL-7635 were simulated by the use of thermal shielding, thermal guards and a flat film resistor mounted directly against the cold junction of the TEB under evaluation with thermal grease. The load resistor is prepared by coating a thin section of mica (3/4 mil thick which is cut to the size of the TEB copper tops) with Aquadag. After drying, connections are made to the Aquadag film with DuPont Air-Dry Silver Conductive Paint. The basic evaluation setup is shown in figure 31. Number 40 gauge thermocouples were used to reduce heat leaks through the thermocouples. Many types of tests may be run in this test system to determine if the device meets the performance requirements under simulated operating conditions.

Considering the type IV units as an example, this is accomplished as follows: The heat sink is heated to a temperature of $125^{\circ}C$ by a resistance heater. A Peltier current is chosen within the current range where the type IV performance is expected to be achieved ($\underline{c}$ 1.5 amperes). Radiation shielding is used at the sides of the TEB. This shield is intimately attached to the heat sink so that the device sees approximately $125^{\circ}C$ from the sides.

The thermal guard is set at the cold junction temperature which is to be achieved: $75^{\circ}C$. This guard is above the TEB at the cold end. The load looks into this radiation condition.

The thermal load is set at 50 milliwatts by passing a current through the film resistor on top of the TEB. The load is determined by I x V. Then, to determine if performance

meets the specifications, it is necessary only to measure the
temperature of the thermal load resistor. At a current of
1.5 amperes the temperature of the thermal load is usually
less than $75^{\circ}C$. The C.O.P. may be determined by measuring
the device voltage.

$$C.O.P. = \frac{\dot{Q}}{IV} .$$

Additional testing may be carried out if desired, such
as the measurement of the temperature of the thermal load at
various electrical currents for given values of $\dot{Q}$. An alterna-
tive method is to adjust the current until the desired tempera-
ture of the thermal load is obtained (in this case $75^{\circ}C$) and
then note the current value. A reasonably accurate value for
$\Delta T_{(max)}$ at $\dot{Q} = 0$, (neglecting radiation loss) may be obtained
by removing the thermal load and varying the current until a
minimum T_c is achieved. To do this, T_h should be maintained
at the specified hot junction temperature. Approximate device
Z may be determined from the $\Delta T_{(max)}$ measurement since:

$$\Delta T_{(max)} = 1/2 \ Z \ T_c^2 .$$

In addition, an extremely simple and reasonably accurate
estimate of performance may be made by measuring only the
voltage drop with no thermal load and T_h at the specified
temperature. The voltage drop corresponding to normal per-
formance is determined by measuring actual operating performance
as described above on several devices. A device voltage drop
deviation either higher or lower than the normal range indi-
cates a defective device. A lower voltage drop indicates bad
or degraded thermoelectric material. A higher than normal
voltage drop indicates high contact resistance. It is, of

course, possible to have a defective device whose voltage drop would fall in the "normal" range. In all of the devices tested none were found which fell in this category. The performance of these devices can be definitely established, however, by this simple technique if followed by the additional simple measurement of A-C resistance. By doing this, this method can be considered an acceptable estimate of device performance. This type of measurement is considerably simpler and less time-consuming than the standard technique described above, though less accurate.

A "heat leak" type of TEB evaluation system was tried. This method was found to be as difficult and as time-consuming as the thermal guard system described previously. Reasonably good agreement was obtained (10%) when the same device was tested in both systems to determine the current that gave the desired performance. Better TEB performance was measured using the heat-leak system.

The heat-leak method used a hot junction heat source similar to that used in the thermal guard system. The thermal guards at the sides of the TEB were used as in the other system. The resistor thermal load and cold junction thermal guard were not used. A square cross-section piece of stainless steel alloy 304 was used as the heat leak. The area of the heat leak was the same as the area of the cold junction. Using the known thermal conductivity of the stainless steel, the distance necessary to provide a 10°C temperature difference with a 50 milliwatt heat flow through the leak was calculated. A No. 40 thermocouple was placed into the heat leak at the required distance from the end. A source of heat was placed at the upper end of the square stainless steel rod. This steel

thermal leak was placed in intimate contact against the TEB under test, with thermal grease. A No. 40 Chromel-Alumel thermocouple was placed at the interface of the heat leak and the TEB cold junction. This heat-leak system is pictured in figure 33.

The hot junction temperature had been maintained at $125^{\circ}C$. The TEB current was then adjusted to the value that gave a $10^{\circ}C$ ΔT between the heat-leak thermocouples. This current then became the value at which the desired TEB performance was obtained.

9.3.2 After evaluation, the thermal grease and oxides are removed from the copper conductors by light blasting with the Airbrasive Unit. The TEB's are now ready for application.

4.4.3.4 <u>Subassembly Operations</u>: The following subassembly operations are a part of the process for constructing TEB's:

a. Preparation of Metallized Micromodule Substrates

Standard 0.010" thick micromodule substrates were purchased with a moly-manganese metallized area. See figure 34. The moly-manganese metallization is supplied plated with copper to facilitate soldering.

The Airbrasive unit is used to cut the desired conductor pattern in the metallization. Figures 35 and 36 show the pattern for the one-junction and two-junction TEB's, respectively. After the pattern has been cut, the pattern is tinned with a thin coating of 95% Sn, 5% Ag solder using standard rosin-alcohol flux. The flux residue is removed with methanol.

b. Preparation of Copper Conductors

Pure annealed copper, 0.005" thick, is used. It is tinned with a thin coat of 95% Sn, 5% Ag solder using
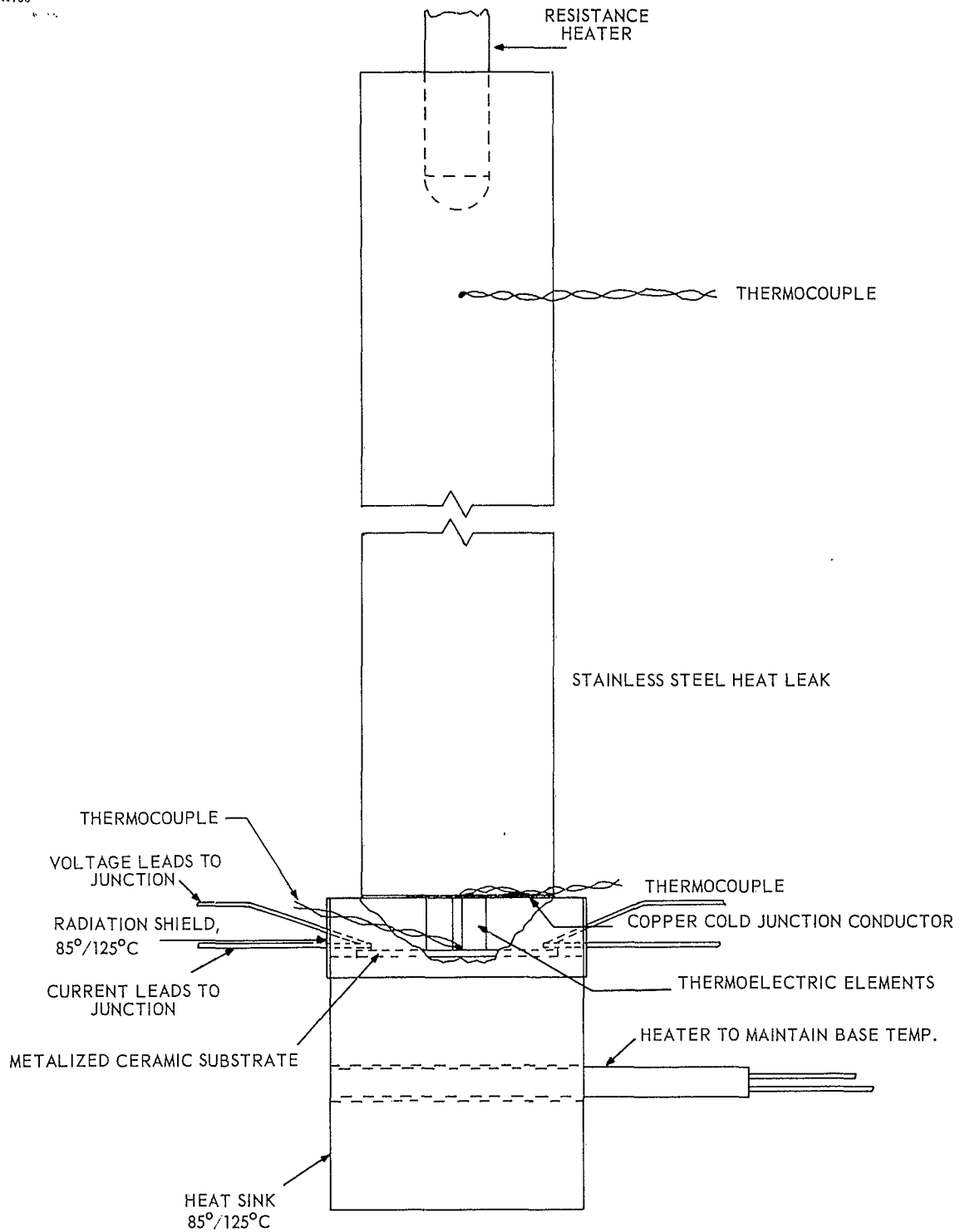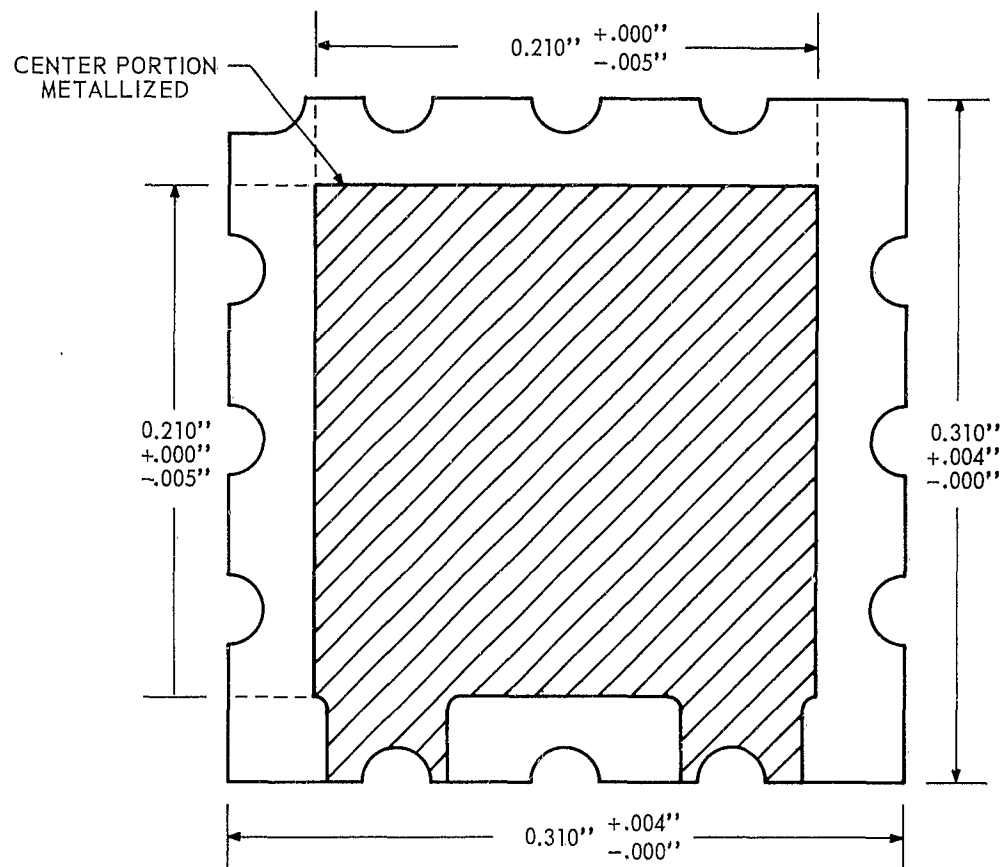
Figure 33.   Heat Leak-Type TEB Tester

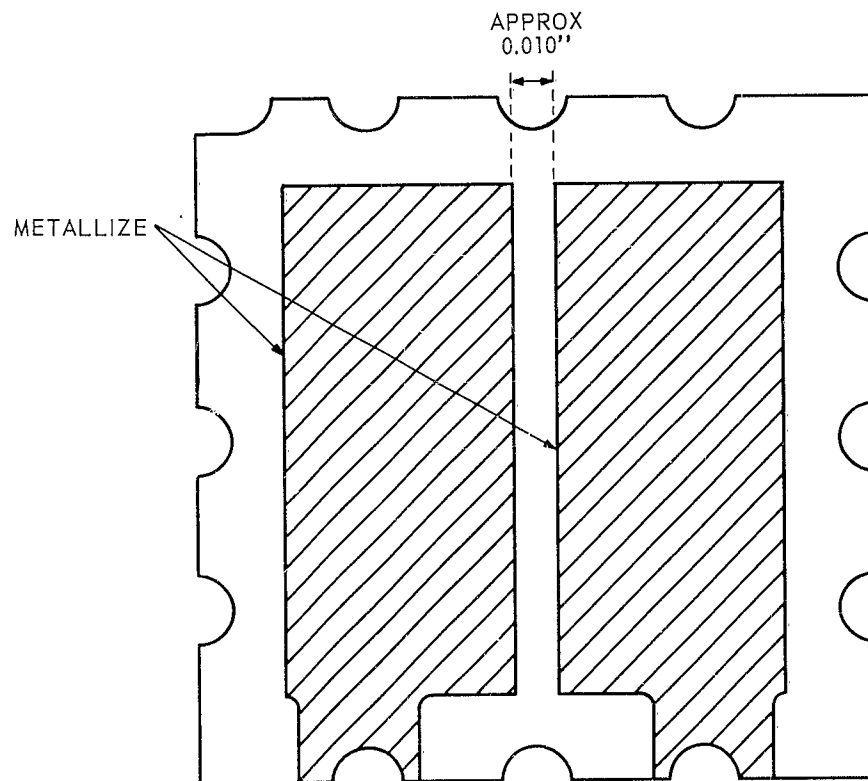Figure 34. Micromodule Substrate, Metalized

Figure 35.   TEB Substrate Pattern (Single Junction)
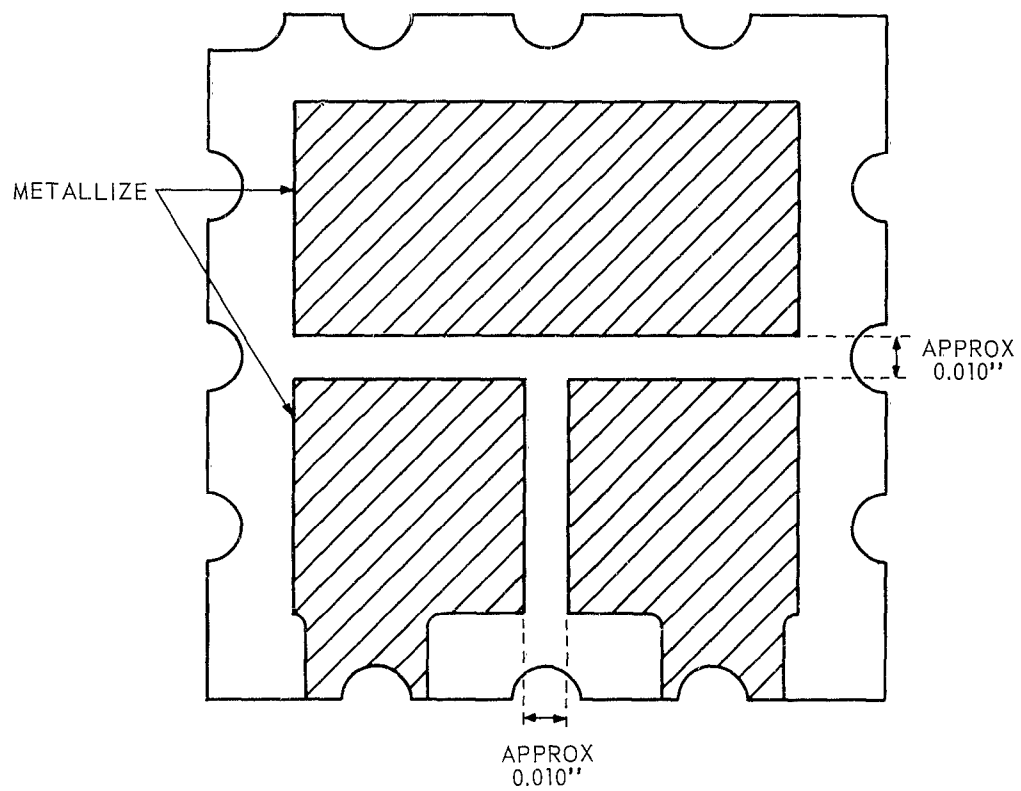
METALLIZE

APPROX
0.010"

APPROX
0.010"

Figure 36.   TEB Substrate Pattern (Two Junction)

rosin-alcohol flux. After tinning, the copper material is cleaned in methanol.

The parts (0.210" x 0.210" for one junction TEB's and 0.100" x 0.210" for two junction TEB's) are punched out on a small hand press specially made for the job. See figure 37.

c. Preparation of 3 Mil Glass Subassemblies

Microscope cover glass, 0.003" thick, is cut into 0.075" x 0.210" pieces on the crystal slicing machine.

The glass is assembled into 90° V-shaped pieces by bonding with A-1 epoxy resin. They are then painted lightly for purposes of identification. The glass subassemblies are shown in figures 11 and 29.

4.4.4 <u>Safety and Other Manufacturing Precautions</u>

The materials which are used in the TEB process offer no unusual hazards. The precautions required for the handling of the materials involved are those standard procedures which are common laboratory and industrial practice, e.g., the handling of flammable solvents.

The bismuth-telluride alloys which constitute the heart of the TEB's are not considered a serious hazard. Tellurium, a component of the Bi_2Te_3 compound, is quite toxic. Therefore, care is taken to eliminate the ingestion of Bi_2Te_3 via any port. Precautions must be taken to keep Bi_2Te_3 particles from open wounds or the ingestion of Bi_2Te_3 dust through the respiratory system. The precautions are:

1. Cover all wounds when working with Bi_2Te_3.

2. Wash hands thoroughly after handling Bi_2Te_3.

3. Perform any operations wet that result in the formation of Bi_2Te_3 dust.
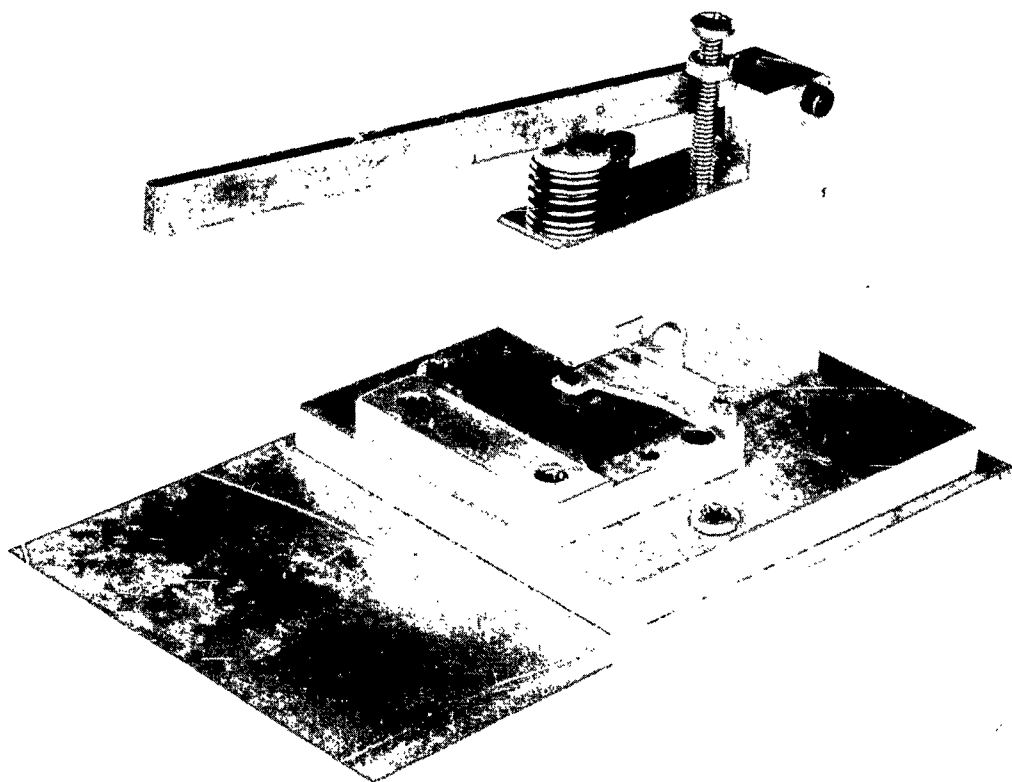
Figure 37. Hand Punch For Copper Conductor Pieces

One other possible hazard exists which results from heating
the material or a device containing the material to the vicinity
of its melting point (585°C). At this temperature the partial
decomposition of the compound and the sublimation of the tel-
lurium occurs. In this regard, the degree of seriousness of
the hazard is similar to that of selenium rectifier burnouts.
No normal operation results in the attainment of such tempera-
tures nor do any of the processing steps require any temperatures
great enough to cause the release of tellurium vapors.

4.5 Evaluation of Experimental TEB's

4.5.1 Results

The data presented in the following subparagraphs was taken with the evaluation systems and using the measurement techniques described in subparagraph 4.4.3.3, step 9.

4.5.1.1 Initial Experimental TEB's: The early experimental devices were capable of meeting the specified performances for TEB's, although they were not as good as the units produced later. Figure 38 shows the characteristics, ΔT vs. I, for a typical early two junction experimental TEB. At the lower currents, the performance was as good as the superior units produced later. At the higher currents, the performance falls off, probably because of increased Joule heating due to greater contact resistance.

4.5.1.2 Interim Experimental TEB Samples Supplied to USAELRDL: With process improvements, better device performance was obtained because of the development of superior contacting procedures (4.4.3.3). Two samples of these improved TEB's were supplied to USAELRDL for evaluation. These were two-junction type TEB's, the performance of which is shown in figures 39, 40, and 41. Figure 39 shows ΔT vs. I for three different thermal loads. Figure 40 is the curve for zero applied thermal load from which $\Delta T_{(max)}$ is obtained for the same device. Figure 41 shows ΔT vs. I with $\dot{Q} = 50$ mw only for a second sample device constructed the same as the first.

4.5.1.3 Final Prototype TEB's:

a. TEB's delivered for evaluation to USAELRDL.

The evaluations data for the 100 TEB's delivered to USAELRDL (25 each of TEB type I, II, III, and IV) is presented in tables XIII through XVI. The devices were evaluated

132

$T_h = 125°C$

$T_{TG} = 75°C$

$\dot{Q} - 50$ MW

COOLER CURRENT, I, AMPERES

\T VS. I CURVE FOR TYPICAL TEB, INITIAL EXPERIMENTAL MODEL
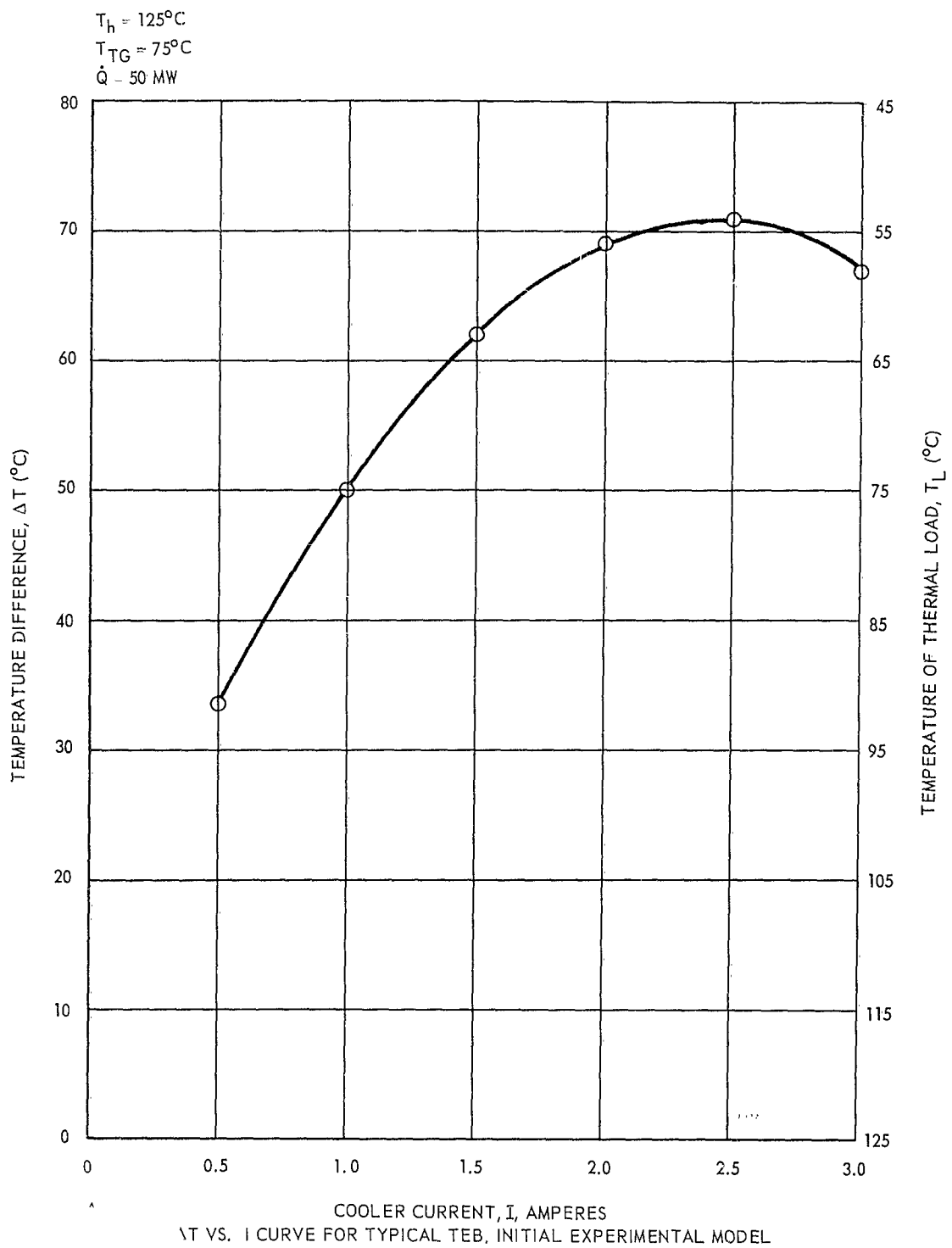
Figure 38. Δ T vs. I Curve For Typical TEB, Initial Experimental
Model (Two Junction)
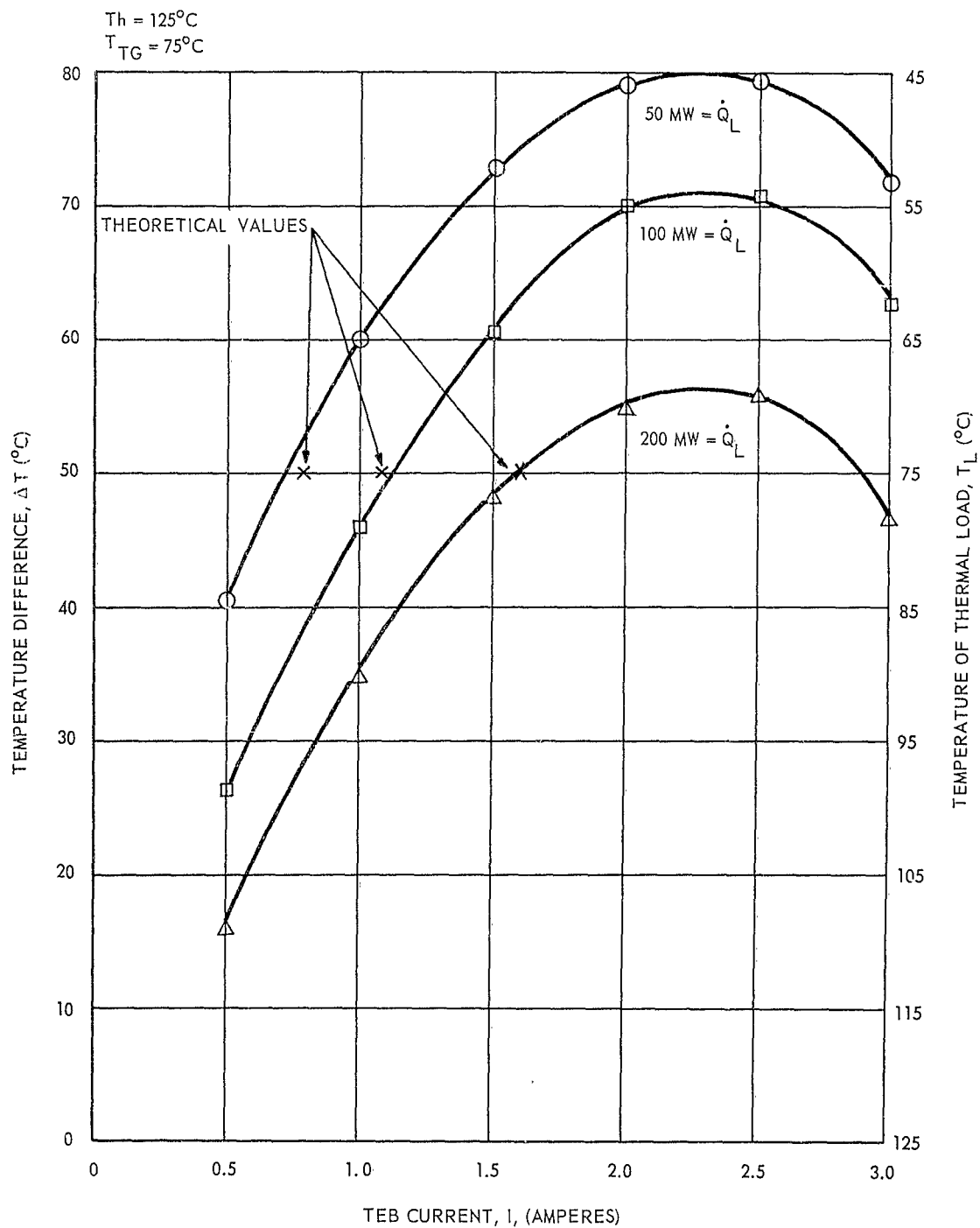
Figure 39.   Δ T vs. I Curve For Interim TEB Sample No. 1 Supplied to
USAELRDL (Two Junction)

Figure 40. Curve For $\Delta T_{(max)}$ Determination For Interim TEB Sample
No. 1 Supplied to USAELRDL (Two Junction)

135

$T_h = 125°C$

$T_{TG} = 75°C$

$\dot{Q}_L = 50$ MW

Figure 41. Δ T vs. I Curve For Interim TEB Sample No. 2 Supplied to USAELRDL (Two Junction)

136

Table XIII

PERFORMANCE DATA, TEB DEVICE, TYPE I (25 UNITS)

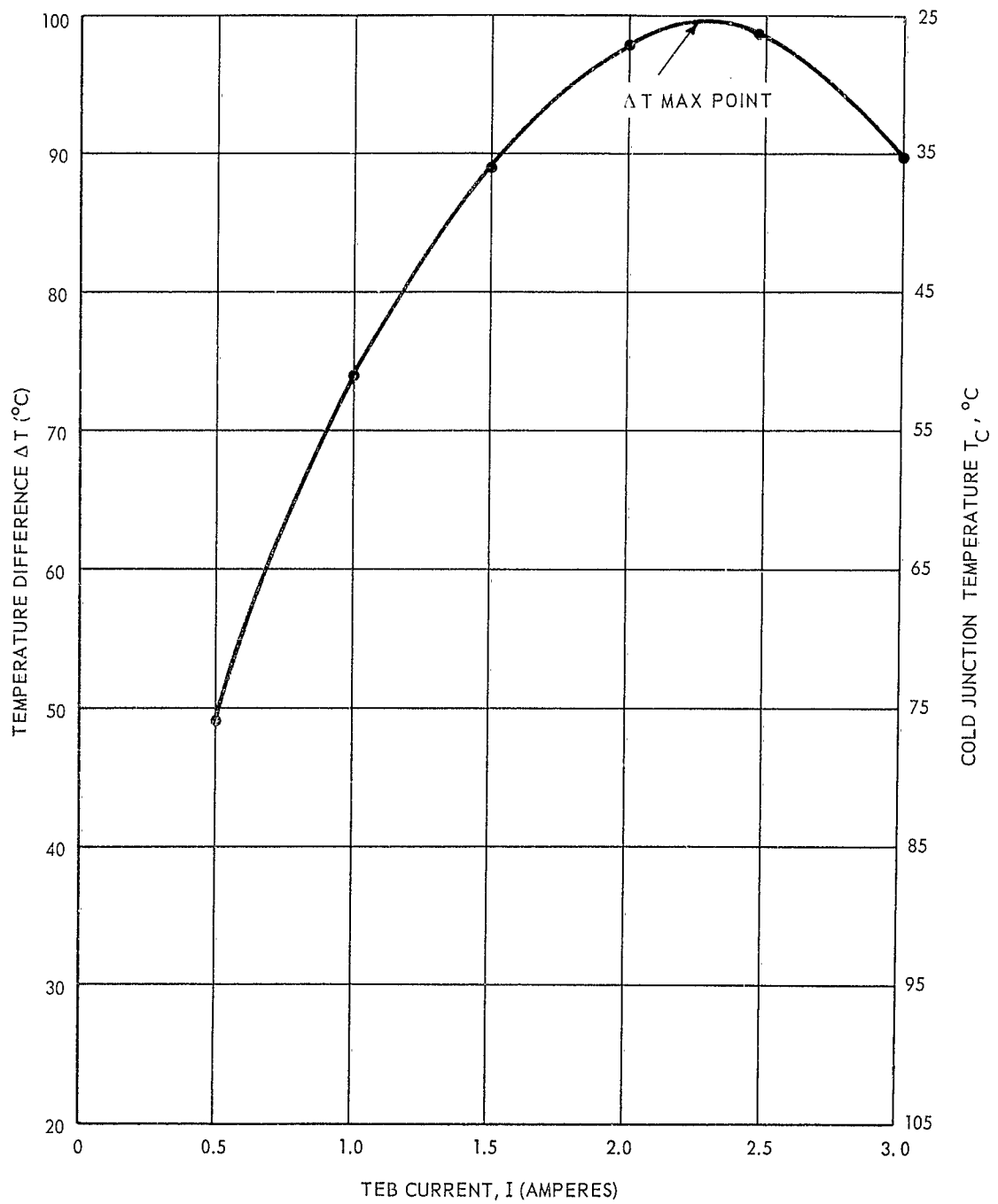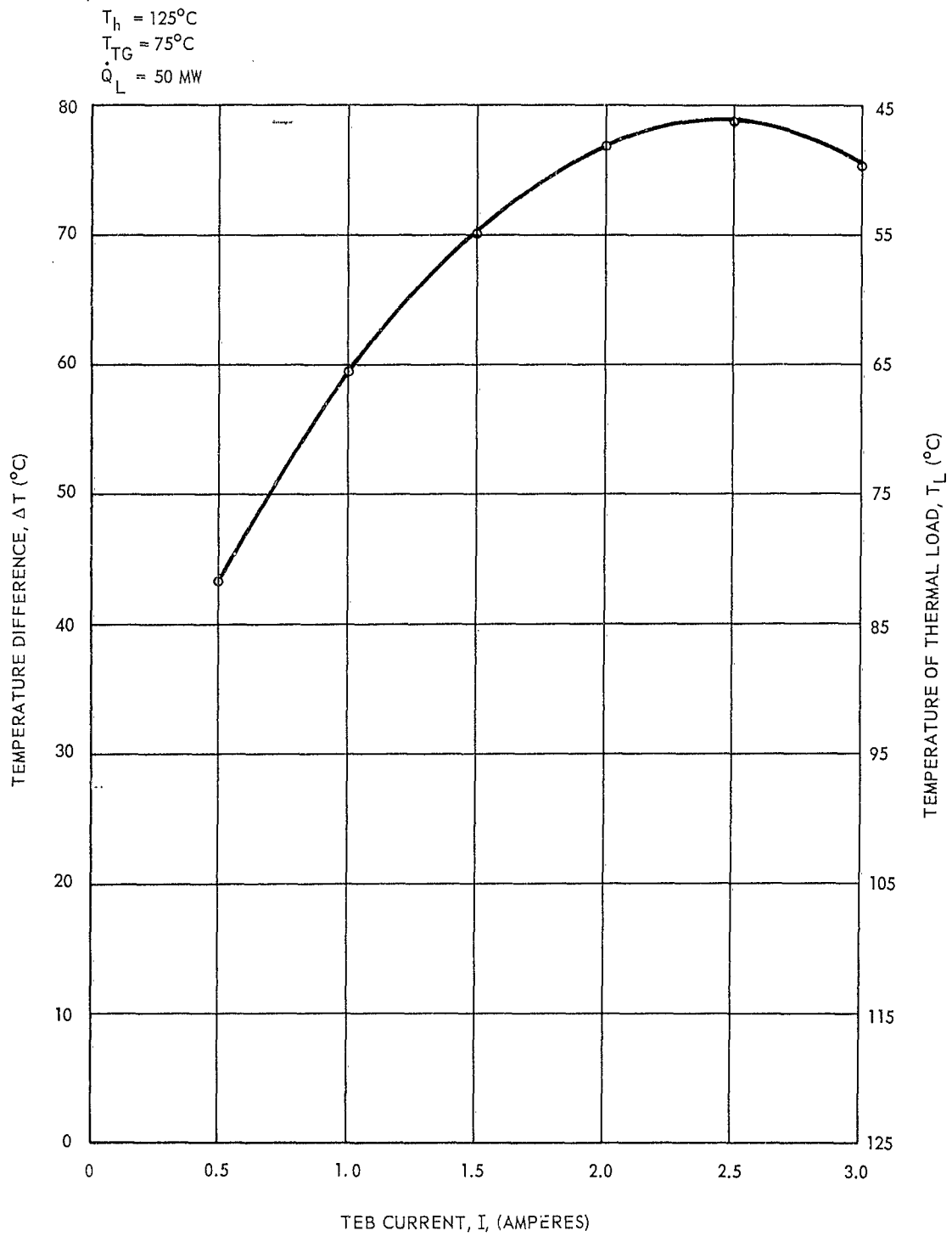| Device No.	I	V	T_c	T_h	$\dot{Q}$
I-1	1 Ampere	0.075 Volt	57.0°C	85°C	0.005 Watt
I-2	"	.110	--	"	"
I-3	"	.097	56.0	"	"
I-4	"	.080	58.0	"	"
I-5	"	.095	--	"	"
I-6	"	.092	--	"	"
I-7	"	.095	56.5	"	"
I-8	"	.097	--	"	"
I-9	"	.092	--	"	"
I-10	"	.080	--	"	"
I-11	"	.080	--	"	"
I-12	"	.075	57.8	"	"
I-13	"	.080	--	"	"
I-14	"	.080	--	"	"
I-15	"	.085	--	"	"
I-16	"	.080	--	"	"
I-17	"	.082	57.5	"	"
I-18	"	.080	58.0	"	"
I-19	"	.100	--	"	"
I-20	"	.100	--	"	"
I-21	"	.100	--	"	"
I-22	"	.085	56.0	"	"
I-23	"	.110	--	"	"
I-24	"	.095	59.0	"	"
I-25	"	.102	--	"	"

Table XIV

PERFORMANCE DATA, TEB DEVICE, TYPE II (25 UNITS)

Device No.	I	V	T_c	T_h	$\dot{Q}$
II-1	1.5 Amperes	0.13 Volt	--	85°C	0.050 Watt
II-2	"	.12	59.3	"	"
II-3	"	.13	--	"	"
II-4	"	.14	59.0	"	"
II-5	"	.13	--	"	"
II-6	"	.12	--	"	"
II-7	"	.13	58.0	"	"
II-8	"	.13	--	"	"
II-9	"	.13	--	"	"
II-10	"	.12	58.2	"	"
II-11	"	.13	58.5	"	"
II-12	"	.12	59.0	"	"
II-13	"	.13	--	"	"
II-14	"	.12	--	"	"
II-15	"	.13	57.5	"	"
II-16	"	.12	--	"	"
II-17	"	.13	--	"	"
II-18	"	.13	58.8	"	"
II-19	"	.12	--	"	"
II-20	"	.12	--	"	"
II-21	"	.12	59.0	"	"
II-22	"	.12	--	"	"
II-23	"	.13	--	"	"
II-24	"	.14	56.0	"	"
II-25	"	.12	--	"	"

138

Table XV

PERFORMANCE DATA, TEB DEVICE, TYPE III (25 UNITS)

Device No.	I	V	T_c	T_h	$\dot{Q}$
III-1	1 Ampere	0.190 Volt	72.0°C	125°C	0.010 Watt
III-2	"	.195	71.0	"	"
III-3	"	.180	--	"	"
III-4	"	.200	70.5	"	"
III-5	"	.180	--	"	"
III-6	"	.180	--	"	"
III-7	"	.180	74.0	"	"
III-8	"	.200	--	"	"
III-9	"	.180	74.6	"	"
III-10	"	.195	--	"	"
III-11	"	.195	72.0	"	"
III-12	"	.190	--	"	"
III-13	"	.200	--	"	"
III-14	"	.195	72.5	"	"
III-15	"	.180	--	"	"
III-16	"	.190	72.0	"	"
III-17	"	.180	--	"	"
III-18	"	.185	--	"	"
III-19	"	.185	--	"	"
III-20	"	.190	--	"	"
III-21	"	.190	--	"	"
III-22	"	.185	73.5	"	"
III-23	"	.185	72.8	"	"
III-24	"	.190	--	"	"
III-25	"	.195	--	"	"

Table XVI

PERFORMANCE DATA, TEB DEVICE, TYPE IV (25 UNITS)

Device No.	I	V	T_c	T_h	$\dot{Q}$
IV-1	1.5 Amperes	0.28 Volt	71.0°C	125°C	0.050 Watt
IV-2	"	.27	--	"	"
IV-3	"	.27	--	"	"
IV-4	"	.28	71.5	"	"
IV-5	"	.28	--	"	"
IV-6	"	.27	--	"	"
IV-7	"	.27	71.0	"	"
IV-8	"	.28	70.0	"	"
IV-9	"	.28	--	"	"
IV-10	"	.27	70.5	"	"
IV-11	"	.28	--	"	"
IV-12	"	.27	--	"	"
IV-13	"	.28	--	"	"
IV-14	"	.27	68.2	"	"
IV-15	"	.28	--	"	"
IV-16	"	.27	71.2	"	"
IV-17	"	.27	--	"	"
IV-18	"	.28	--	"	"
IV-19	"	.28	70.2	"	"
IV-20	"	.27	--	"	"
IV-21	"	.26	--	"	"
IV-22	"	.29	--	"	"
IV-23	"	.28	68.0	"	"
IV-24	"	.27	--	"	"
IV-25	"	.28	67.8	"	"

by measuring the voltage on each device and then by measuring the T_c at a given current under the operating conditions specified for TEB types I, II, III, and IV.

b. Complete TEB Evaluations.

Twelve devices of the same kind as delivered to USAELRDL were evaluated to a much more complete degree. The results for these units are given in figures 42 through 49. Figures 42 through 45 show the ΔT vs. I characteristics for constant $\dot{Q}$ values of 5, 10, or 50 mw. Figures 46 through 49 show the ΔT vs. $\dot{Q}$ curves at various constant currents for some of the same devices, taken from the previous data. These equations are linear according to the relationship given by Ioffe[35],

$$\Delta T = \Delta T_{(max)} - \frac{\dot{Q}}{K} .$$

In these figures, data is also given for $\Delta T_{(max)}$ for $\dot{Q} = 0$. The devices are distinguished by several numbers after the letters TEB. The first number I, II, III, or IV represents the device type as defined by table X, the second number is that of the device, i.e., one through twelve. Finally, the letters C or D indicate, respectively, whether the device was tested without or with its glass encapsulation. This code also applies to the final prototype TEB's delivered to USAELRDL.

4.5.2 Discussion of Results

4.5.2.1 Introduction: The usual equation giving device performance under type I to IV operating conditions is

$$\dot{Q} + K\Delta T + 1/2 \, I^2 \, r' = \overline{S} T_c I$$

where $\overline{S}$, K, r' refer to the thermoelectric material and $\dot{Q}$ refers to the applied heat load.

141

TEB-1-2 C&D

FOR Q̇=0 { (C) ΔT MAX = 83.6° AT 2.4A
{ (D) ΔT MAX = 51.6° AT 2.35A

TEMPERATURE OF THERMAL LOAD, TL (°C)

TEMPERATURE DIFFERENCE ΔT (°C)

TEB CURRENT, I (AMPERES)

TEB - TYPE I - NO. 2, Tc AND ΔT vs I (AT Q̇=5mw AND Th=85°C)

TEB-1-2-C

TEB-1-2-D

SPEC LIMIT

Th = 85°C
TTG = 60°C
Q̇L = 5 MW

TEB-1-4 C&D

FOR Q̇=0 { (C) ΔT MAX = 72.4° AT 2.2A
{ (D) ΔT MAX = 46.3° AT 2.45A

TEMPERATURE OF THERMAL LOAD, TL (°C)

TEMPERATURE DIFFERENCE ΔT (°C)

TEB-I-4C

TEB-I-4D

SPEC LIMIT

Th = 85°
TTG = 60°C
Q̇L = 5 MW

TEB-1-1 C&D

FOR Q̇=0 { (C) ΔT MAX = 84.5° AT 2.55A
{ (D) ΔT MAX = 58° AT 2.4A

TEMPERATURE OF THERMAL LOAD, TL (°C)

TEMPERATURE DIFFERENCE ΔT (°C)

TEB CURRENT, I (AMPERES)

TEB - TYPE I - NO. 1, Tc AND ΔT vs I (AT Q̇=5mw AND Th=85°)

TEB-I-1-C

TEB-I-1-D

SPEC LIMIT

Th = 85°C
TTG = 60°C
Q̇L = 5mw

TEB-1-3 C&D

FOR Q̇=0 { (C) ΔT MAX 84.4° AT 2A
{ (D) ΔT MAX 57.6° AT 2.25A

TEMPERATURE OF THERMAL LOAD, TL (°C)

TEMPERATURE DIFFERENCE ΔT (°C)

TEB-I-3-C

TEB-I-3-D

SPEC LIMIT

Th = 85°C
TTG = 60°C
Q̇L = 5 MW

1

Figure 42. Performance Data, TEB, Type I

TEMPERATURE OF THERMAL LOAD, T_L (°C)

TEB-II-2 C&D

FOR Q̇=0 { (C) ΔT MAX = 83.8° AT 2.4A
(D) ΔT MAX = 51.0° AT 2.35A

TEB-II-2-C

TEB-II-2-D

SPEC LIMIT

TEB CURRENT, I (AMPERES)

TEB-TYPE II NO 2, T_c AND ΔT vs. I AT Q̇=50mw AND T_h=85°C

TEMPERATURE DIFFERENCE ΔT (°C)

T_h=85°C
T_{TG}=60°C
$Q̇_L$=50 MW

TEMPERATURE OF THERMAL LOAD, T_L (°C)

TEB-II-4C&D

FOR Q̇=? { (C) ΔT MAX = 72.0° AT 2.2A
(D) ΔT MAX = 46.3° AT 2.45A

SPEC LIMIT

TEB-II-4-C

TEB-II-4-D

TEMPERATURE DIFFERENCE ΔT (°C)

T_h=85°C
T_{TG}=60°C
$Q̇_L$=50 MW

TEMPERATURE OF THERMAL LOAD, T_L (°C)

TEB-II-1-C&D

FOR Q̇=0 { (C) ΔT MAX = 84.5° AT 2.55A
(D) ΔT MAX = 58° AT 2.4A

TEB-II-1-C

TEB-II-1-D

SPEC LIMIT

TEB CURRENT, I (AMPERES)

TEB-TYPE II-NO. 1, T_c AND ΔT vs. I AT Q̇=50mw AND T_h=82°C

TEMPERATURE DIFFERENCE ΔT (°C)

T_h=85°C
T_{TG}=60°C
$Q̇_L$=50 MW

TEMPERATURE OF THERMAL LOAD, T_L (°C)

TEB-II-3-C&D

FOR Q̇=? { (C) ΔT MAX = 84.4° AT 2.25A
(D) ΔT MAX = 57.6° AT 2.25A

TEB-II-3-C

TEB-II-3-D

SPEC LIMIT

TEMPERATURE DIFFERENCE ΔT (°C)

T_h=85°C
T_{TG}=60°C
$Q̇_L$=50 MW

1

Figure 43.   Performance Data, TEB, Type II

143

R4647

TEB - III - 7 - C & D

FOR Q̇ ~ 0 {(C) ΔT MAX = 93.4° AT 2.15A / (D) ΔT MAX = 73.9° AT 2.05A}

TEMPERATURE OF THERMAL LOAD, T_L (°C)

TEB - III - 7 - C

TEB - III - 7 - D

SPEC LIMIT

T_h = 125°C
T_{TG} = 75°C
$\dot{Q}_L$ = 10 MW

TEMPERATURE DIFFERENCE, ΔT (°C)

TEB CURRENT, I (AMPERES)

TEB - TYPE III - NO. 7, T_c AND ΔT VS. I AT Q = 10MW AND T_h = 125°C

TEB - III - 9 - C & D

FOR Q̇ ~ 0 {(C) ΔT MAX = 91° AT 2.0A / (D) ΔT MAX = 67.9° AT 1.9A}

TEMPERATURE OF THERMAL LOAD, T_L (°C)

TEB - III - 9 - D

TEB - III - 9 - C

SPEC LIMIT

T_h = 125°C
T_{TG} = 75°C
$\dot{Q}_L$ = 10 MW

TEMPERATURE DIFFERENCE ΔT (°C)

TEB - III - 6 - C

FOR Q̇ ~ 0 (C) ΔT MAX = 90.4° AT 2.5 A

TEMPERATURE OF THERMAL LOAD, T_L (°C)

TEB - III - 6 - C

SPEC LIMIT

T_h = 125°C
T_{TB} = 75°C
$\dot{Q}_L$ = 10 MW

TEMPERATURE DIFFERENCE ΔT (°C)

TEB CURRENT, I (AMPERES)

TEB - TYPE III - NO. 6, T_c AND ΔT VS. I AT Q = 10MW AND T_h = 125°C

TEB - III - 8 - C & D

FOR Q̇ ~ 0 {(C) ΔT MAX = 90.2° AT 2.25A / (D) ΔT MAX = 71.8° AT 2.2A}

TEMPERATURE OF THERMAL LOAD, T_L (°C)

TEB - III - 8 - D

TEB - III - 8 - C

SPEC LIMIT

T_h = 125°C
T_{TG} = 75°C
$\dot{Q}_L$ = 10 MW

TEMPERATURE DIFFERENCE ΔT (°C)

1

Figure 44. Performance Data, TEB, Type III

TEMPERATURE OF THERMAL LOAD, T_L (°C)

TEB - IV - 7 C&D
FOR $\dot{Q} \sim 0$ {(C): ΔT MAX = 73.9° AT 2.15A
{(D): ΔT MAX = 73.9° AT 2.05A

SPEC LIMIT

TEB - IV - 7 - D

TEB - IV - 7 - C

T_h = 125°C
T_{TG} = 75°C
$\dot{Q}_L$ = 50 MW

TEMPERATURE DIFFERENCE, ΔT (°C)

TEB CURRENT, I (AMPERE)
TEB - TYPE IV - NO. 7, T_c AND ΔT VS. I AT $\dot{Q}$ = 50MW, T_h = 125°C

TEMPERATURE OF THERMAL LOAD, T_L (°C)

TEB - IV - 9 - C&D
FOR $\dot{Q} \sim 0$ {(C): ΔT MAX = 91° AT 2.0A
{(D): ΔT MAX = 67.9° AT 1.9A

SPEC LIMIT

TEB - IV - 9 - D

TEB - IV - 9 - C

T_h = 125°C
T_{TG} = 75°C
$\dot{Q}_L$ = 50 MW

TEMPERATURE DIFFERENCE, ΔT (°C)

TEMPERATURE OF THERMAL LOAD, T_L (°C)

TEB - IV - 6 - C
FOR $\dot{Q} \sim 0$ (C) ΔT MAX = 90.4° AT 2.5A

SPEC LIMIT

TEB - IV - 6 - C

T_h = 125°C
T_{TG} = 75°C
$\dot{Q}_L$ = 50 MW

TEMPERATURE DIFFERENCE, ΔT (°C)

TEB CURRENT, I (AMPERES)
TEB - TYPE IV - NO. 6, T_c AND ΔT VS. I AT $\dot{Q}$ = 50MW, T_h = 125°C

TEMPERATURE OF THERMAL LOAD, T_L (°C)

TEB - IV - 8 - C&D
FOR $\dot{Q} \sim 0$ {(C): ΔT MAX = 90.2° AT 2.25A
{(D): ΔT MAX = 71.8° AT 2.2A

SPEC LIMIT

TEB - IV - 8 - D

TEB - IV - 8 - C

T_h = 125°C
T_{TG} = 75°C
$\dot{Q}_L$ = 50 MW

TEMPERATURE DIFFERENCE, ΔT (°C)

1

Figure 45. Performance Data, TEB, Type IV
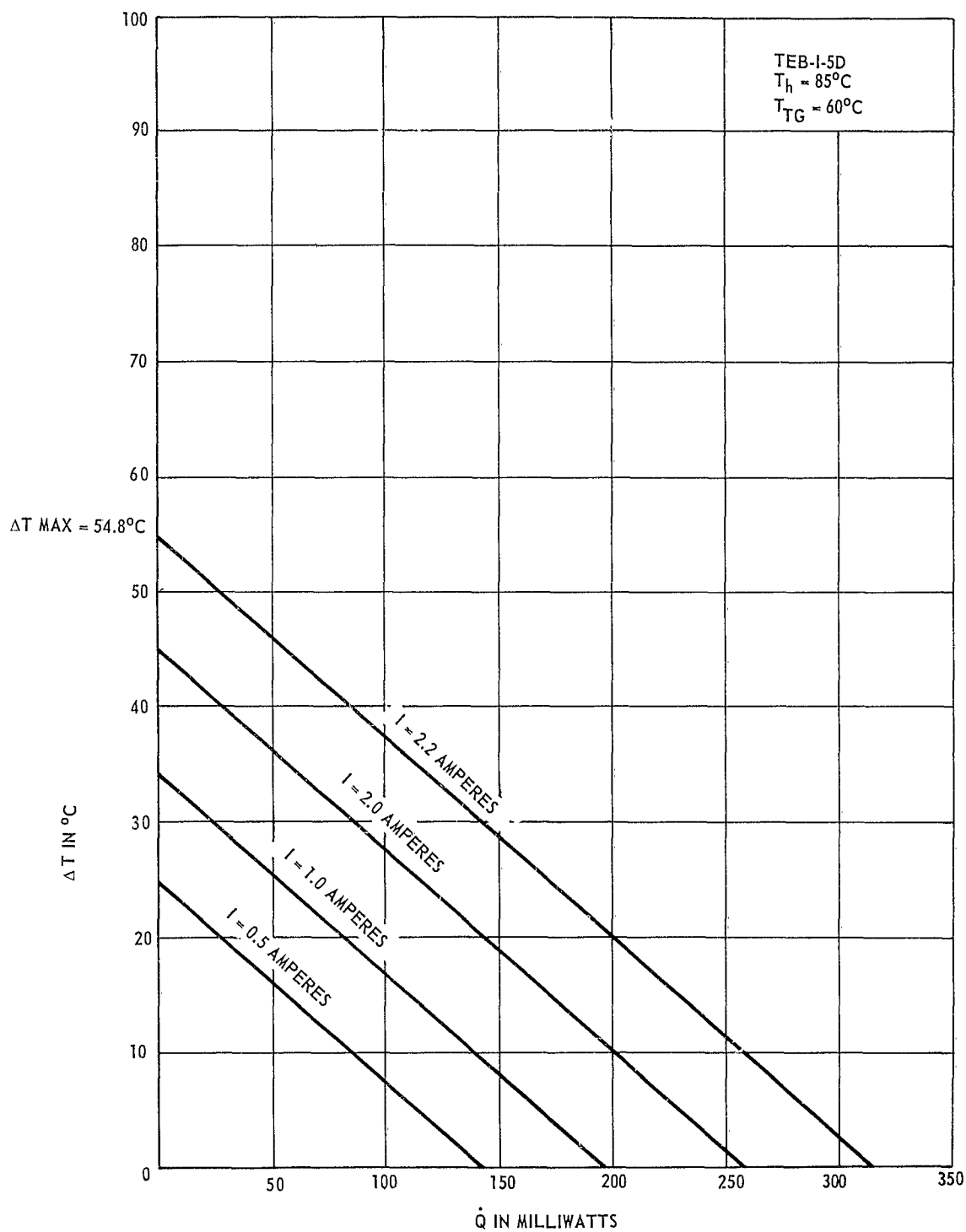
Figure 46.   TEB, Type I-D, No. 5, $\dot{Q}$ vs. Δ T, With T_h = 85 °C, Showing
Typical Types I and II Performance With Glass Encapsulation

146
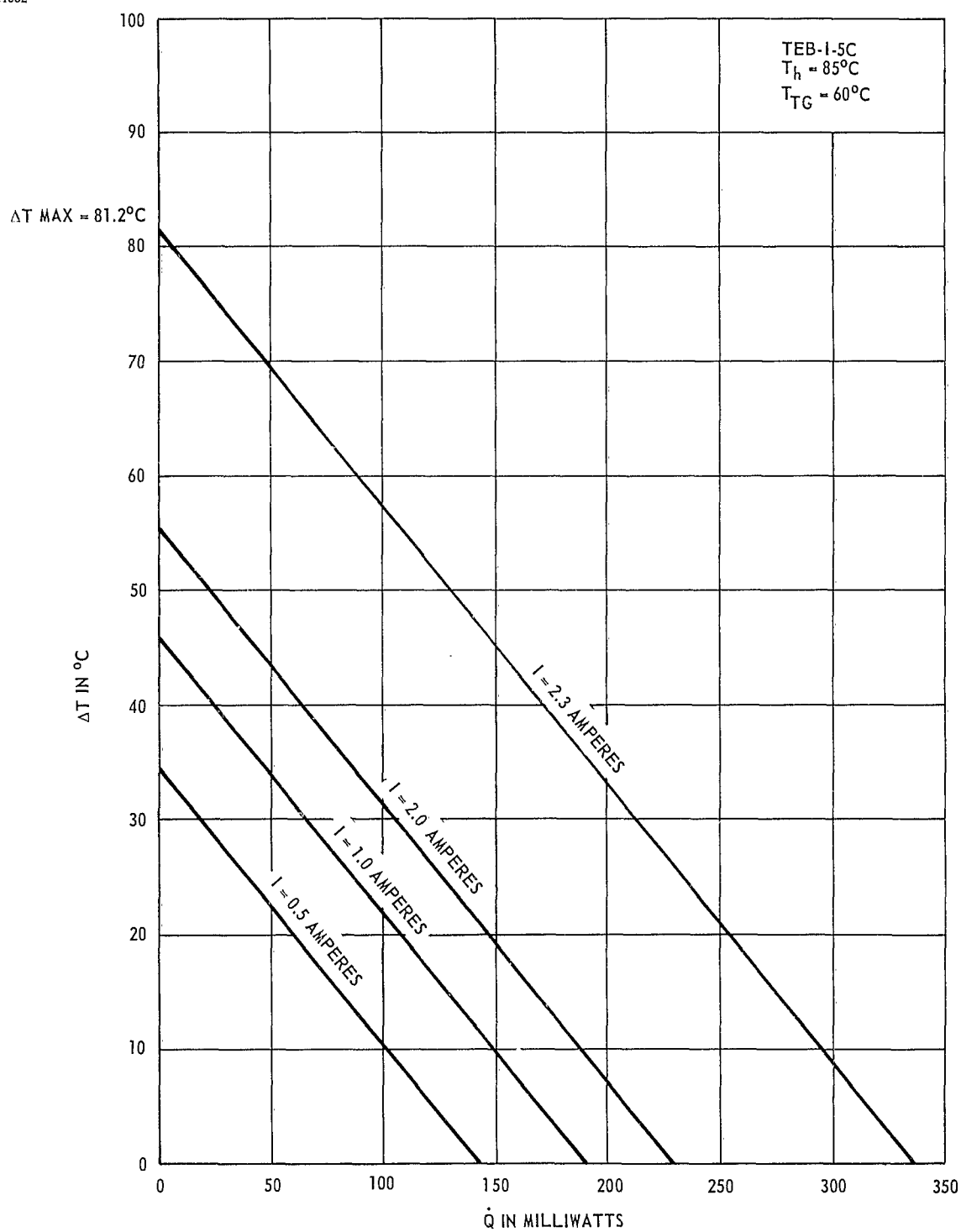
Figure 47. TEB, Type I-C, No. 5, $\dot{Q}$ vs. ΔT, With T_h = 85°C, Showing Typical Types I and II Performance Without Glass Encapsulation

147
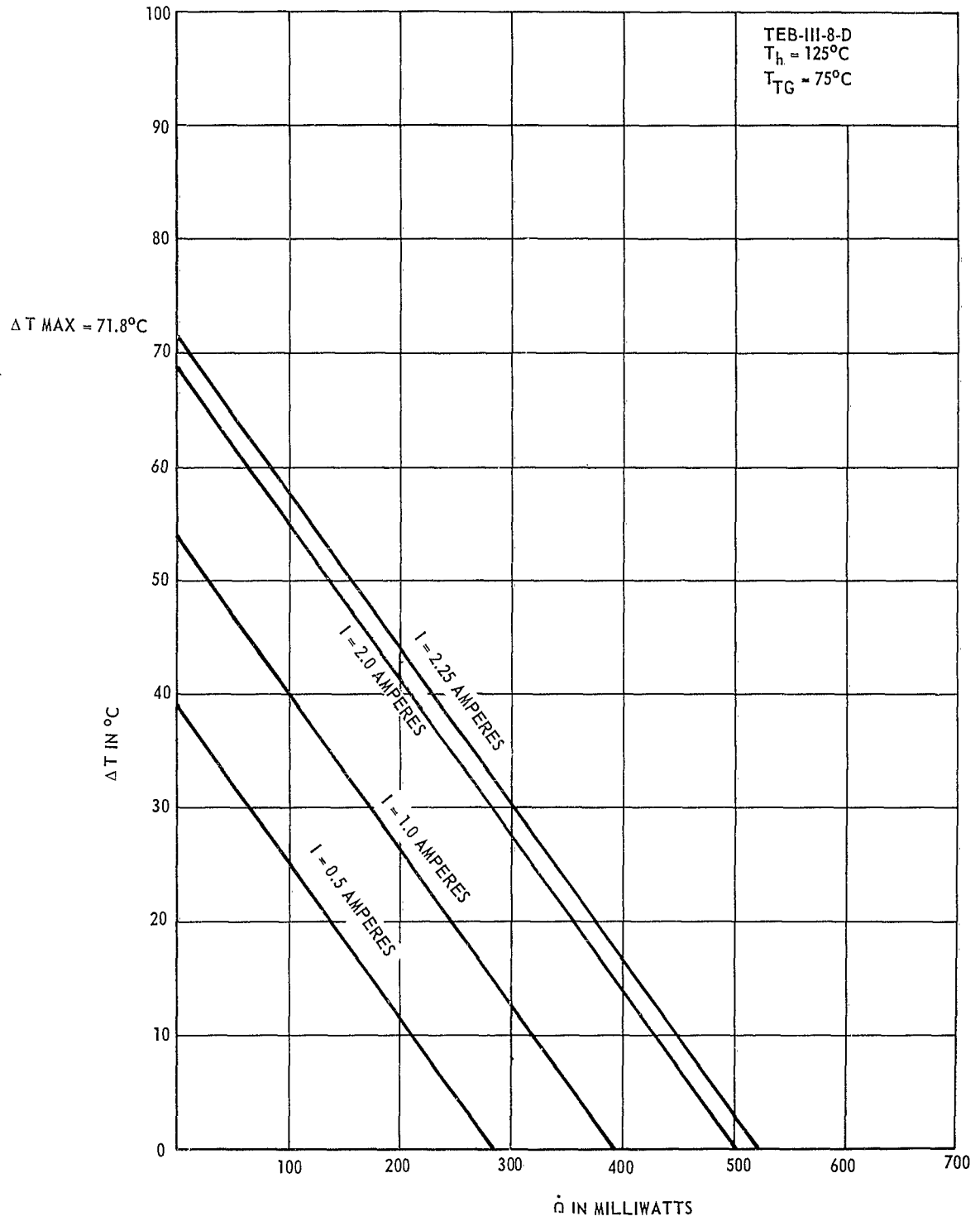
Figure 48.   TEB, Type III-D, No. 8, $\dot{Q}$ vs. Δ T, With T_h = 125°C, Showing
Typical Types III and IV Performance With Glass Encapsulation

148
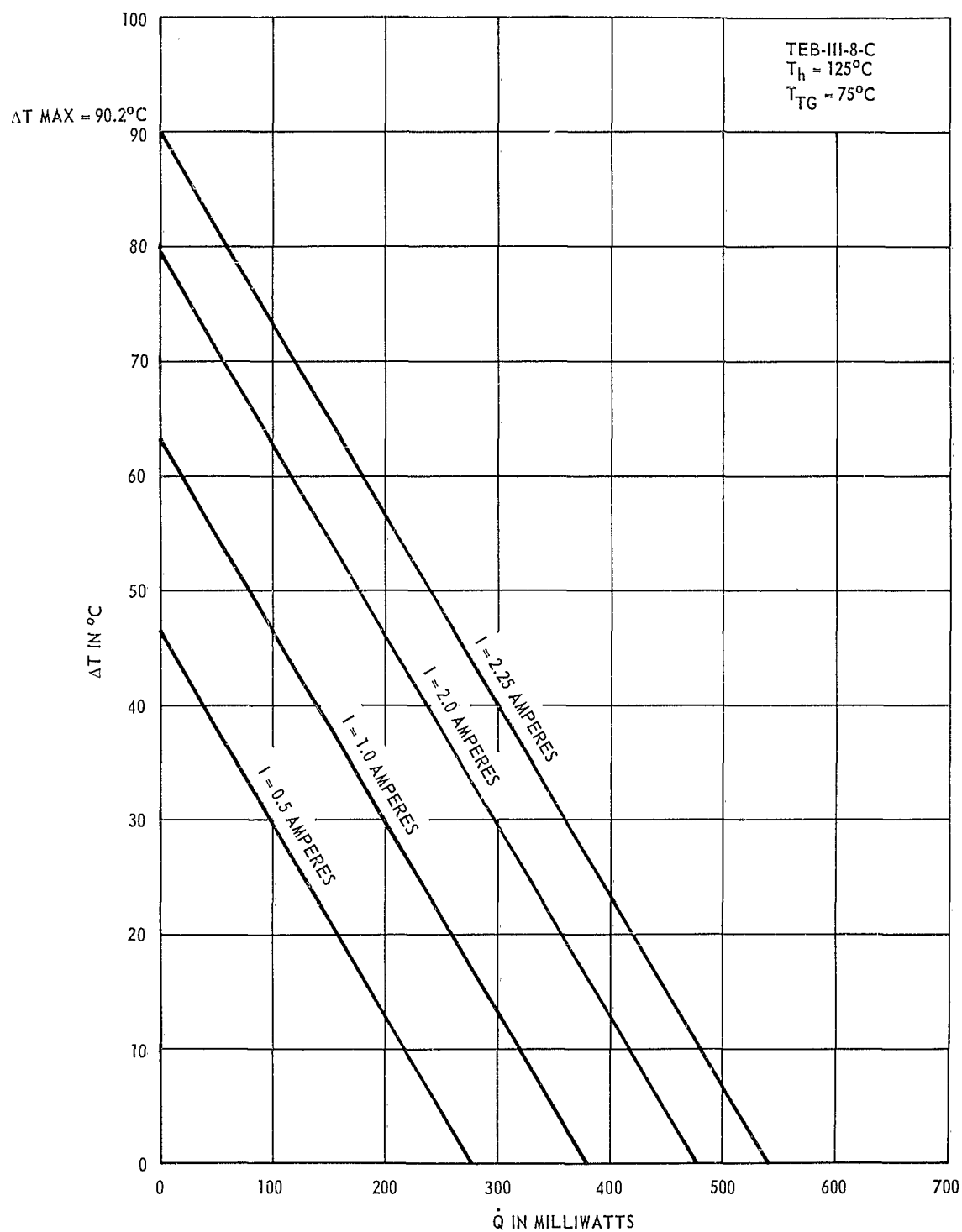
Figure 49.   TEB, Type III-C, No. 8, $\dot{Q}$ vs. ΔT, With T_h = 125°C, Showing
Typical Types III and IV Performance Without Glass Encapsulation

149

The left side of this equation represents the heat flowing into the cold junction, while the right side represents the heat flowing out of the cold junction because of Peltier heat absorption. This theoretical equation neglects two correction terms, K_r and $K_{(insulation)}$, which should be included on the left side of the equation.

$$\dot{Q}_t = \dot{Q} + \dot{Q}_r + \dot{Q}_{(insulation)} + K(T_h - T_c) + 1/2\ I^2 r' = \overline{S}T_c I$$

or

$$\dot{Q}_t = \dot{Q} + \left[K + K_r + K_{(insulation)} \right] (T_h - T_c) + 1/2\ I^2 r' = \overline{S}T_c I$$

(1) $\dot{Q}_r$ is the heat transferred by radiation exchange between T_h and T_c through the nonthermoelectric parts of the heat exchange area $\overline{A}$. $\dot{Q}_r$ and K_r are given by

$$\dot{Q}_r = \sigma \overline{A}(\overline{\varepsilon}_1 T_h^4 - \overline{\varepsilon}_2 T_c^4) \quad \text{and} \quad K_r = \dot{Q}_r / (T_h - T_c)$$

where $\overline{\varepsilon}_1$ and $\overline{\varepsilon}_2$ are the emissivities of the surfaces at T_h and T_c respectively and K_r is the effective thermal conductance attributable to the radiation flux.

(2) $\dot{Q}_{(insulation)}$ is the heat conducted through the glass encapsulation (and air if the TEB device is tested or used in air).

$$\dot{Q}_{(insulation)} = K_{(insulation)}\ \Delta T$$

$$K_{(insulation)} = \frac{k_{(insulation)} A'}{L}$$

The terms $\dot{Q}_{(insulation)}$ and $K_{(insulation)}$ are further defined in the glossary.

Taking these excess heat fluxes $\dot{Q}_r$ and $\dot{Q}_{(insulation)}$ and
their associated thermal conductances K_r and $K_{(insulation)}$
into account, we can calculate the effective figure of merit
Z'' of the device from:

$$Z'' = \frac{\overline{S}^2}{(r + r_c)(K + K_r + K_{(insulation)})}$$

$$= \frac{Z}{(1 + \dfrac{r_c}{r})(1 + \dfrac{K_r + K_{(insulation)}}{K})}$$

where the materials figure of merit

$$Z = \frac{\overline{S}^2}{r\,K} = \frac{\overline{S}^2}{\overline{\rho}\,\overline{k}}$$

4.5.2.2 <u>Comparison of Experimental and Theoretical</u>
<u>Performance</u>: The data for the interim devices given in figure
39 may be checked against theory. Assuming the device $Z'' =$
2.5×10^{-3} $(^{\circ}K)^{-1}$, $(\overline{S} = 440\ \mu v/^{\circ}C$, $\overline{\rho} = 10^{-3}$ ohm-cm, $\rho_c = 10^{-5}$
ohm-cm^2, $K = 3.52 \times 10^{-3}$ watts$/^{\circ}K$), the calculated theoretical
values (see figure 4) shown in figure 39 by the points indi-
cated by 'x' indicate reasonable theoretical agreement.

The theoretical agreement for the data presented for the
twelve final prototype TEB's under type I, II, III, and IV
conditions (table X) is also reasonable, as may be seen from
figures 50 to 57. These curves represent plots of average and
extreme values of ΔT from the data presented in figures 42
to 45, inclusive, for type I to IV devices without glass encap-
sulation (C), and with glass encapsulation (D). The theoretical
current values for $Z'' = 2.5 \times 10^{-3}(^{\circ}K)^{-1}$ which should give the
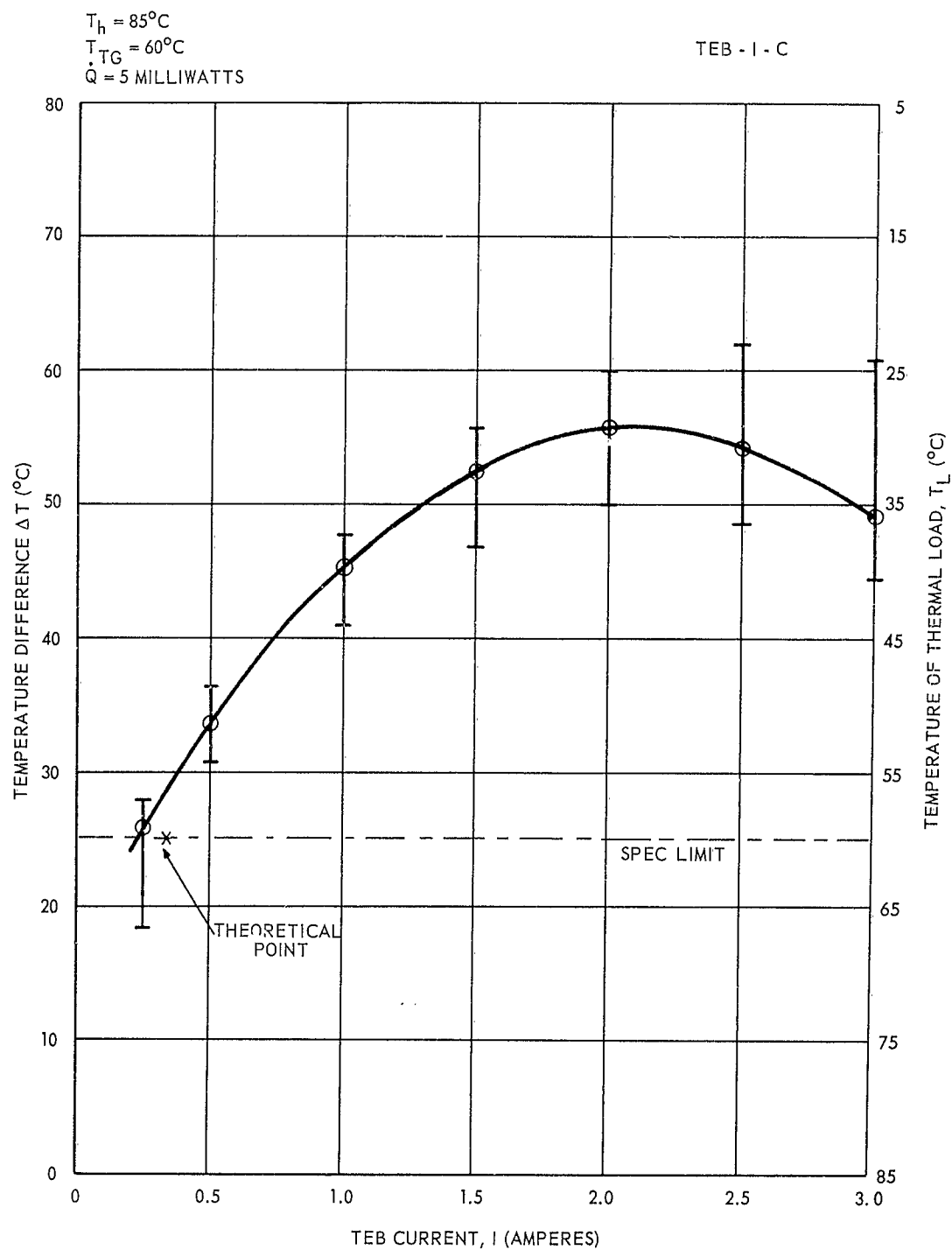
Figure 50.   TEB, Type I-C, Average ΔT vs. I Curves For $\dot{Q}$ = 5 mw

152
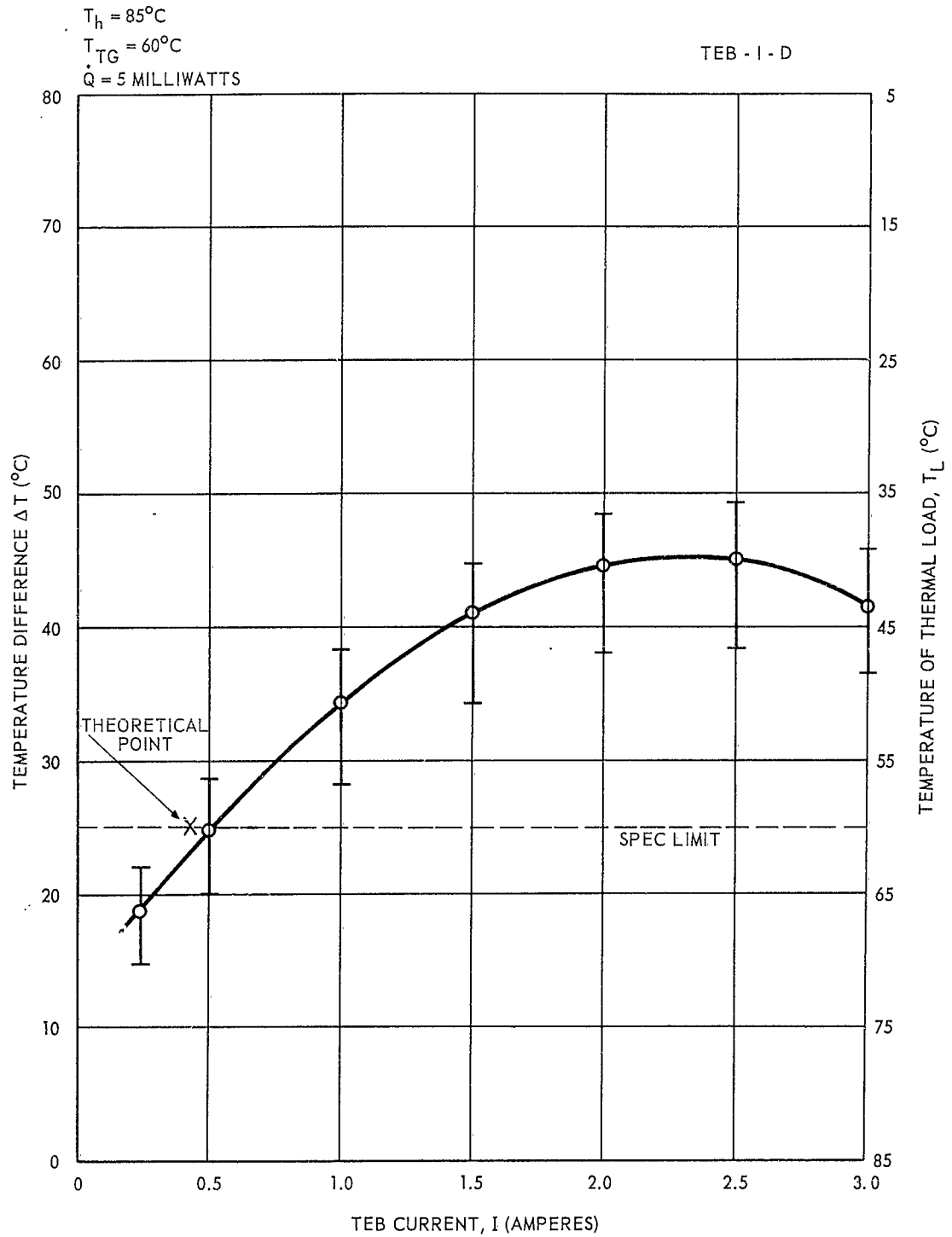
Figure 51. TEB, Type I-D, Average ΔT vs. I Curves For $\dot{Q}$ = 5 mw

153
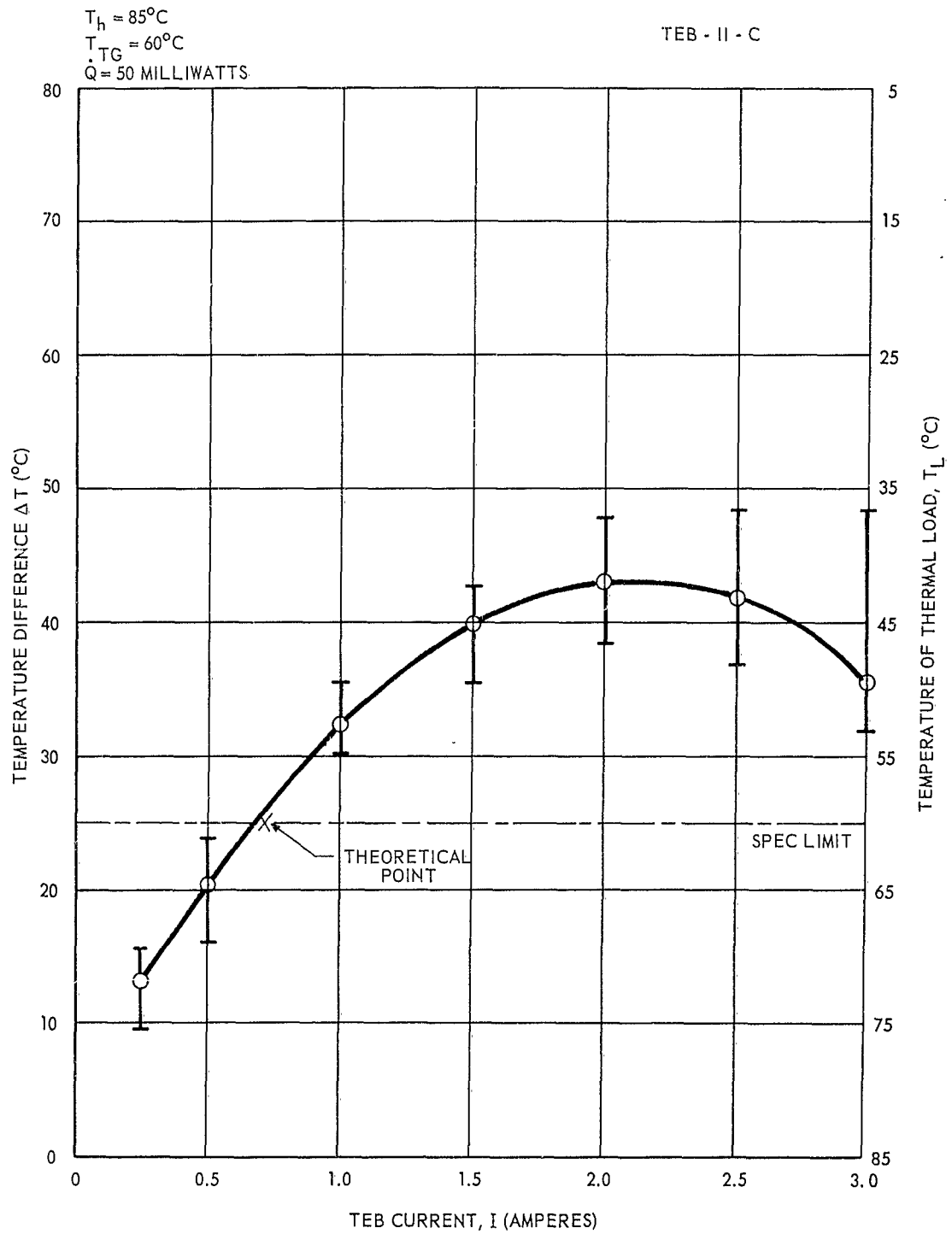
Figure 52.   TEB, Type II-C, Average ΔT vs. I Curves For $\dot{Q}$ = 50 mw
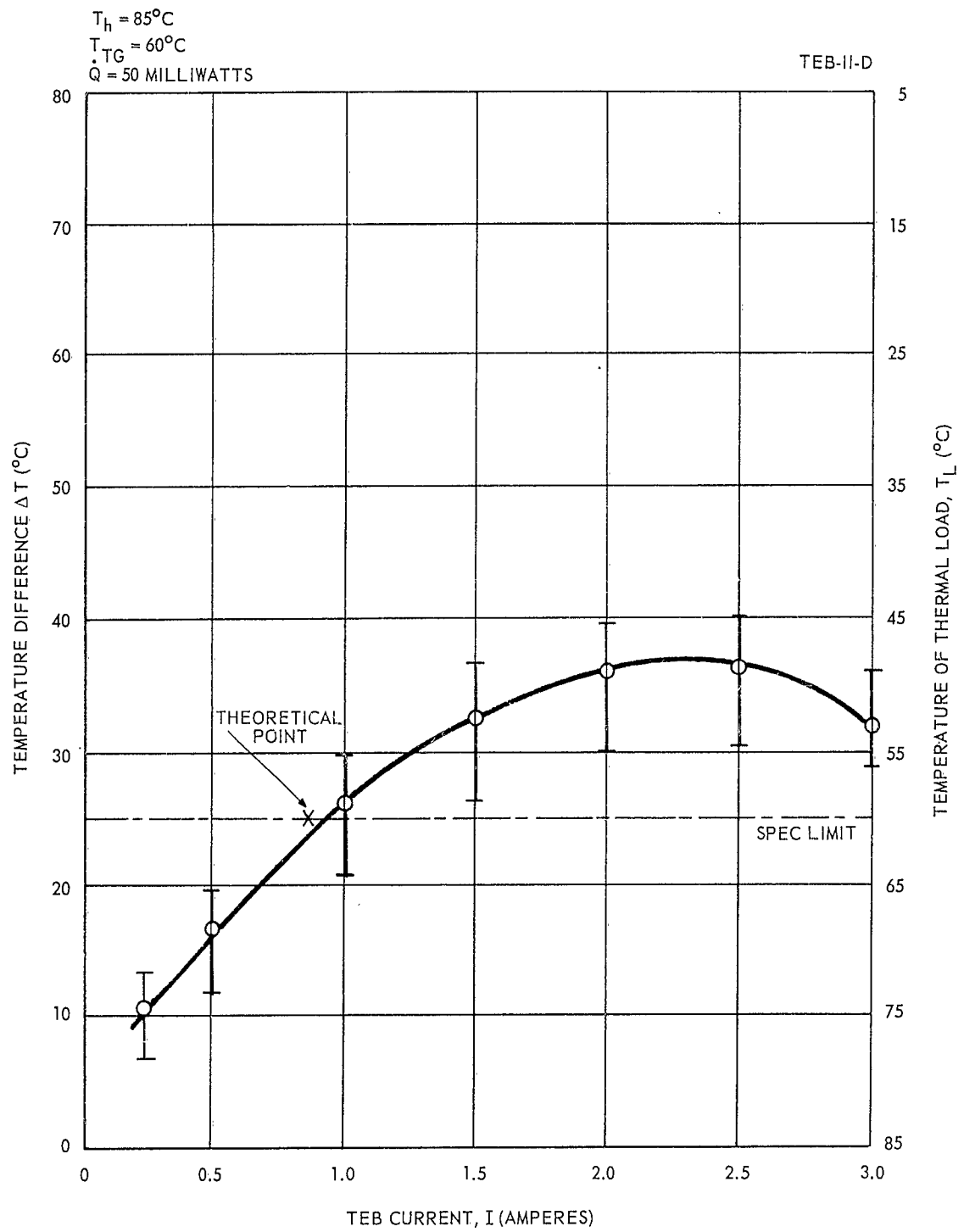
Figure 53.   TEB, Type II-D, Average Δ T vs. I Curves For $\overset{\bullet}{Q}$ = 50 mw
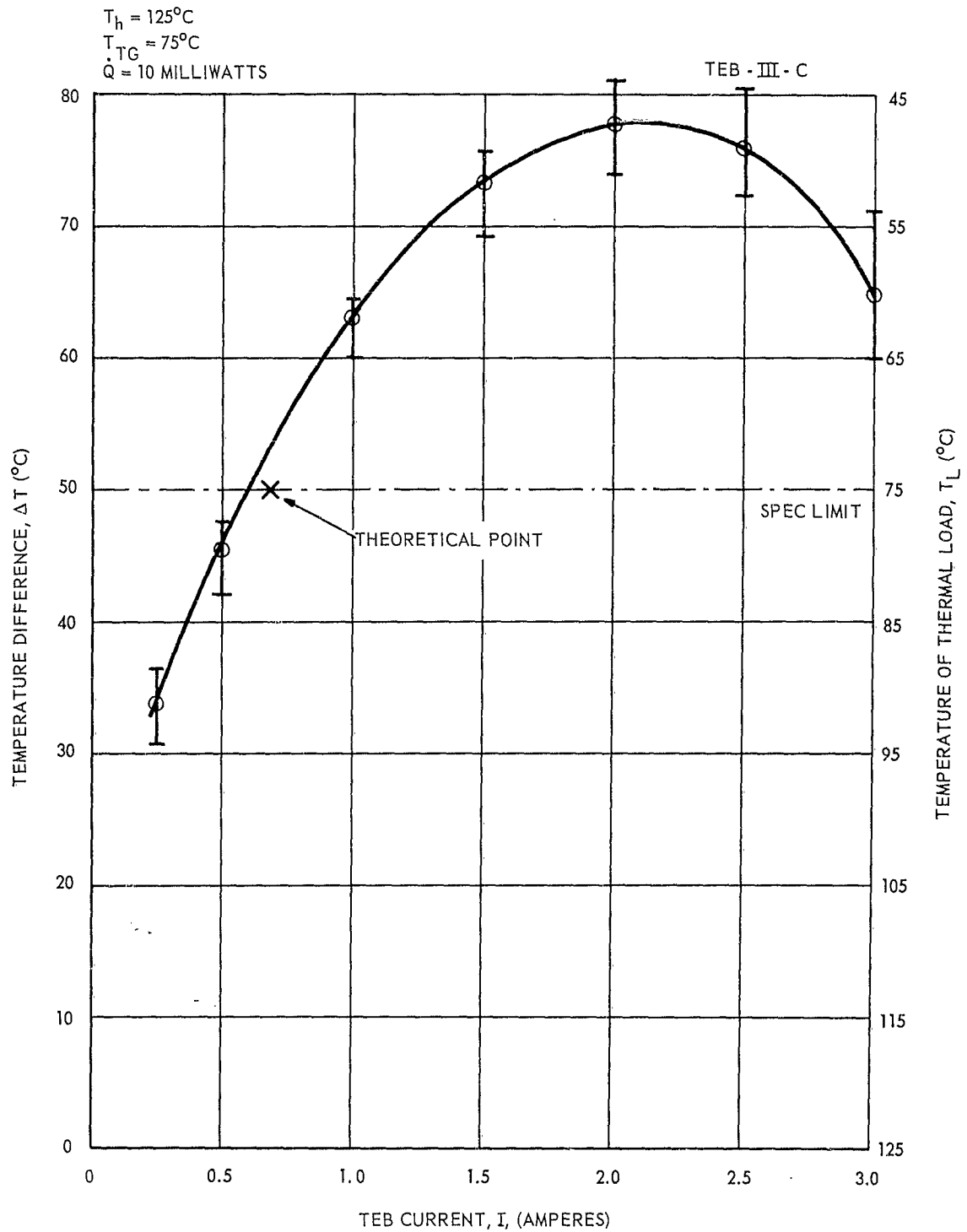
Figure 54.   TEB, Type III-C, Average Δ T vs. I Curves For $\dot{Q}$ = 10 mw
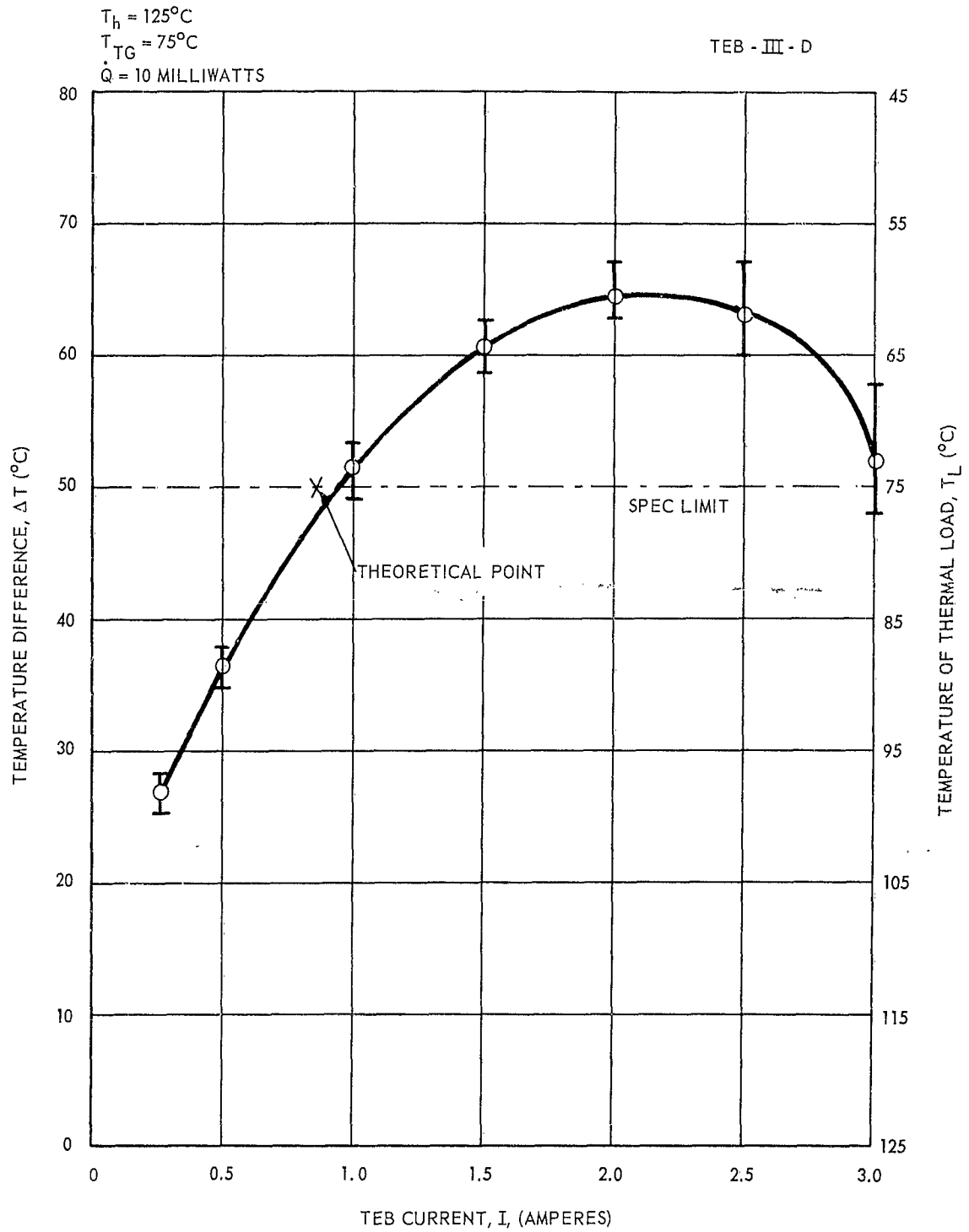
Figure 55. TEB, Type III-D, Average ΔT vs. I Curves For $\dot{Q}$ = 10 mw

$T_h = 125°C$

$T_{TG} = 75°C$

$\dot{Q} = 50$ MILLIWATTS
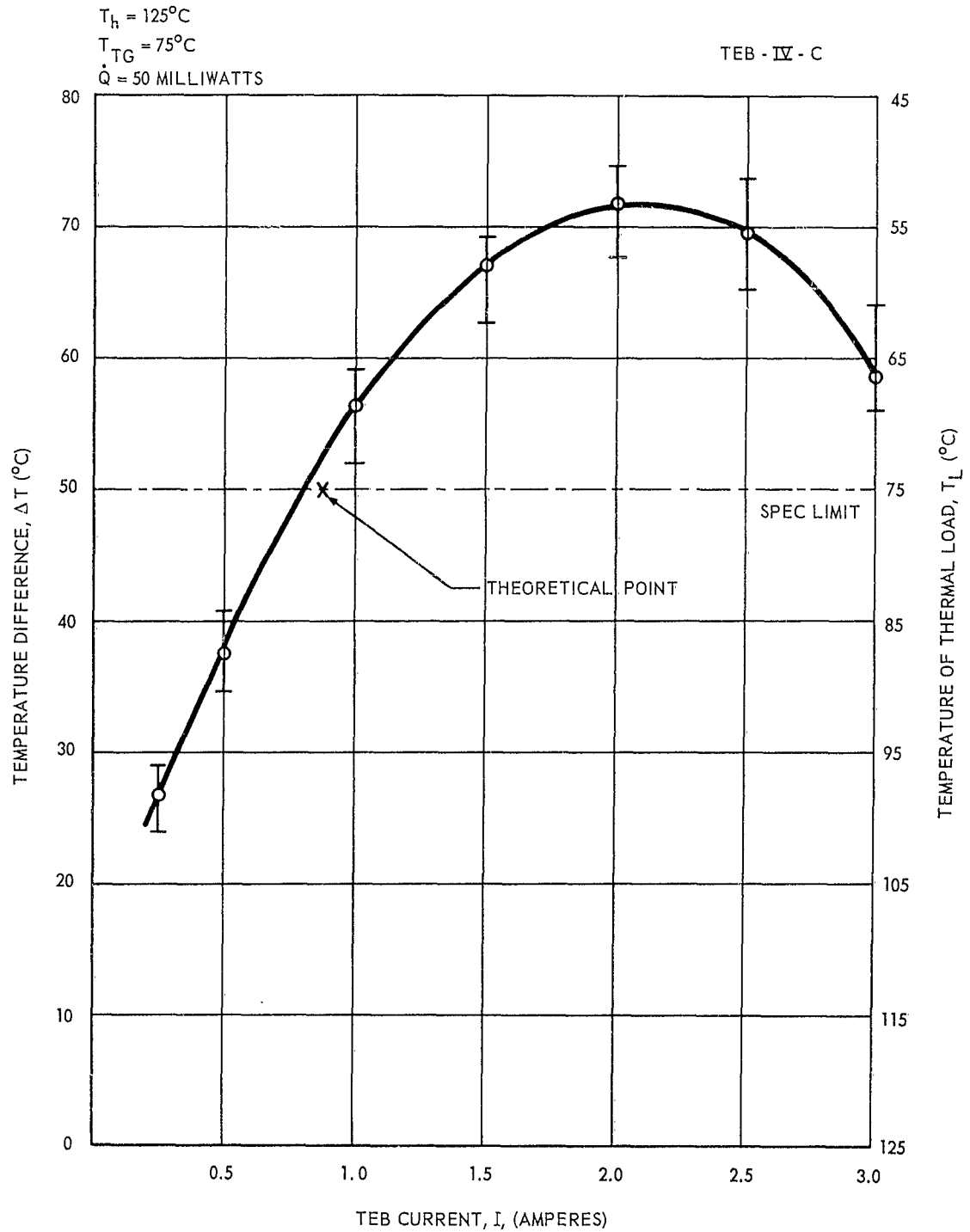
TEB - IV - C

Figure 56. TEB, Type IV-C, Average ΔT vs. I Curves For $\dot{Q} = 50$ mw
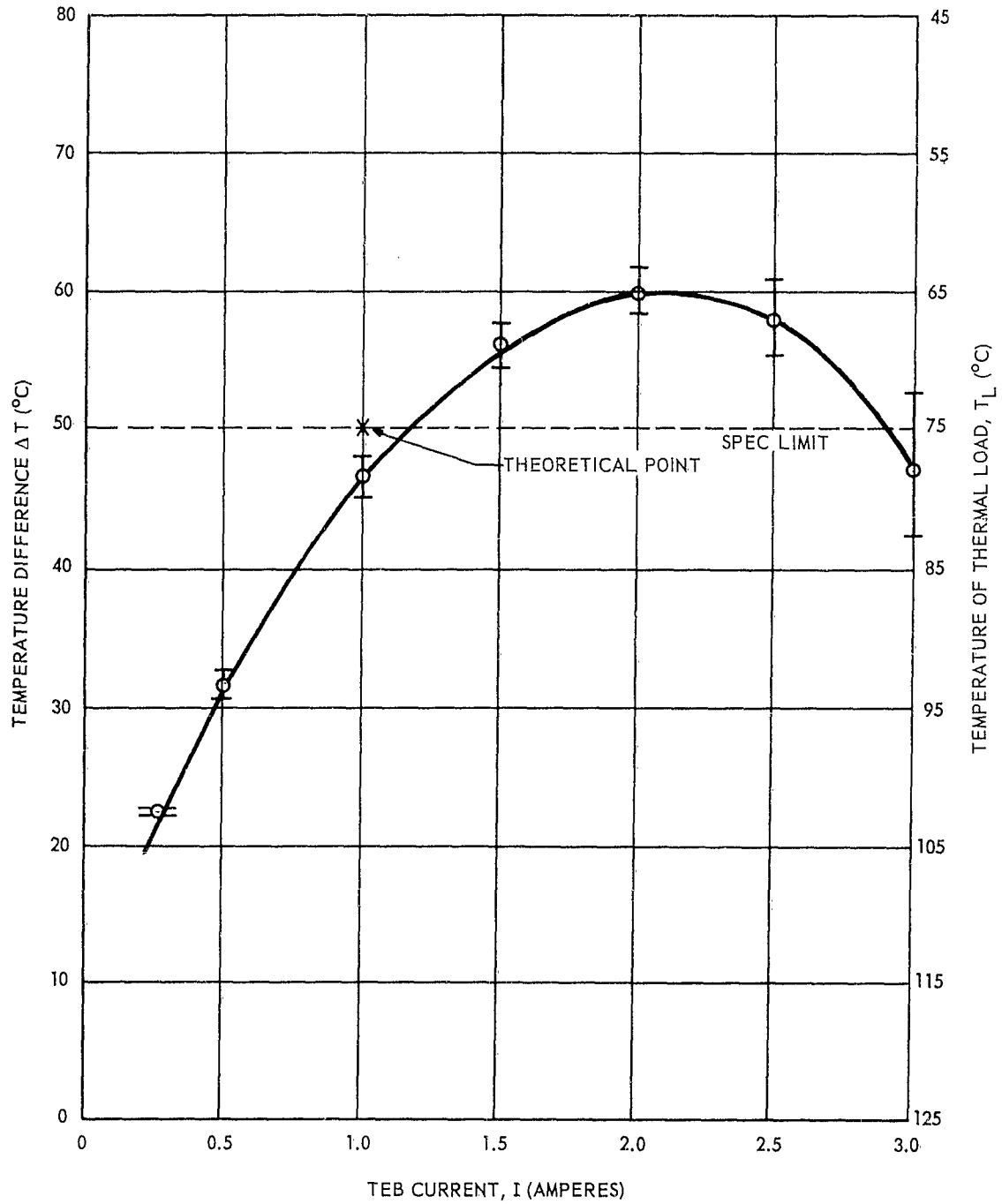
Figure 57.   TEB, Type IV-D, Average Δ T vs. I Curves For $\dot{Q}$ = 50 mw

159

desired type I through IV performance are plotted on the curves
for devices without glass encapsulation by points designated
by 'x'. (See table XI.) Agreement between the theoretical
and experimental currents at the operating points indicated
by table X is satisfactory. It would thus seem that the
behavior of the TEB device can be represented by device figure
of merit of $Z'' = 2.5 \times 10^{-3} \, (^{\circ}K)^{-1}$. The parameters of the
thermoelectric material measured by the Z-meter technique gave
a materials figure of merit Z of $2.83 \times 10^{-3} \, (^{\circ}K)^{-1}$. The
difference between Z'' and Z may be explained by the discussion
and equations in 4.5.2.1. Using the equations in that section,
$\dot{Q}_r \cong 4.9$ mw for type III and IV conditions. This value was
calculated assuming that the average emissivity associated with
$T_h = 125^{\circ}C$ is $\bar{\varepsilon}_1 \cong 0.30$ and the average emissivity associated
with $T_c = 75^{\circ}C$ is $\bar{\varepsilon}_2 \cong 0.44$. The surface at T_c consists of
partially oxidized copper. The handbook emissivity values for
the emissivity for a pure copper surface is $\varepsilon \cong 0.1$, but for
copper oxide it is 0.6. Assuming the surface at T_c is approxi-
mately 90% oxidized, the selected value of $\bar{\varepsilon}_2$ is obtained.
The surface at T_h is partly alumina ($\varepsilon \cong 0.2$) and partially
oxidized copper. Using the known proportions of partially
oxidized copper and alumina, an approximate average value of
0.3 for the emissivity of the surface at T_h was estimated.
Thus, the correction terms ρ_c and $\dot{Q}_r$ are such as to account
adequately for the difference between the measured materials
figure of merit, Z and Z''.

Using the value of $0.0076 \, \frac{watts}{cm^{\circ}K}$ for the thermal con-
ductivity of glass, the Z'' for the glass encapsulated modules
is calculated as explained in 4.5.2.1 with the result

$z'' \cong 2.1 \times 10^{-3} (^{\circ}K)^{-1}$, using the calculated values for $\dot{Q}_{(insulation)}$ and $\dot{Q}_r$ for type I to IV conditions. The approximate calculated heat flow, $\dot{Q}_{(insulation)}$, for values of $T_h = 85^{\circ}C$ and $T_c = 60^{\circ}C$ (types I and II) is 16 mw and for $T_h = 125^{\circ}C$ and $T_c = 75^{\circ}C$ (types III and IV), $\dot{Q}_{(insulation)}$ is 32 mw. The theoretically calculated values for ΔT under type I to IV conditions are given by the theoretical point (x) on the curves of figures 51, 53, 55, and 57. The agreement between theory and experiment is good. The important effect of the glass encapsulation is clearly shown by comparing the C and D curves in figures 50 to 57.

5.   CONCLUSIONS

The TEB device requirements defined in USAELRDL Technical
Requirements SCL-7635 and summarized in table X have been met
with currents considerably less than the three amperes specified
as the upper limit. The average current, as shown in figures
50 to 57 for type I, II, III, and IV operation without glass
encapsulation, was 0.25, 0.7, 0.6, and 0.8 amps, respectively.
With glass encapsulation, the corresponding average currents
were 0.5, 0.95, 0.92, and 1.17 amps. Thus, the method of encapsu-
lation is of critical importance. The theoretical curves of
figures 3 and 4 indicate that, for operation at $C.O.P._{(max)}$,
$\dot{Q}_{(max)}$, and the crossover point between them, currents of 1.3,
3.5, and 2.1 amps, respectively, are required. It is thus
apparent that the TEB devices constructed will operate at
greater C.O.P. for higher heat loads than those specified by
type I to IV conditions. This point was emphasized in para-
graph 4.3.2, on design calculations, where the limiting factor
was the technological limit to the area of cross section of
the thermoelectric legs attainable.

No unusual difficulties were encountered in manufacturing
25 units of each type (I to IV) called for by SCL-7635, but
the development of semiautomatic methods will be important for
quantity production.

Worthwhile improvements could be used in TEB device per-
formance, which may be achieved principally by reducing radiation
heat leakage and heat leak through the glass encapsulation.

The device performance was limited by technological limits
placed on the TEB device height. A higher C.O.P. could have
been achieved under the specified heat loads only by advances

in the state of the art of producing thermoelectric legs of smaller cross-sectional area, as explained in paragraph 4.3.2. This cross-sectional area was limited by the present technology, which could be extended to reduce this area by a factor of between approximately 5 and 10 times. As shown in figures 3 and 4, considerable excess pumping capacity has been introduced into the devices, and operation at higher heat loads and currents would result in operation in the most favorable region between C.O.P.$_{(max)}$ and $\dot{Q}_{(max)}$. It is expected that this extra heat-pumping capacity available at currents less than 3 amps will be of value in the practical applications of TEB devices to the temperature control of temperature-critical electronic components.

6. RECOMMENDATIONS

Although the devices developed in the present contract easily meet the specified type I to IV operational requirements, several worthwhile improvements can be made. These improvements are discussed below.

6.1 Improvements Related to the Present Device Configurations

These include:

a. Improved encapsulation procedures to make the fabrication process less time consuming and to reduce thermal conduction through the encapsulation.

b. Emissivity control to reduce the radiation flux through the spaces not occupied by thermoelectric material. For instance, the surfaces at T_c and T_h could be plated to have as low an emissivity as possible.

c. A thorough experimental device analysis should be conducted on one device of each type to check the theoretical predictions of figures 3 and 4 together with extensions to higher heat loads and additional temperatures.

d. Extensive life tests should also be performed on TEB devices under operational conditions.

6.2 Improvement in Configurational and Thermal Design

These include development work to:

a. Reduce the height of TEB devices to one-half, or less, their present values so that the devices can be fitted into a smaller space.

b. Extend the TEB devices for operation at higher heat loads (1 watt, or higher), using the design criteria for minimum current and higher voltage of operation. This may be achieved by using 16 or more legs of reduced cross-sectional area.

c. Improve the heat-transfer characteristics and simplify fabrication procedures using thermoelectric legs integrated with BeO ceramic micromodule wafers of high thermal conductance and high electrical resistance. The electrical conduction paths could be formed by various methods, such as metal plating and selective etching.

6.3 Additional Cooling Design Concepts

These include:

a. The direct integration of thermoelectric cooling legs into the temperature-sensitive device. Thus, a temperature-sensitive transistor could be mounted onto a BeO micromodule wafer and the thermoelectric cooling legs connected directly to the transistor mounting wafer. Alternatively, the thermo-electric legs could be incorporated directly into the transistor can. These procedures would have the advantage of enabling a precise matching of the thermoelectric TEB design to the specific cooling requirements of a specific temperature-sensitive component.

b. Thermoelectrically cooling a whole micromodule stack instead of a specific component.

c. Thermoelectrically cooling a complete chassis instead of an individual component or module stack by thermoelectrically cooled and dehumidified air.

It is anticipated that all four approaches to solid-state electronic cooling (that is, the TEB micromodule approach, the matched individual specific component approach, the micromodule stack approach, and the thermoelectric cooling of the chassis by dry thermoelectrically cooled air) will have certain advantageous areas of application.

7. IDENTIFICATION OF KEY TECHNICAL PERSONNEL

During the period of this contract, the following key personnel participated in the work discussed in this report.

7.1 Man-Hours Expended

Name	Title	Man-Hours
Nicholas Fuschillo	Head, Solid-State Physics Section	150
Paul A. Mullin*	Physicist	200
F. Kent Eggleston	Principal Engineer	300
Forest K. Luckett**	Solid-State Technician	600
Orville B. Van Blaricon	Design Engineer	150
Eugene B. Stewart***	Senior Thermoelectric Technician	60
	Total	1,460

7.2 Personnel Résumés

Résumés of the key personnel assigned to this project follow:

---

*Mr. Mullin replaced Mr. John D. Boardman on this program; the latter was called into the U.S. Air Force.

**Mr. Luckett was transferred to this program after the departure of Mr. Stewart.

***Mr. Stewart left Melpar in June 1962.

Nicholas Fuschillo received B.S. and M.S. degrees in physics at the University of London; he presented a dissertation on the control and measurement of temperatures from the lowest to the highest attainable. He received a Ph.D. degree in 1952 at the University of Leeds, where he studied with E. C. Stoner and F. E. Hoare. There, he worked in the low-temperature laboratory and did thesis research on thermoelectric effects in liquid and solid metals and alloys, as well as on precision low-temperature gas and thermoelectric thermometry. He continued research in the Department of Engineering Physics at Cornell University, where he studied the mechanical properties and audiofrequency attenuation in metallic single crystals from 2° to 400°K.

In 1954, Dr. Fuschillo was appointed assistant professor of physics at Pennsylvania State University, where he taught classical mechanics and solid-state physics at the first-year graduate and senior undergraduate levels, as well as second-year courses in atomic and nuclear physics, electricity, magnetism, and thermodynamics. His research activities were principally in nuclear magnetic resonance as applied to the study of surfaces, radiation damage, molecular diffusion, and rotation, as well as in the thermal and mechanical properties of high polymers, molecular crystals, and molecular radiation damage.

Dr. Fuschillo went to the Franklin Institute of the State of Pennsylvania in 1957 as the head of the Magnetics and Semiconductors Branch. In addition to directing the Institute's industrial co-operative programs in thermoelectricity and fine-particle magnetics, he initiated and supervised research programs

for the government in superconducting and semiconductor r-f
thermal detectors as well as organic and plastic semiconductors.
He initiated the Institute's magnetic spin resonance laboratory,
and was administratively responsible for government research
programs in metallic-magnetic materials and ferrites. In 1959,
Dr. Fuschillo went to C.B.S. Laboratories as Head of the Solid-
State Physics Department. There, he supervised research
involving photoconductive, semiconductor, magnetic, and thin-
film materials and devices.

Dr. Fuschillo is a fellow of the Physical Society and
of the Institute of Physics, and a member of the American
Physical Society, the Institute of Metals, Sigma Xi, Gamma
Alpha, and the Physics Club of Philadelphia.

Dr. Fuschillo is the author or coauthor of over 20 articles
published in the journals of learned societies, and the author
of several chapters in copyrighted, scientific books.

Dr. Fuschillo is also the author or coauthor of nearly
20 scientific papers presented to scholarly organizations or
groups.

Paul A. Mullin received a B.S. degree in physics at Drexel
Institute of Technology June 1961. He had 24 months of co-
operative experience with Bendix Radio in the air traffic-
control problem; wide-band video-amplifier design and testing
of toroidal coils; passive impedance-matching devices; setting
down design parameters for simple digital computer circuits;
and building a multipurpose pulse generator from another
engineer's design.

In July 1961, Mr. Mullin came to Melpar as a physicist
in the Solid-State Physics Section of the Research Division.

There, he has been working on the design theory of thermoelectric power generators and refrigerators, thermoelectric materials development, and the theory of photovoltaic diode power generators.

Mr. Mullin is presently enrolled in the University of Maryland graduate-degree program, working on a M.S. degree in solid-state physics.

F. Kent Eggleston majored in physics at Wabash College and Ohio State University. He went to the Battelle Memorial Institute in 1952 as a technician in the Solid-State Devices Division. There, he worked on the development of germanium and silicon diodes, electrical properties of aluminum antimonide, TiO_2 rectifiers, and cadmium sulphide photocells; he gained experience in diode and transistor testing, barrier layer capacitance, Hall effect, and minority carrier lifetime and other physical measurements.

Mr. Eggleston went to the Delco Division of General Motors Corporation in October 1955 as project engineer with the Advanced Devices Group of the Semiconductor Research and Engineering Department. There, he worked on the development of the first Delco Radio germanium power transistors (2N173 and 2N174), silicon power rectifiers by the diffusion technique, silicon solar cells and germanium-diffused collector power transistors, and germanium RF and VHF mesa transistors, for which he also developed special equipment required for microfabrication techniques.

He went to Ohio Semiconductors, Inc., in January 1958 as Chief, Device Development Section. There, he was responsible

for the development of Hall effect and magneto-resistance devices of InSb and InAs; he was promoted to manager of the Device Engineering Division, with responsibilities for the development of thermoelectric cooling devices. He supervised the development of the first marketed thermoelectric cooling units early in 1959 and the first commercial Hall effect device, the Halltron. Thermoelectric cooling devices were emphasized, and several special-purpose thermoelectric coolers and refrigerators were constructed.

At Delco and Ohio Semiconductors, Mr. Eggleston had experience in process development and production; he was in charge of groups responsible for process development of the subassembly parts for production rates of 10,000 transistors a day, and the production of marketable Hall effect and thermoelectric devices.

In April 1961, Mr. Eggleston was assigned to the Solid-State Physics Section of Melpar as senior research engineer in the Solid-State Devices Branch. There, he is responsible for research and development programs in diode, transistor, and thermoelectric devices.

He has presented papers to the IRE and the AIEE entitled, respectively, "Galvanomagnetic Devices of InSb and InAs" and "High-Temperature Titanium Dioxide Rectifiers." He is a member of the IRE and of the American Management Association.

Forest K. Luckett was educated at the National Radio Institute and the Ohio Technical Institute. He is a fully qualified watchmaker and micro solid-state device technician. Mr. Luckett has had 17 years of experience in watch and custom jewelry repair and manufacturing preceding 4 years of experience in

the semiconductor devices field. He is particularly skilled in the following areas of solid-state device technology: Fabrication and design of thermoelectric, Hall effect and magnetoresistance devices and their testing and evaluation; material and active device preparation; vacuum deposition and electrochemical plating technology; metallography and photography as well as photolithographic techniques.

At Melpar, Mr. Luckett has been specializing in integrated monocrystalline microcircuit fabrication and in the construction of novel experimental active elements. He is particularly talented in the fabrication of microdevices and in other tasks which require an unusual manipulative ability combined with great patience and care.

Eugene B. Stewart received a certificate in electronics technology from the Ohio Technical Institute in 1959.

At Melpar, Mr. Stewart did development work on computer equipment microcircuits. Previously, he was doing research and development work on thermoelectric devices for application to commercial products. He had also done work on the application of thermoelectrics to chemical warfare projects, and has constructed a special diffusion furnace and associated control equipment.

Mr. Stewart came to Melpar in September 1961. At the Ohio Semiconductors Division of Tecumseh Products, 1959-1961, he was an engineering assistant in a laboratory group doing thermoelectric research and development work. There, he also did research and development in micro.Hall-effect devices and power magnetoresistors.

171

In 1959, he worked with Bell Telephone Laboratories as a technical aide.

With the Battelle Memorial Institute from 1956 to 1959, he was an electronics technician on design and construction of test sets and various test and control equipment.

Mr. Stewart served in the U.S. Air Force from 1951-1955, working principally in statistical services and terminating as statistical specialist in the Comptroller's Division with the rating of staff sergeant.

Orville B. Van Blaricon has had 24 years of experience as a master machinist, model maker, and mechanical designer. He went to Ohio Semiconductors, Inc., in 1958 as supervisor of the Experimental Model Shop. Mr. Van Blaricon is experienced in the mechanical forming operations on semiconductor materials (transistor, Hall effect, and thermoelectric), i.e., slicing, lapping, dicing, polishing, and ultrasonic cutting.

Mr. Van Blaricon is currently in charge of the Technical Operations Laboratory of the Solid-State Physics Section in the Research Division of Melpar. In this position, he is responsible for mechanically preparing semiconductor materials, providing experimental machine shop and model-making capability, scientific glass blowing, and mechanical design services to the Solid-State Physics Section.

8. REFERENCES

1. R. R. Heikes and R. W. Ure, _Thermoelectricity: Science and Engineering_, Interscience Publishers, New York, N.Y. (1961), p. 463, Eq. 15.14.

2. _Ibid._, p. 464, Eq. 15.15.

3. _Ibid._, p. 464, Eq. 15.16.

4. _Ibid._, p. 463, Eq. 15.11.

5. A.F. Ioffe, _Semiconductor Thermoelements and Thermoelectric Cooling_, Infosearch Limited, London (1957), p. 118, Eq. 67.

6. Heikes and Ure (reference 1), p. 464, Eq. 15.22.

7. _Ibid._, p. 465, Eq. 15.24.

8. Ioffe (reference 5), p. 97, Eq. 10.

9. _Ibid._, p. 99, Eq. 15.

10. Heikes and Ure (reference 1) p. 472, Eq. 15.45.

11. _Ibid._, p. 464, Eq. 15.18.

12. _Ibid._, p. 464, Eq. 15.19.

13. _Ibid._, p. 465, Eq. 15.24.

14. _Ibid._, p. 465, Eq. 15.25.

15. _Ibid._, p. 466, Eq. 15.26.

16. _Ibid._, p. 466, Eq. 15.27.

17. _Ibid._, p. 466, Eq. 15.28.

18. _Ibid._, p. 470, Eq. 15.36.

19. _Ibid._, p. 470, Eq. 15.38.

20. *Ibid.*, p. 471, Eq. 15.39.

21. *Ibid.*, p. 471, Eq. 15.40.

22. *Ibid.*, p. 471, Eq. 15.41.

23. *Ibid.*, p. 470, Eq. 15.37.

24. *Ibid.*, p. 471, Eq. 15.42.

25. I.B. Cadoff and E. Miller, *Thermoelectric Materials and Devices*, Reinhold Publishing Corp., New York, (1960), p. 253, Eq. 5.

26. *Ibid.*, p. 253, Eq. 8.

27. *Ibid.*, p. 255, Eq. 13.

28. *Ibid.*, p. 255, Eq. 16.

29. *Ibid.*, p. 255, Eq. 14.

30. *Ibid.*, p. 255, Eq. 18.

31. *Ibid.*, p. 256, Eq. 19.

32. *Ibid.*, p. 256, Eq. 20.

33. *Ibid.*, p. 257.

34. T.C. Harman (reference 25), chapter 6.

35. Ioffe (reference 5), p. 152.

36. R. H. Vought (reference 25) p. 271, Eq. 24.

UNITED STATES ARMY ELECTRONICS RESEARCH & DEVELOPMENT AGENCY
STANDARD DISTRIBUTION LIST
RESEARCH AND DEVELOPMENT CONTRACT REPORTS

<u>Copies</u>

OASD (R&E)
ATTN: Technical Library
Room 3E1065
The Pentagon
Washington 25, D.C.   1

Chief of Research and Development
OCS, Department of the Army
Washington 25, D. C.   1

Commanding General
U.S. Army Materiel Command
ATTN: R&D Directorate
Washington 25, D.C.   1

Commanding General
U.S. Army Electronics Command
ATTN: AMSEL-AD
Fort Monmouth, New Jersey   1

Director, U.S. Naval Research Laboratory
ATTN: Code 2027
Washington 25, D.C.   1

Commander, Aeronautical Systems Division
ATTN: ASAPRL
Wright-Patterson Air Force Base, Ohio   1

Hq, Electronic Systems Division
ATTN: ESAL
L.G. Hanscom Field
Bedford, Massachusetts   1

Commander, Air Force Cambridge Research Laboratories
ATTN: CRO
L.G. Hanscom Field
Bedford, Massachusetts   1

a

Commander, Air Force Command & Control Development
Division
ATTN: CRZC
L.G. Hanscom Field
Bedford, Massachusetts   1

Commander, Rome Air Development Center
ATTN: RAALD
Griffiss Air Force Base, New York   1

Commander, Armed Services Technical Information
Agency
ATTN: TISIA
Arlington Hall Station
Arlington 12, Virginia   20

Chief, U.S. Army Security Agency
Arlington Hall Station
Arlington 12, Virginia   2

Deputy President
U.S. Army Security Agency Board
Arlington Hall Station
Arlington 12, Virginia   1

Commanding Officer
Harry Diamond Laboratories
ATTN: Library, Room 211, Building 92
Washington 25, D.C.   1

Corps of Engineers Liaison Office
U.S. Army Electronics Research and Development
Laboratory
Fort Monmouth, New Jersey   1

AFSC Scientific/Technical Liaison Office
U.S. Naval Air Development Center
Johnsville, Pennsylvania   1

USAELRDL Liaison Office
Rome Air Development Center
ATTN: RAOL
Griffiss Air Force Base, New York   1

Commanding Officer
U.S. Army Electronics Materiel Support Agency
ATTN: SELMS-ADJ
Fort Monmouth, New Jersey   1

Marine Corps Liaison Office
U.S. Army Electronics Research and
Development Laboratory
ATTN: SELRA/LNR
Fort Monmouth, New Jersey   1

Commanding Officer
U.S. Army Electronics Research and
Development Laboratory
ATTN: Director of Research or Engineering
Fort Monmouth, New Jersey   1

Commanding Officer
U.S. Army Electronics Research and
Development Laboratory
ATTN: Technical Documents Center
Fort Monmouth, New Jersey   1

Commanding Officer
U.S. Army Electronics Research and
Development Laboratory
ATTN: SELRA/ADJ (FU #1)
Fort Monmouth, New Jersey   1

Advisory Group on Electron Devices
346 Broadway
New York 13, New York   2

Commanding Officer
U.S. Army Electronics Research and
Development Laboratory
ATTN: SELRA/TNR
Fort Monmouth, New Jersey   3

(FOR RETRANSMITTAL TO ACCREDITED BRITISH AND CANADIAN
GOVERNMENT REPRESENTATIVES)

C

Commanding General
U.S. Army Combat Developments Command
ATTN: CDCMR-E
Fort Belvoir, Virginia   1

Commanding Officer
U.S. Army Combat Developments Command,
Communications-Electronics Agency
Fort Huachuca, Arizona   1

Director, Fort Monmouth Office
U.S. Army Combat Developments Command,
Communications-Electronics Agency
Building 410
Fort Monmouth, New Jersey   1

AFSC Scientific/Technical Liaison Office
U.S. Army Electronics Research and
Development Laboratory
Fort Monmouth, New Jersey   1

Commanding Officer and Director
U.S. Navy Electronics Laboratory
San Diego 52, California   1
                                                    ─────────
                                                         52

Melpar, Incorporated
DA36-039-sc-89212
Final Report
Addendum to Standard Distribution List

Copies

General Instruments Corporation
Thermoelectric Division
ATTN: Mr. Howard Hagler
65 Gouverneur Street
Newark 4, New Jersey   1

Astropower, Incorporated
Solid State Devices Laboratory
ATTN: Dr. R. E. Smith
2968 Randolph Avenue
Costa Mesa, California   1

Radio Corporation of America
Surface Communications Division
ATTN: Mr. Donald Mackey
Building 1-4
Camden 2, New Jersey   1

Commanding Officer
U.S. Army Electronics Research and
Development Laboratory
Fort Monmouth, New Jersey
ATTN: SELRA/PE (Division Director)   1
ATTN: SELRA/PE (Dr. E. Both)   1
ATTN: SELRA/PEP (Mr. R. A. Gerhold)   1
ATTN: SELRA/PEP (Dr. H. J. Degenhart)   1
ATTN: SELRA/PEP (Mr. H. C. Frankel)   14
ATTN: SELRA/PSP (Dr. E. Kittl)   1
ATTN: SELRA/PFM (Mr. H. L. Mette)   1

                            Total Number of Copies   75

e

UNCLASSIFIED

AD-_____ Accession No._____

Melpar, Inc., Falls Church, Virginia. THERMOELECTRIC THERMAL-BARRIER MICROELEMENTS, by F. K. Eggleston, P. A. Mullin, and N. Fuschillo. October 1962. 174 p. incl. illus. tables (Task 3A99-15-002-03) (Final Report) (Contract DA 36-039 SC-89212)

Unclassified report

Thermoelectric heat pumps were designed and constructed to serve as Thermoelectric Thermal-Barrier Microelements. These devices have been designed to protect and cool heat-sensitive elements within a micromodule stack from adjacent heat-generating elements.

Devices with capabilities of cooling from 85° to 60°C with thermal loads of 5 to 50 milliwatts and from 125° to 75°C with thermal loads of 10 to 50 milliwatts have been designed, constructed, and evaluated in accordance with Signal Corps Technical Requirement SCL-7635. One hundred devices were manufactured and delivered.

Important features of these thermoelectric heat pumps are: Miniature size, 0.310" x 0.310" (micromodule substrate size) x less than 0.1" high; low operating currents, from 0.25 to 1.5 amperes.

UNCLASSIFIED

1. Thermoelectric heat pumps - Design
2. Thermoelectric heat pumps - Construction
3. Cooling devices - Design
4. Cooling devices - Construction
5. Cooling devices - Evaluation
I. Eggleston, F. K., et al
II. U.S. Army Electronics Research and Development Laboratory
III. Contract DA 36-039 SC-89212

AVAILABLE from Astia

DESCRIPTORS (Cooling, Electronics, Heat Pumps, Miniaturization, Micromodules, Peltier, Thermoelectricity)

UNCLASSIFIED